PHYSICAL REVIEW
LETTERS

VOLUME 7 SEPTEMBER 1, 1961 NUMBER 5

CRITICAL DRIFT VELOCITY OF IONS IN LIQUID HELIUM

G. Careri, S. Cunsolo, and P. Mazzoldi
Istituto di Fisica dell'Università di Roma, Roma, Italy

(Received August 7, 1961)

We have measured the drift velocity $\langle v_D \rangle$ of positive ions in liquid helium II in the temperature range 1.06 to 0.927°K as a function of the applied electric field. We have found that above a critical field strength E_c the drift velocity no longer increases linearly with the increasing field, but suffers a discontinuity. While the value of this critical field E_c depends on the temperature, the corresponding critical velocity $\langle v_c \rangle$ appears to be a temperature-independent quantity in the range so far investigated.

The apparatus used to measure the mobility is a time-of-flight method, which has been more fully described by one of us.[1] Essentially one measures the drift velocity from the time taken by the ions to go from a grid to an electrode, which is connected to a vibrating reed electrometer by a suitable filter. Two apparatus have been used, with different electrode distances and different ionization sources, and they gave identical results.

The reproducibility of our drift velocity data was within ±2%, while the mobility $\mu = \langle v_D \rangle / E$ derived in this way is affected by a further common systematic error, due to the uncertainty in the absolute value of the square wave voltage which was estimated to rise up to ±2%. In this range our absolute values of the zero-field mobility were reproducible on different days, and were also in agreement with those measured by Reif and Meyer[2] and by ourselves[3] by different techniques.

Some typical results of this investigation are reported in Fig. 1 in the customary way, as a plot of the mobility versus the applied field. A glance at this graph shows that below the critical

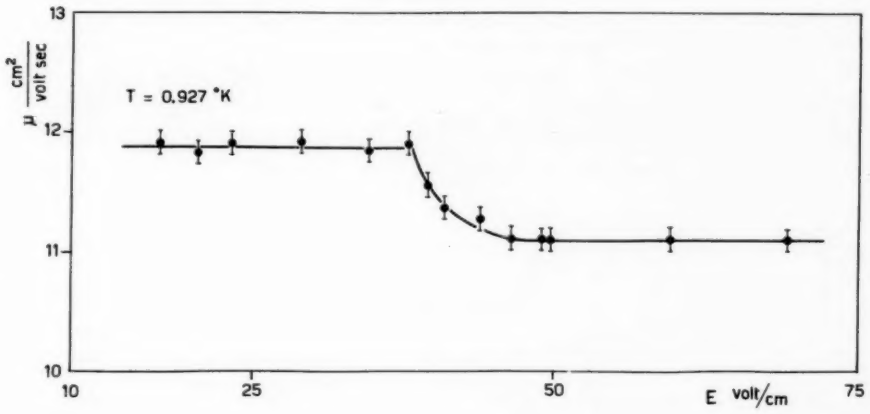

FIG. 1. Experimental values of the mobility at T=0.927°K as a function of the applied electric field E.

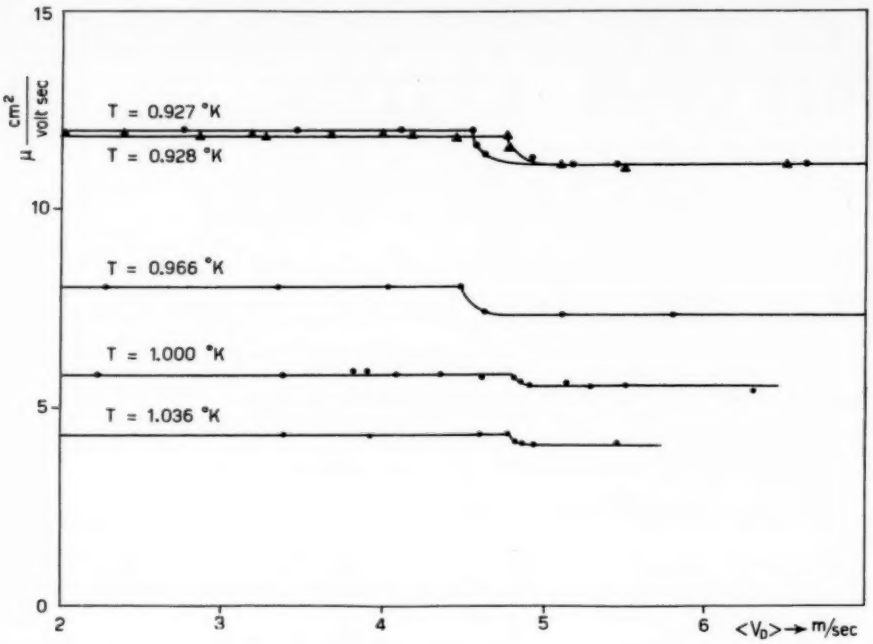

FIG. 2. Plot of the mobility versus drift velocity at different temperatures.

field of 37 v/cm the mobility is indeed field independent, but above it the mobility sharply decreases to a lower constant value. The sharp change in the mobility is well outside the experimental error, and also the discontinuity is clear from the shape of the curve around E_c.

In Fig. 2 we give the results of some runs made at different temperatures in a plot of mobility versus drift velocity, particularly convenient to show that the discontinuity always falls around the same value of the drift velocity, while the mobility changes by a factor of 3. For the sake of clarity the experimental errors in the mobility and drift velocity are not shown in this plot. In Table I we give the critical velocities so far detected under different experimental conditions. Each value of $\langle v_c \rangle$ is evaluated as the mean value of the two measured drift velocities where the break was found; the uncertainty in $\langle v_c \rangle$ indicated in the table is therefore one half of the value of this range. These values of $\langle v_c \rangle$ cluster in the range $\langle v_c \rangle = 4.70 \pm 0.15$ m/sec, indicating indeed the existence of a threshold independent of the temperature.

Table I. Observed critical velocities.

Run	T (°K)	$\langle v_c \rangle$ (m/sec)
3B	1.036	4.79 ± 0.10
3A	1.000	4.83 ± 0.10
5A	0.966	4.56 ± 0.15
4A	0.928	4.77 ± 0.10
8A	0.927	4.56 ± 0.10

In one run we were able to achieve still higher drift velocities, and a second discontinuity was observed as shown in Fig. 3. This second discontinuity appeared at a value $\langle v_c \rangle = 9.22 \pm 0.20$,

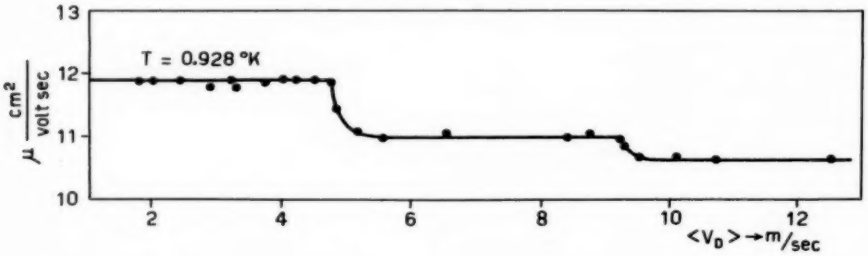

FIG. 3. A similar plot to Fig. 2 for one temperature and for an extended range of drift velocities.

which is larger than the first one by a factor of 1.96 ± 0.08, as if a repetition of this phenomenon can exist at a velocity twice as large.

The change in the mobility values at the discontinuity is never larger than 10% and therefore this phenomenon may easily escape observation in a plot of the mobility versus field when few experimental points are taken, and may then be confused with a slight and continuous field dependence. We believe this to be the reason why Reif and Meyer[2] did not notice this phenomenon at 0.98°K, where they were interested only in the zero-field mobility. It is also clear that at temperatures higher than the ones reported here it becomes progressively harder or downright impossible to detect this discontinuity. Some preliminary runs performed in this laboratory, at temperatures lower than 0.90°K, indicate that this discontinuity in the mobility is more difficult to detect there because of the superimposed continuous decrease. Reif and Meyer[2] have concentrated their work on the field dependence of the mobility essentially below this temperature, and have thoroughly investigated this continuous decrease in terms of mean-free-path phenomena. Therefore we believe our experimental work not to be in contrast with their data, but instead to provide a fine structure of the mobility versus field curve which is observable only in a narrow temperature range.

An interpretation of the meaning of the critical drift velocities detected in these experiments is not easily found in the current picture[4] of the ionic motion in liquid helium II. The sharpness of the transition and the stepwise shape of the curve rules out any approach in terms of hot ions, which is customary to explain the decrease of the mobility with the increasing field strength when the drift velocity is comparable to the thermal velocity of the ions. On the other hand, we know that these velocities are much too low to be possibly explained in terms of inelastic processes involving the creation of one roton or phonon.

As a further possibility one may suggest the same argument now used to explain the critical flow phenomena, which involves the creation of quantized vortex lines. The creation of one quantized vortex ring of atomic size behind every ion in motion would easily provide a critical velocity of the magnitude observed here, and would also give an account of the observed multiplicity in terms of different quantum numbers of circulation. However, if the Feynman[5] expression for the vortex ring energy and momentum are used, the effective mass of the ion turns out to be as large as 10^4 helium atom masses. Details of the calculation are not given here, but this figure follows simply from the energy and momentum conservation conditions.[2] Such a value of the effective mass is much larger than the estimated[6,7] static mass, and seems rather inconsistent.

One final remark should be made concerning the unexpectedly sharp onset of the drop in mobility. The only two possible explanations which suggest themselves are (1) a very sharply peaked velocity distribution due to a large effective mass of the ion, or (2) a kind of cooperative interaction with a large number of nearby ions through the long-range Coulomb forces.

The lack of a proper theoretical treatment of this problem does not allow us at the present time to come to a more definite conclusion.

Experiments are planned in this laboratory to extend these measurements over a wider range of field strengths and temperatures by an improved technique.

---

[1]S. Cunsolo, Nuovo cimento (to be published).
[2]F. Reif and L. Meyer, Phys. Rev. 119, 1164 (1960).
[3]G. Careri, F. Scaramuzzi, and J. O. Thomson, Nuovo cimento 13, 186 (1959).
[4]For a discussion on the behavior of ions in liquid helium, see also G. Careri, Progress in Low-Temperature Physics (North-Holland Publishing Company, Amsterdam, 1961), Vol. 3, p. 58.
[5]R. P. Feynman, Progress in Low-Temperature Physics (North-Holland Publishing Company, Amsterdam, 1955), Vol. 1, p. 17.
[6]K. R. Atkins, Phys. Rev. 116, 1339 (1959).
[7]J. de Boer and A. 't Hooft, Proceedings of the Seventh International Conference on Low-Temperature Physics (University of Toronto Press, Toronto, 1960), p. 510.

CALCULATED SHAPE OF THE FERMI SURFACE OF COPPER

B. Segall
General Electric Research Laboratory, Schenectady, New York
(Received July 12, 1961)

The electronic properties of copper have recently become the subject of intensive study by a wide variety of experimental methods.[1] One important result of these investigations has been the general verification of the Pippard model[2] for the Fermi surface, which is nearly spherical over the main part of the surface (called the "belly") and which is pulled out in the ⟨111⟩ directions to form eight "necks" which contact the Brillouin zone surface. It is the purpose of this Letter to note that our recently completed band-structure calculations[3] on Cu not only have led to results consistent with the Pippard model but have also predicted interesting distortions of the "belly" which have just been observed experimentally.[4] Also we will present an explanation for the distortions and will discuss the importance of this effect for the other noble metals.

The calculations were carried out by the Green's function method[5] using two different crystal potentials. The first one, which is perhaps most appropriate for the d bands, was used initially by Chodorow.[6] For the second potential, we computed the Coulomb and exchange contributions separately for the different angular momenta from renormalized Cu Hartree-Fock functions. Only the results for the latter potential, which we believe to be somewhat more realistic than the former, will be discussed here although the other results are in semiquantitative agreement with them and lead to similar conclusions about the Fermi surface.[7]

Our results[3] show that the Fermi surface associated with the calculated energy bands contacts the hexagonal zone surface and the calculated ratio of neck to belly radii is 0.22 ± 0.02 in good agreement with the experimental ratio[1,4] of about 0.20. Also, for these bands, the onset of interband optical transitions would occur for transitions between the d bands around the upper L_3 state and the Fermi surface at about 2.6 ev in fair accord with the observed 2.2-ev value.

To study the Fermi surface in more detail, we have determined the intersections of the constant energy surfaces with a (110) plane (Fig. 1). The estimated Fermi energy is -0.19 ry. Aside from the sizable region of contact with the zone surface (for $E = E_F$), the principal feature of interest in these curves is that the belly is pulled out in the ⟨100⟩ directions and is contracted in the ⟨110⟩ directions. The occurrence of these appreciable distortions is at variance with the generally held belief that the main section of the surface is very nearly spherical.

Bearing out these results are the recently reported studies of the shape of the Cu Fermi surface by Morse et al.[4] using the magnetoacoustic effect which clearly show these deviations from sphericity. It is clear from their diagram that their observed and our calculated distortions are comparable. We find $k_F(100)/k_F(110) \approx 1.09$.

The explanation for the occurrence of these distortions involves the "repulsion" of conduction band states by the relatively high-lying d-band states of the same symmetry. In Fig. 2 are shown some of the bands of interest for this discussion. Now, the calculations[3] show that the lowest conduction band state at the end of the [100] axis has the p-like symmetry X_4'. As d-band states of this symmetry cannot occur, this state is not "re-

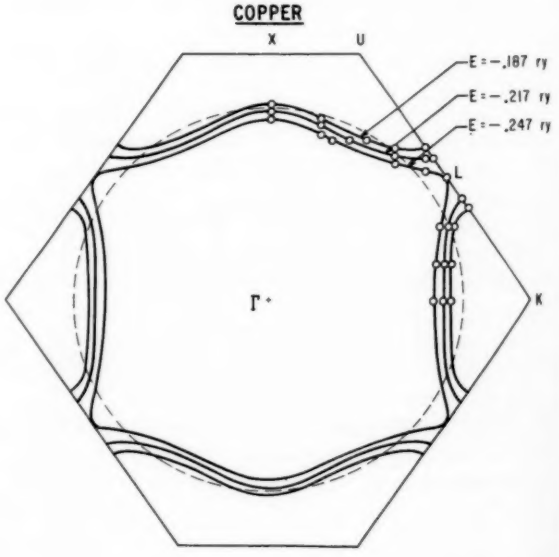

FIG. 1. The intersections of a (110) plane with calculated constant energy surfaces for Cu and with a free electron Fermi sphere (dashed curve). The estimated Fermi energy is -0.19 ry.

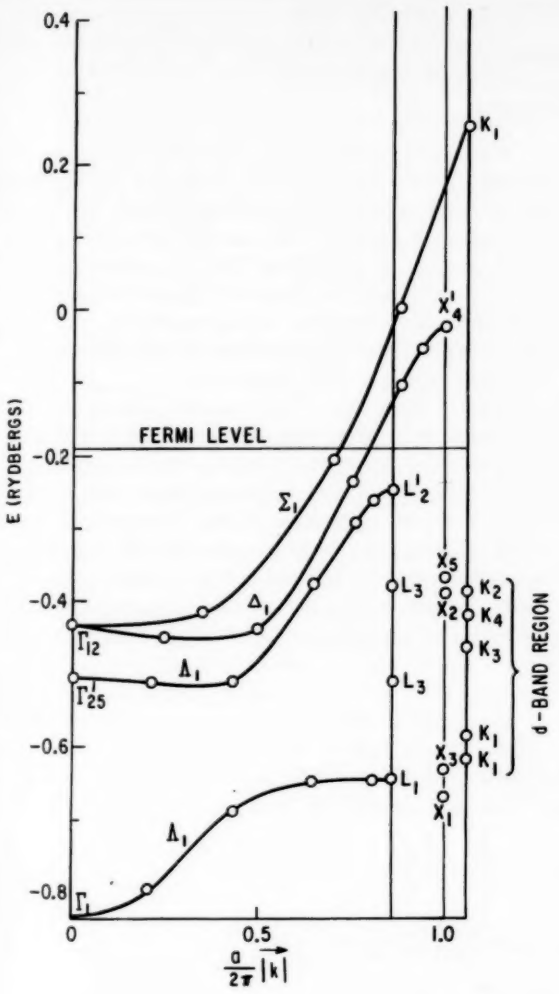

FIG. 2. The Cu energy bands in the conduction and d-band regions for the Λ_1, Δ_1, and Σ_1 states in the [111], [100], and [110] directions, respectively. For clarity, most of the calculated d-band curves were not drawn in.

pelled." Conduction band states "near" X_4' will, of course, have very small admixtures of d functions and consequently will only be affected weakly by the lower states. In the [110] direction, on the other hand, the conduction band (Σ_1 symmetry) "interacts" fully with the d band all the way out to the zone surface where it has K_1 symmetry. The argument also applies to the other noble metals as our calculations for them[8] also indicate that the lowest conduction band states at X and L are p-like. It is interesting to note that Morse et al. have also observed these distortions in Au. Inasmuch as the d bands in Ag are expected to be lower than in Cu and Au, we would predict smaller distortions in that metal.

It is thus seen that, contrary to opinions often expressed in the past about the possibility of calculating meaningful energy bands for such a metal, the calculated bands lead to a Fermi surface in good agreement with the one determined by experiment. Of course, as the many-electron effects have not been treated adequately and the electron-phonon coupling has been neglected, we cannot expect these bands to describe all the electronic properties of this metal without the introduction of corrections for these correlation effects.

The details of the calculations will be published shortly.

The author wishes to thank Miss E. L. Kreiger for her invaluable help with the numerical computations.

---

[1]This work is reviewed in The Fermi Surface, edited by W. A. Harrison and M. B. Webb (John Wiley & Sons, Inc., New York, 1960), in the articles by D. Shoenberg, p. 74; J. R. Klauder and J. E. Kunzler, p. 125; A. F. Kip, p. 146; G. E. Smith, p. 172; and R. W. Morse, p. 214.

[2]A. B. Pippard, Phil. Trans. Roy. Soc. London A250, 325 (1957).

[3]The essential results and conclusions discussed in this paper were given in B. Segall and E. L. Kreiger, Bull. Am. Phys. Soc. 6, 10 (1961), and in B. Segall, Bull. Am. Phys. Soc. 6, 231 (1961). The latter talk has been written up as General Electric Research Laboratory Report No. RL-2785G which is available upon request. Also, see B. Segall, reference 1, p. 314.

[4]R. W. Morse, A. Myers, and C. T. Walker, J. Acoust. Soc. Am. 33, 699 (1961).

[5]W. Kohn and N. Rostoker, Phys. Rev. 94, 1111 (1954), and F. S. Ham and B. Segall (to be published).

[6]M. Chodorow, thesis, Massachusetts Institute of Technology, 1939 (unpublished).

[7]More recently G. A. Burdick (private communication) has also calculated $E(\vec{k})$ for Chodorow's potential and his results agree with ours.

[8]B. Segall, Bull. Am. Phys. Soc. 6, 145 (1961); 6, 231 (1961).

TOPOLOGY OF THE FERMI SURFACE OF COPPER

Glenn A. Burdick
Massachusetts Institue of Technology, Cambridge, Massachusetts
(Received July 7, 1961)

Segall[1] has reported calculations of the Fermi surface of copper by the Green's function method of Kohn and Rostoker, using both the potential of Chodorow,[2] and other modified potentials. In this laboratory[3] we have been engaged since 1954 in programming the augmented plane wave method suggested by Slater[4] in 1937 for the digital computer, and in making calculations of energy bands by this method. The author has used these programs to compute the energy versus k for copper, for the equivalent of 2048 points in the first Brillouin zone and for the highest 6 bands which are fully or partially filled. The potential derived by Chodorow for d electrons was used in the computations, which were done on an IBM-709 computer at the M.I.T. Computation Center.

The purpose of this report is to point out that we are in agreement with the results of Segall, namely, that there is very close agreement between the Fermi surface for copper as proposed by Pippard[5] and the one as theoretically computed by the author. The major features of this surface are the "necks" which project out from the "belly" region in the ⟨111⟩ directions and intersect the Brillouin zone edge at the center of the hexagonal faces. The author also finds a slight bulge (in the form of an "egghead") in the ⟨100⟩ directions.

Figure 1 shows the Fermi surface cross section as formed by a plane passing through the origin and bisecting two opposite sides of a hexagonal face. Several neighboring zones have been drawn to facilitate the definition of characteristic dimensions of the surface. The experimental values for the dimensions as defined in Fig. 1 were obtained from ultrasonic attenuation experiments[6] and are listed along with the author's theoretical values in

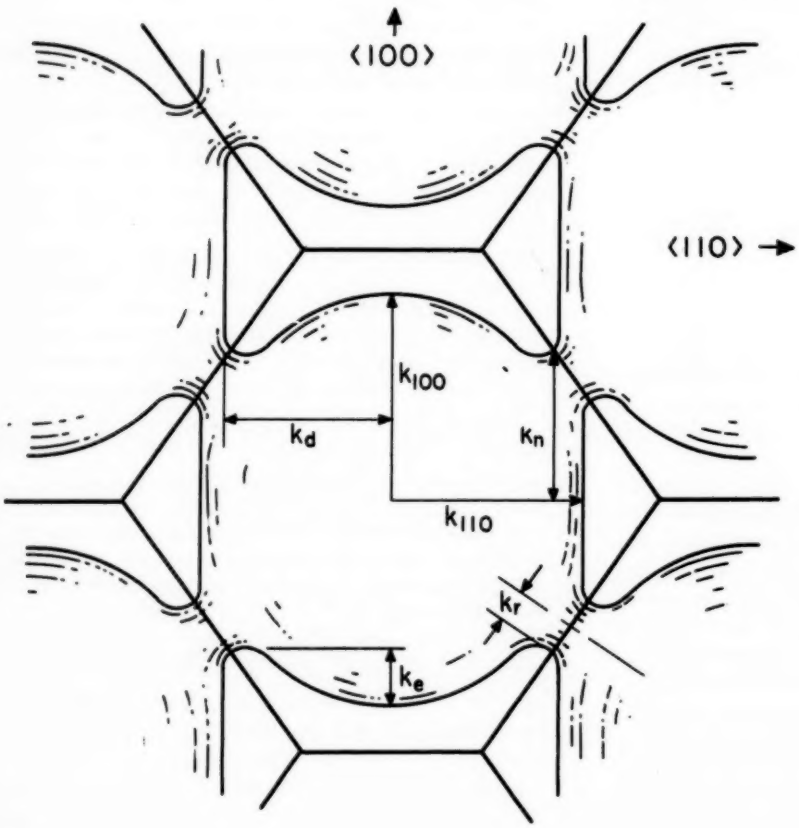

FIG. 1. The ⟨110⟩ cross section for the Fermi surface of copper.

Table I. Experimental values[a] for the dimensions as defined in Fig. 1. For comparison, the radius of the sphere having one-half the volume of the Brillouin zone is $k_S = 1.44$.

	Morse	Burdick
k_{100}	1.41	1.51 ± 0.03
k_{110}	1.38	1.39 ± 0.03
k_d	1.22	1.21 ± 0.03
k_n	1.10	1.11 ± 0.02
k_e	0.32	0.44 ± 0.06
k_γ	0.24	0.24 ± 0.03; 0.22 ± 0.06

[a]All values are to be multiplied by the factor 10^{-19}.

Table I. The possible computational errors are as indicated but the author has no information concerning the possible experimental errors. The dimensions are given in cgs momentum units. The two theoretical values listed for k_γ correspond to the "neck" radius as computed along a line passing through the center of the hexagonal face and one corner and along a line passing through the center and the midpoint of one edge, respectively. As can be seen from an examination of Table I, the only difference in topology is that the author's "belly" region in the plane of the figure is slightly more egg-shaped than the experimental model indicates. However, even this difference is a slight one.

As those who heard the two talks of Segall before the American Physical Society (referred to above) will realize, these results agree closely with his, thereby giving important verification of the fact that energy bands as computed by different methods can agree with each other and with experiment to a greater extent than has been generally realized.

The details of the computations, the density-of-states curve, and a discussion of the energy band structure will be published at a later date.

[1]B. Segall and E. L. Kreiger, Bull. Am. Phys. Soc. 6, 10 (1961); B. Segall, Bull. Am. Phys. Soc. 6, 231 (1961). We are greatly indebted to Dr. Segall for private communication of many of his results.

[2]M. I. Chodorow, Ph.D. thesis, Massachusetts Institute of Technology, 1939 (unpublished).

[3]Quarterly Progress Reports, Solid-State and Molecular Theory Group, April 15, 1954 to date (unpublished), contributions from D. J. Howarth, M. M. Saffren, J. H. Wood, and others.

[4]J. C. Slater, Phys. Rev. 51, 846 (1937).

[5]A. B. Pippard, Phil. Trans. Roy. Soc. London A250, 325 (1957).

[6]Robert W. Morse, in The Fermi Surface of Metals, edited by W. A. Harrison and M. B. Webb (John Wiley & Sons, Inc., New York, 1960), p. 214 ff.

CALCULATION OF THE CRYSTAL FIELD SPLITTING

R. G. Shulman and S. Sugano
Bell Telephone Laboratories, Murray Hill, New Jersey

(Received July 21, 1961)

By starting with wave functions determined by nuclear magnetic resonance measurements[1] in $KNiF_3$, we have been able to calculate a value for the cubic crystal field splitting which is in good agreement with the observed value. The cubic crystal field splitting, $10Dq$, is the energy separation between the orbital triplet t_{2g} and the e_g doublet which arise from the d levels split by a cubic field. Measured values of $10Dq$ have been used with considerable success to explain optical and magnetic properties. However, it has not yet been possible to calculate a value which agrees with experiment. We follow the method of Tanabe and Sugano,[2] the main difference being the use of molecular orbitals with Hartree-Fock atomic functions as our basis set. We define

$$10Dq \equiv E(t_2^5 e^3\,{}^3T_2) - E(t_2^6 e^2\,{}^3A_2) = (\Psi_e|h|\Psi_e) - (\Psi_t|h|\Psi_t), \quad (1)$$

in which the wave functions are assumed to be

$$\Psi_e = N_e^{-1/2}[\Phi_e - \lambda_e \psi_e], \quad (2)$$

$$\Psi_t = N_t^{-1/2}[\Phi_t - \lambda_t \psi_t]. \quad (3)$$

In these expressions Φ_e and Φ_t (subscript t is abbreviation for t_2) may be the Ni^{++} $3d_{x^2-y^2}$ and $3d_{xy}$ functions, respectively, with Watson's Hartree-Fock radial functions.[3] Furthermore, $\Psi_e = \mu_{\sigma e}\chi_\sigma + \mu_{se}\chi_s$ and $\mu_{\sigma e}^2 + \mu_{se}^2 = 1$ while χ_σ, χ_s,

Table I. Values of the matrix elements listed in the first column are shown in the second in atomic units. In the third column the contributions to $10Dq$ from the differences between the e_g and t_{2g} energies are listed in cm^{-1}. The calculated value of 5270 cm^{-1} agrees fairly well with the experimental[a] value of 7250 cm^{-1}.

Matrix element	Value (a.u.)	Contribution to $10Dq$ (cm^{-1})
$(\Phi_e\|h\|\Phi_e)$	+0.1201	-3580
$(\Phi_t\|h\|\Phi_t)$	+0.1364	
$(\Phi_e\|h\|\Psi_e)$	-0.1510	+16 320
$(\Phi_t\|h\|\Psi_t)$	-0.0559	
$(\Psi_e\|h\|\Psi_e)$	-0.3300	-7470
$(\Psi_t\|h\|\Psi_t)$	-0.0847	
Calculated $10Dq$		+5270
Observed $10Dq$		+7250[a]

[a]K. Knox, R. G. Shulman, and S. Sugano, Bull. Am. Phys. Soc. 5, 415 (1960).

and $\chi_t = \psi_t$ are the normalized appropriate linear combinations of fluoride ion $2p_\sigma$, $2s$, and $2p_\pi$ orbitals, respectively. The fluoride ion $2s$ and $2p$ atomic orbitals were Froese's Hartree-Fock functions.[4] The fluorine $1s$ functions were shrunk into the nuclei. The augmentation parameters for Ψ_e of $\lambda_e\mu_{\sigma e} \equiv \lambda_\sigma$ and $\lambda_e\mu_{se} \equiv \lambda_s$ were determined from the nuclear magnetic resonance measurements[1] of the F^{19} nucleus in a single crystal of $KNiF_3$. The values[5] were $(\lambda_e\mu_{\sigma e})^2 = 3\times0.0369$ and $(\lambda_e\mu_{se})^2 = 3\times0.00451$.

The first order Hartree-Fock Hamiltonian employed in (1) is

$$h = -\tfrac{1}{2}\Delta + V_M + V_L, \tag{4}$$

in which Δ is the kinetic energy operator and V_M is the Coulomb and exchange potential of all the Ni^{++} electrons and nucleus. The contribution of the ligands is

$$V_L = V_L^{\,0} + V_L^{\,K} + V_L^{\,E}, \tag{5}$$

in which

$$V_L^{\,0} = \sum_{i=1}^{6} \frac{1}{|r - R_i|}$$

is the point-charge potential of six ligands centered at R_i;

$$V_L^{\,K} = \sum_{i=1}^{6} -\frac{8}{|r - R_i|} + \int d\tau_2 r_{12}^{-1} \sum_{k=2s,\,2p} |\Phi_{ik}(2)|^2$$

is Kleiner's correction[6] of the point-charge potential which arises from the imperfect screening of the fluorine nuclei by their electrons whose atomic orbitals are Φ_{ik}; finally

$$V_L^{\,E} = -\sum_{i=1}^{6} \int d\tau_2 r_{12}^{-1} \sum_{k=2s,\,2p} \Phi_{ik}^*(2)\Phi_{ik}(1)P_{12}$$

is the exchange interaction introduced in the previous paper,[2] where P_{12} is the permutation operator of electrons 1 and 2. All the two-center integrals were calculated on an IBM-7090 with Switendick and Corbató's program.[7] The results are presented in Table I.

Table II. Separate contributions to the nickel diagonal terms of the components of V_L.

	$V_L^{\,0}$	$V_L^{\,K}$	$V_L^{\,E}$
$(\Phi_e\|V_L\|\Phi_e)$	1.58687	-0.03017	-0.02396
$(\Phi_t\|V_L\|\Phi_t)$	1.58055	-0.02069	-0.01082
Difference	0.00632	-0.00948	-0.01314

The nickel diagonal term makes a negative contribution to $10Dq$. This term represents the approximation in which the effects of the ligands are treated as perturbations upon the nickel ion energy levels. The separate contributions to this term of $V_L^{\,0}$, $V_L^{\,K}$, and $V_L^{\,E}$ are shown in Table II. Although the individual exchange terms are small, they make a larger contribution than the total Coulomb interaction because of the cancellation[8] of the contributions from $V_L^{\,0}$ and $V_L^{\,K}$ which allows the difference between exchange terms for e and t_2 to dominate. In Table II, the difference between N_t and N_e is not taken into account because its effect is negligible.

In order to calculate the contributions of the transfer integral and fluorine diagonal terms to $10Dq$, it is necessary to know the value of λ_t since the nuclear magnetic resonance measurements only determine λ_σ and λ_s. λ_t may be determined nonempirically by minimizing the corresponding bonding orbital energy. Such a nonempirical method can be also applied to the determination of λ_σ and λ_s, and a comparison between their calculated and observed values would be very interesting.

In the present calculation, however, we employed the following method in order to avoid the tedious calculation of important three-center integrals of the type $(\Phi_{3d}|V_{jL}|\Phi_{ik})$ appearing in the transfer integrals; a three-center integral

for the e orbital was determined so that the observed λ_e minimizes the e bonding orbital energy. Then, using the calculated overlap integrals to relate the three-center integral for the t_2 orbital to that for the e orbital, λ_t was determined by minimizing the energy, with the result that $\lambda_t = 0.286$. The large value of λ_t is consistent with our previous findings.[1] Furthermore, the values of the three-center integrals thus determined were found to be reasonable. The three-center integrals are being evaluated independently so that we will be able to compare calculated and observed values of λ_σ and λ_S. However, the reasonable values derived for the three-center integrals in the above-mentioned procedure confirm the observed values of λ_σ and λ_S. It is interesting to observe that the $V_L{}^E$ term makes an important contribution to the $10Dq$ in the transfer integral also.

In all energy determinations we have assumed a potential well model in which the $NiF_6{}^{-4}$ complex is located in a constant potential arising from the rest of the crystal. This model can be proven to be a good approximation. It also explains the observation that the cubic field parameter is insensitive to distant ions beyond the ligands. All of these assumptions, calculations, and additional refinements will be discussed more fully in future publications.

In conclusion we can say:

(1) The traditional concept of the cubic crystal field should be changed: The nickel diagonal term gives a negative contribution to the crystal field splitting. Its contribution comes mainly from the exchange interaction between d electrons and ligand electrons. The transfer integral term is the only term which makes a positive contribution to $10Dq$. Roughly speaking, this contribution is reduced by a factor of ~50% by the negative contribution of the fluorine diagonal term. Although this relation is found in our specific problem numerically, it is generally applicable. This will be discussed in the future.

(2) The molecular orbital model is successful in explaining both the nuclear magnetic resonance experiments and the cubic crystal field parameter in a consistent way. The value of $10Dq$ calculated from this model is 5300 cm^{-1}, in reasonable agreement with the observed value of 7250 cm^{-1}.

It is a pleasure to thank A. C. Switendick, Mrs. W. Mammel, and R. Kornegay for help in the machine calculation and L. C. Allen for an important suggestion.

---

[1] R. G. Shulman and K. Knox, Phys. Rev. Letters 4, 603 (1960).

[2] Y. Tanabe and S. Sugano, J. Phys. Soc. Japan 11, 864 (1956).

[3] R. E. Watson, Phys. Rev. 118, 1036 (1960).

[4] C. Froese, Proc. Cambridge Phil. Soc. 53, 206 (1957).

[5] These values are lower than the values previously reported of 3×0.049 and 3×0.0050, respectively, because we have included accurate values of the susceptibility which are now available and which is responsible for 70% of the change. Also, we have included two contributions by Marshall to the determination of the hyperfine interaction which correct for the nonspherical nature of the Ni^{++} ions.

[6] W. H. Kleiner, J. Chem. Phys. 20, 1784 (1952).

[7] A. C. Switendick and F. J. Corbató, Quarterly Progress Report, October 15, 1959, Solid-State and Molecular Theory Group, Massachusetts Institute of Technology, Cambridge, Massachusetts (unpublished).

[8] A. J. Freeman and R. E. Watson, Phys. Rev. 120, 1254 (1960), have calculated $V_L{}^0$ and $V_L{}^K$ in $Cr(H_2O)_6{}^{+3}$ with Hartree-Fock functions and have shown their combined effect to be very small.

FERROMAGNETIC INTERACTION IN EuO

B. T. Matthias and R. M. Bozorth*
Bell Telephone Laboratories, Murray Hill, New Jersey

and

J. H. Van Vleck
Harvard University, Cambridge, Massachusetts
(Received August 3, 1961)

We have found that a europium oxide of the formula EuO becomes truly ferromagnetic at 77°K with a saturation moment of close to 7 Bohr magnetons. This is thus the first rare earth oxide to be found to become ferromagnetic, and with the exception of CrO_2 the only oxide to our knowledge that has true ferromagnetic coupling.

We were led to this discovery by somewhat contradictory results on ferromagnetic intermetallic rare earth compounds.[1] There it was found that $EuIr_2$ becomes ferromagnetic near 70°K and has an extremely small saturation moment. It was clear from measurements of lattice constants of this cubic compound that europium had a $4f^6$ configuration corresponding to trivalent europium and so would not be expected to have a ferromagnetic moment.[2] A compound having a Curie point of 70°K and very small moment seemed to be a severe contradiction. One possible explanation was the presence of an impurity strongly ferromagnetic below 70°K. $EuIr_2$ had been formed in a quartz tube by having molten europium react with finely divided iridium powder, and the presence of oxides was thus a likely possibility. The magnetic behavior of Eu_2O_3 is known and normal. EuO was the other alternative.

The latter compound was formed by reacting stoichiometric amounts of Eu and Eu_2O_3 at 1220°C in a quartz tube. The product was a brown crystalline powder. X-ray examination by Mrs. V. B. Compton showed it to have a NaCl structure with a lattice constant of 5.141 A, corresponding to a density of 8.21. A few unidentified faint lines were present on the x-ray film. This lattice constant agrees with that previously reported for material obtained by the reduction of Eu_2O_3 with lanthanum metal.[3]

The existence of strong ferromagnetism in EuO, and a Curie point (77°) very near to that observed for $EuIr_2$ (70°) shows immediately that the presence of a few percent of EuO might easily give rise to the anomalous results obtained with $EuIr_2$.

As shown in Fig. 1, above the Curie point the susceptibility of EuO is represented within the experimental error by a formula of the type $\chi = C/(T-\theta)$, where the Curie constant C has the value $7.9N\beta^2/3k$ to be expected for an ^8S configuration. This fact shows unequivocally that the europium ion is divalent and isoelectronic with Gd^{+++} as one would expect from the degree of oxidation. The linearity of $1/\chi$ in T is, if anything, more accurate than one would expect, for the Weiss-Curie law is always but an approximation theoretically.

Figure 2 shows the data for the ferromagnetic region. The saturation at 0°K, determined by extrapolation linear in $1/H$, is 6.9 Bohr magnetons, and within the limits of error is equal to the theoretical $Jg = 7$. The broken line is that calculated for spontaneous magnetization using the Brillouin function for $J = 7/2$ with the parameter $a = (7/3) \times (M/M_0)/(T/\theta)$. At low temperatures the triangular points are obtained by extrapolation (using $1/H$) of the smoothed data for $H = 8$ and 12 koe at selected temperatures. Just below the Curie point (obtained by the Weiss-Forrer method, W.F. in the figure) the extrapolation is to $H = 0$, on the as-

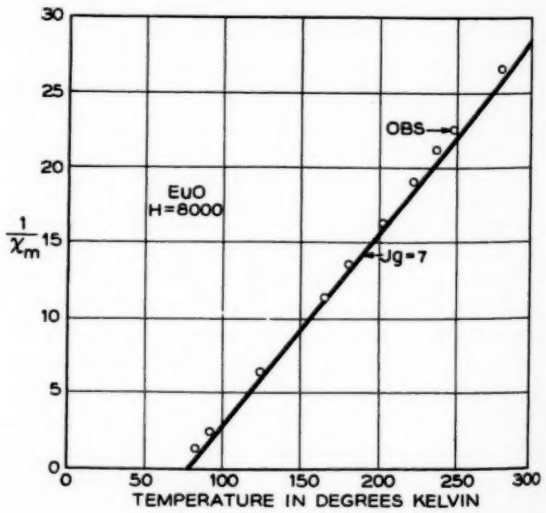

FIG. 1. Reciprocal molecular susceptibility of EuO: experimental points, and theoretical line drawn through ferromagnetic Curie point (77°K) with slope for $Jg = 7$, $\mu_{eff} = 7.94$.

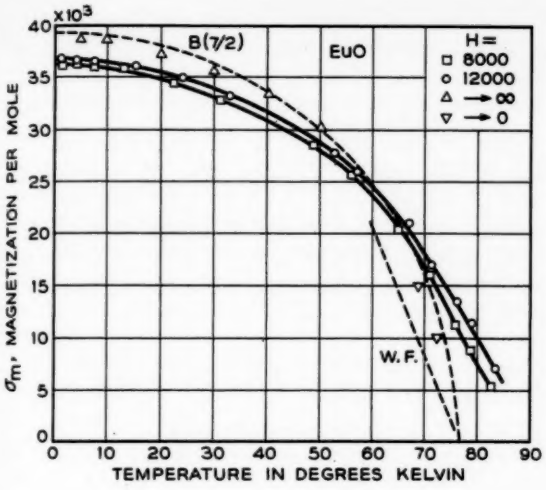

FIG. 2. Magnetization of EuO vs temperature in ferromagnetic region. Broken line, Brillouin curve for $J=\frac{7}{2}$, $\theta=77°$. Triangles, extrapolation of experimental data to $H=\infty$ (high M) or $H=0$ (low M). W.F., Weiss-Forrer extrapolation $(\sigma_m)_{H=0}$ vs T, to determine the Curie point.

sumption that here the crystal anisotropy is zero and the applied field increases the magnetization above the spontaneous value.

At low temperatures the magnetic moment per unit volume, based on 7β and a density of 8.25, is high:

$$4\pi M = 24\,100.$$

This may be compared with the values of $4\pi M$ for iron (21 700), gadolinium (about 25 000), and for metallic dysprosium[4] (about 38 000).

Measurement of the pressed powder on a megohm meter indicated a resistivity of 10^9 to 10^{10} ohms.

The measurements are of interest as furnishing one of the clearest examples of exchange interaction in a material in which the atomic orbitals are substantially the same as for the free ions, since this is always the case for $4f$ electrons in the middle of the rare earth period in nonconducting compounds.

We will not attempt to enter into the question of the precise mechanism responsible for the ferromagnetic exchange coupling. It is certainly not the Yosida mechanism resulting from the polarization of conduction electrons, since EuO is an insulator. Conceivably, direct overlap may be the cause, but in our opinion indirect exchange via excited states is more likely.

We are grateful to Mrs. V. B. Compton for permission to quote the results of her x-ray measurements on $EuIr_2$ and EuO.

---

* Present address: Tokyo University, Tokyo, Japan.

[1]R. M. Bozorth, B. T. Matthias, H. Suhl, E. Corenzwit, and D. D. Davis, Phys. Rev. 115, 1595 (1959).

[2]J. H. Van Vleck, Magnetic and Electric Susceptibilities (Cambridge University Press, New York, 1936).

[3]H. A. Eick, N. C. Baenziger, and L. Eyring, J. Am. Chem. Soc. 78, 5147 (1956).

[4]D. R. Behrendt, S. Legvold, and F. H. Spedding, Phys. Rev. 109, 1544 (1958).

QUANTIZATION OF FLUX IN A SUPERCONDUCTING CYLINDER

John Bardeen
University of Illinois, Urbana, Illinois
(Received July 31, 1961)

Recent experiments of Deaver and Fairbank[1] and of Doll and Näbauer[2] have shown that the flux in a superconducting cylindrical tube is quantized. That the flux should be quantized in units of hc/e was originally suggested by London[3]; the experiments indicate units of about half this amount. Onsager[4] predicted such a result on the basis that an effective charge $e^* = -2e$, representing that of a pair, should be used. We shall show that in tubes of very small diameter and with wall thickness of the order of the penetration depth the unit may depend on dimensions and be somewhat smaller than $hc/2e$.

The theory has been discussed by Byers and Yang,[5] who showed that it is essential to take into account the statistical distribution of quasi-particle excitations, and that one could expect a flux quantum of $hc/2e$ on the basis of the microscopic theory. They considered, as we shall do here, states with current flow which exist with nonintegral values of flux.

We shall use the Gor'kov version[6] of the Ginzburg-Landau (G-L) theory[7] to discuss the effect. By use of the method of "thermal" Green's functions, Gor'kov showed that the G-L equations, originally given on a phenomenological basis, may be derived from the microscopic theory provided that the temperature is sufficiently close to T_c so that the local London equations are valid for the electrodynamics. The only difference from the original version is that an effective charge $e^* = -2e$, evidently that of a pair, appears in place of $-e$. Since in the experiments, the flux is frozen in as the specimen is cooled below T_c, the theory is valid in the significant temperature range.

Gor'kov showed that the effective wave function, $\Psi(\vec{r})$, of the G-L theory may be taken to be proportional to the local value of the energy gap. We shall take a different normalization for Ψ than that used by Gor'kov, one that is closer to the original G-L theory. We shall define it so that Ψ_0, the equilibrium value of Ψ, is such that $|\Psi_0|^2 = \rho_s/\rho$, where ρ_s is the density of superconducting electrons of the two-fluid model and $\rho = Nm$, the total density. The Schrödinger-like equation for Ψ may then be written

$$-\frac{h^2}{8\pi^2 m^*}\left(\frac{\partial}{\partial \vec{r}} - \frac{2\pi i e^*}{hc}A(\vec{r})\right)^2\Psi - \alpha\Psi + \beta|\Psi|^2\Psi = 0, \quad (1)$$

where $m^* = 2m$ and $e^* = -2e$, representing the charge and mass of a bound pair. This equation then corresponds to that of the center-of-mass motion of the pair. The free-energy difference between superconducting and normal states is given by integrating over space and multiplying by $N/2$, the number of pairs at $T = 0°\mathrm{K}$:

$$F_s - F_n = \frac{N}{2}\int\left\{-\frac{h^2}{8\pi^2 m^*}\Psi^*\left(\frac{\partial}{\partial \vec{r}} - \frac{2\pi i e^*}{hc}A(\vec{r})\right)^2\Psi - \alpha|\Psi|^2 + \tfrac{1}{2}\beta|\Psi|^4\right\}d\tau. \quad (2)$$

The density of mass flow is

$$J = \frac{N}{2}\left\{-\frac{ih}{4\pi}\left[\Psi^*\frac{\partial\Psi}{\partial \vec{r}} - \Psi\frac{\partial\Psi^*}{\partial \vec{r}}\right] - \frac{e^*}{c}|\Psi|^2 A(\vec{r})\right\}. \quad (3)$$

In the absence of fields and currents, the free-energy minimum, for $|\Psi_0|^2 = \alpha/\beta = \rho_s/\rho$, is $F_s - F_n = -H_c^2/8\pi = -N\alpha^2/(4\beta)$, where $H_c(T)$ is the critical field for bulk material.

Gor'kov derived the values of α and β from the microscopic theory.[8] They can be expressed in terms of H_c and the penetration depth, $\lambda(T)$. Since $\rho_s/\rho = \lambda_L^2/\lambda^2$, where $\lambda_L^2 = mc^2/(4\pi e^2 N)^{1/2}$ is the London penetration depth, we have

$$\alpha = H_c^2\lambda^2/(2\pi N\lambda_L^2); \quad \beta = H_c^2\lambda^4/(2\pi N\lambda_L^4). \quad (4)$$

These apply whether or not elastic scattering by impurities or other imperfections is important provided that the appropriate value for the penetration depth is used. Limiting expressions[8,9] valid near T_c are

$$\lambda_L^2/\lambda^2 = 2(1-t), \quad l \gg \xi_0; \quad (5)$$

$$\lambda_L^2/\lambda^2 = 2.73(1-t)(l/\xi_0), \quad l \ll \xi_0; \quad (6)$$

where $t = T/T_c$, l is the mean free path, and ξ_0 is the coherence distance. The limit $l \ll \xi_0$ applies to thin films.

In the absence of a magnetic field, a wave function $\Psi = \Psi_0 e^{i\vec{q}\cdot\vec{r}}$ corresponds to a momentum $m^* v_s = \hbar q/2\pi$ where v_s is the velocity of the center of mass. The net current is $\rho_s v_s$ and the increase in free energy $\frac{1}{2}\rho_s v_s^2$, in accordance with the two-fluid model.[10] A superconductor is characterized by a value of ρ_s different from zero.

To discuss the quantization of flux, we shall suppose that the specimen is in the form of a thin film of thickness $d \leq 2\lambda$ on the surface of a cylindrical tube of radius r and circumference $L = 2\pi r$. The current density will then be substantially uniform across the film. One may simplify the mathematics by taking x to be a linear coordinate measuring distance around the circumference and require periodic boundary conditions, $\Psi(x+L) = \Psi(x)$. If Φ is the flux through the tube, the vector potential A_x is a constant equal to Φ/L.

An appropriate periodic solution of the G-L equation is[3]

$$\Psi = \exp[2\pi i n x/L]\Psi_0, \tag{7}$$

where n is an integer. For an arbitrary flux Φ one may choose n so that the residual wave vector

$$q = (2\pi/L)(n - e^*\Phi/hc) \tag{8}$$

is in the interval $-\pi/L < q < \pi/L$. The velocity $v_S = hq/(2\pi m^*)$ and the free-energy increase will then be as small as possible.

The electric current density, $I = e^*\rho_S v_S/m^*$, is quite large even for small values of q. A value $q = \pi/L$, with $L \sim 1$ cm, gives $v_S \sim 1$ cm/sec and a current density $I \sim 10^3\, \rho_S/\rho$ amp/cm^2 in a typical metal. Generally a much smaller current density is required to produce a unit of flux, so that it is favorable to minimize the free energy by reducing q and thus v_S to nearly zero. There will then be very nearly an integral number of flux units in the cylinder. Values of q corresponding to odd multiples of π/L would also give zero current (with a different pairing condition), but with a free-energy maximum rather than a minimum.[5]

Appreciable values of q which would give non-integral units of flux can be expected only if the thickness of the film and the radius of the cylinder are very small. When the external field is removed, the flux is produced entirely by the current flowing in the film, so that

$$\Phi = 4\pi^2 r^2 I d/c. \tag{9}$$

Setting $I = e^*\rho_S hq/(8\pi m^2)$, we may solve for q and find

$$q = 2\lambda^2 e^*\Phi/(r^2 dhc), \tag{10}$$

where $\lambda^2 = m^2c^2/(4\pi e^2\rho_S)$. Substituting in (8) and solving for Φ, we find

$$\Phi = (nhc/2e)(1 + 2\lambda^2/rd)^{-1}. \tag{11}$$

Thus we find that for tubes of very small radius, the flux quantum may be appreciably less than $hc/2e$. It is possible that the value of $0.4\,hc/e$ observed by Doll and Näbauer may be accounted for in this way. The lead tube which they used had a diameter of only 0.01 mm and λ may have been abnormally large because of scattering in the film. It should be noted that λ and thus the unit of flux may change with temperature.

This work was done at the Summer Institute for Theoretical Physics, University of Wisconsin, sponsored by the National Science Foundation. The author is indebted to E. Wigner, R. G. Sachs, and other members of the Institute for informative discussions.

---

[1]B. S. Deaver, Jr., and W. M. Fairbank, Phys. Rev. Letters 7, 43 (1961).

[2]R. Doll and M. Näbauer, Phys. Rev. Letters 7, 51 (1961).

[3]F. London, Superfluids (John Wiley & Sons, New York, 1950), p. 152.

[4]L. Onsager (private communication); Phys. Rev. Letters 7, 50 (1961).

[5]N. Byers and C. N. Yang, Phys. Rev. Letters 7, 46 (1961).

[6]L. P. Gor'kov, J. Exptl. Theoret. Phys. (U.S.S.R.) 36, 1918 (1959); 37, 833 (1960) [translations: Soviet Phys. – JETP 9, 1364 (1959); 10, 593 (1960)].

[7]V. L. Ginzburg and L. D. Landau, J. Exptl. Theoret. Phys. (U.S.S.R.) 20, 1064 (1950).

[8]J. Bardeen, L. N. Cooper, and J. R. Schrieffer, Phys. Rev. 108, 1175 (1957).

[9]P. B. Miller, Phys. Rev. 113, 1209 (1959).

[10]J. Bardeen, Phys. Rev. Letters 1, 399 (1959). It is mainly the two-fluid model, valid for all temperatures, which is required for the present discussion.

QUANTIZATION OF THE FLUXOID IN SUPERCONDUCTIVITY

J. B. Keller and B. Zumino
New York University, New York, New York
(Received August 16, 1961)

It was predicted by London[1] that the magnetic fluxoid in a superconductor should be quantized in units of $2\pi\hbar c/e$. On the basis of the electron pair idea of Schafroth[2] and Cooper,[3] Onsager[4] suggested that the quantum unit should be half that of London, since the charge of a pair is twice the charge of the electron. Onsager's prediction was confirmed in recent experiments of Deaver and Fairbank[5] and of Doll and Näbauer[6] on superconducting cylindrical tubes. Theoretical discussions of the phenomenon have been given by Byers and Yang,[7] Blatt,[8] and Bardeen.[9] Bardeen showed that the quantum of flux is smaller than the natural unit $\pi\hbar c/e$ for a tube thinner than the penetration depth.

It is our purpose to show that in a superconductor the fluxoid is always quantized in multiples of the natural unit even though the flux may be quantized in smaller units. Our demonstration is based upon the assumption that there exists an effective wave function Ψ for electron pairs. We also assume that $|\Psi|^2$ is the number density of pairs and that the supercurrent density $\vec{J}$ is given by the usual quantum mechanical formula

$$\vec{J}=\frac{-ie\hbar}{2m}(\Psi^*\nabla\Psi-\Psi\nabla\Psi^*)-\frac{2e^2}{mc}|\Psi|^2\vec{A}. \tag{1}$$

Here $\vec{A}$ is the vector potential and we have used the fact that the charge and mass of a pair are twice those of an electron. These assumptions have been verified by Gor'kov[10] in his derivation of the Ginzburg-Landau[11] semiphenomenological theory from the microscopic theory of Bardeen, Cooper, and Schrieffer.[12]

Following London, we define the fluxoid Φ_C through a closed curve C by the equation

$$\Phi_C=\int_C(\vec{A}+c\Lambda\vec{J})\cdot d\vec{s}, \tag{2}$$

where

$$\Lambda=m/(2e^2|\Psi|^2). \tag{3}$$

From Eq. (1) it follows that

$$\vec{A}+c\Lambda\vec{J}=-(i\hbar c/4e)\nabla\ln(\Psi/\Psi^*). \tag{4}$$

Then Eq. (2) becomes

$$\Phi_C=-(i\hbar c/4e)[\ln(\Psi/\Psi^*)]. \tag{5}$$

In Eq. (5), square brackets denote the change in the enclosed quantity upon traversing C once. From Eqs. (4) and (5) it follows that Φ_C has the same value for any two curves which can be deformed into each other without leaving the superconductor. Therefore Φ_C vanishes for a curve which can be shrunk to a point. For a curve which cannot be shrunk to a point because it encircles a hole in the superconductor, we write $\Psi=ae^{iS}$, where a and S are real; then $\ln(\Psi/\Psi^*)=2iS$. Since Ψ must be single valued, S can change only by $2\pi n$ where n is an integer, so Eq. (5) yields

$$\Phi_C=n(\pi\hbar c/e). \tag{6}$$

This is the result we sought. It is a characteristic feature of superconductors which distinguishes them from normal conductors even when they are pervaded by magnetic fields, as is the case for specimens which are thin compared to the penetration depth λ. From (6) it follows that the fluxoid remains constant in time in the superconducting state, since it must change continuously and n is an integer. When $\vec{J}=0$ along C, Eq. (2) shows that Φ_C is just the magnetic flux through C. Then the flux itself is a multiple of the natural unit. This is the fact which was verified experimentally.

Bardeen's result can be deduced easily from Eq. (6) by considering a thin cylindrical tube of radius r and thickness $d\leq\lambda$. We assume that the current $\vec{J}$ is constant throughout the tube and in the circumferential direction and that the density $|\Psi|^2$ is also constant. Then the total current per unit length of tube is $d|\vec{J}|$ and it produces a flux $\Phi=4\pi^2r^2d|\vec{J}|/c$ through the hole. The line integral of $\vec{A}$ in Eq. (2) is just Φ if C is a circle of radius r concentric with the axis, so Eqs. (2) and (6) yield

$$\Phi+2\pi rc\Lambda|\vec{J}|=n(\pi\hbar c/e). \tag{7}$$

Upon introducing the penetration depth $\lambda=(mc^2/8\pi e^2|\Psi|^2)^{1/2}$ and eliminating $|\vec{J}|$ in terms of Φ, we obtain from Eq. (7)

$$\Phi=n\frac{\pi\hbar c}{e}\left(1+\frac{2\lambda^2}{rd}\right)^{-1}. \tag{8}$$

This is just Bardeen's result. Our derivation shows that an experimental verification of Eq. (8) would verify the quantization of the fluxoid in natural units. The penetration depth λ becomes in-

finite as the temperature T approaches the critical temperature T_c from below. Therefore when T is sufficiently near T_c and d is finite, λ is much greater than d and so Eq. (8) applies. This shows that the unit of flux quantization tends to zero as T tends to T_c. Since $|\vec{J}|$ is proportional to Φ it also tends to zero and so does the density $|\Psi|^2$. However, the ratio $|\vec{J}|/|\Psi|^2$, which occurs in the fluxoid, tends to $ne\hbar/mr$.

When the tube is not thin compared to λ, we have obtained the quantum of flux through the hole as well as the magnetic field as a function of radial distance from the axis by solving Maxwell's equations for $\vec{A}$ with $\vec{J}$ given by Eq. (1). By using these results we have computed the Ginzburg-Landau expression for the free energy of the equilibrium states. It is the sum of a surface energy proportional to n^2 and the free energy in the absence of a magnetic field, which is independent of the quantum number n. When n is small and the tube is thick compared to λ, the surface energy is negligible. In any case these equilibrium values must be interpreted as local minima with respect to small deviations from equilibrium.

We wish to thank Professor C. N. Yang for a stimulating discussion of his microscopic theory.

[1]F. London, Superfluids (John Wiley & Sons, Inc., New York, 1950), Vol. 1, p. 152.
[2]M. R. Schafroth, Phys. Rev. 96, 1149, 1442 (1954).
[3]L. N. Cooper, Phys. Rev. 104, 1189 (1956).
[4]L. Onsager (private communication); see also Phys. Rev. Letters 7, 50 (1961).
[5]B. S. Deaver and W. M. Fairbank, Phys. Rev. Letters 7, 43 (1961).
[6]R. Doll and M. Näbauer, Phys. Rev. Letters 7, 51 (1961).
[7]N. Byers and C. N. Yang, Phys. Rev. Letters 7, 46 (1961).
[8]J. M. Blatt, Phys. Rev. Letters 7, 82 (1961).
[9]J. Bardeen, this issue [Phys. Rev. Letters 7, 162 (1961)].
[10]L. P. Gor'kov, J. Exptl. Theoret. Phys. (U.S.S.R.) 36, 1918 (1959) [translation: Soviet Phys. – JETP 9, 1364 (1959)].
[11]V. L. Ginzburg and L. D. Landau, J. Exptl. Theoret. Phys. (U.S.S.R.) 20, 1064 (1950). See also V. L. Ginzburg, Nuovo cimento 2, 1234 (1955).
[12]J. Bardeen, L. N. Cooper, and J. R. Schrieffer, Phys. Rev. 108, 1175 (1957).

ELECTRICALLY INDUCED SHIFT OF THE F^{19} RESONANCE FREQUENCY IN MnF_2[†]

P. S. Pershan and N. Bloembergen
Gordon McKay Laboratory, Harvard University, Cambridge, Masschusetts

(Received August 2, 1961)

The predicted linear effect of an applied electric field on the magnetic hyperfine interaction[1] has been found experimentally in antiferromagnetic MnF_2. We believe this is the first such observation, although the quadratic variation with E of the hyperfine splitting in the Cs atom has been reported earlier.[2]

The F^{19} resonance,[3] which occurs at 159.970 Mc/sec without external magnetic field at 4.2°K, was detected with the spectrometer built by Kushida for the investigation of the pressure dependence of the same resonance.[4]

A plane parallel slab, 1 mm × 5 mm × 20 mm, was cut from a single crystal of MnF_2 with the [100] direction perpendicular to the broad face. Metal electrodes were applied to the broad face by silver paint that was fired at 1000°F. Contacts were then attached with indium solder. A dc voltage up to 9700 volts could be applied from a battery of dry cells. It was necessary to use rf chokes to isolate the high-voltage line from the tank circuit. At the highest field, $E = 0.97 \times 10^5$ volts/cm, the F^{19} resonance is completely resolved into two components. In Fig. 1 the recordings of the absorption derivative are reproduced for zero field and three values of the applied electric field. They are compatible with a linear absolute shift $\Delta\nu_E = 5$ kc/sec for each of the four F^{19} nuclei in the unit cell, if $E = 10^4$ volts/cm is applied in the [100] direction, as shown in Fig. 2. The separation of the two components is of course twice the shift.

For an arbitrary direction of E the line should split into four components. Only the component of $\vec{E}$ pointing from each F^{19} nucleus to the nearest Mn^{++} ion is effective in shifting the resonance of that nucleus. If $E = 10^4$ volts/cm is applied along a [110] direction, half the F^{19} nuclei will keep an undisplaced resonance, while one quarter will be displaced by 7.1 kc/sec and the remaining quarter by -7.1 kc/sec.

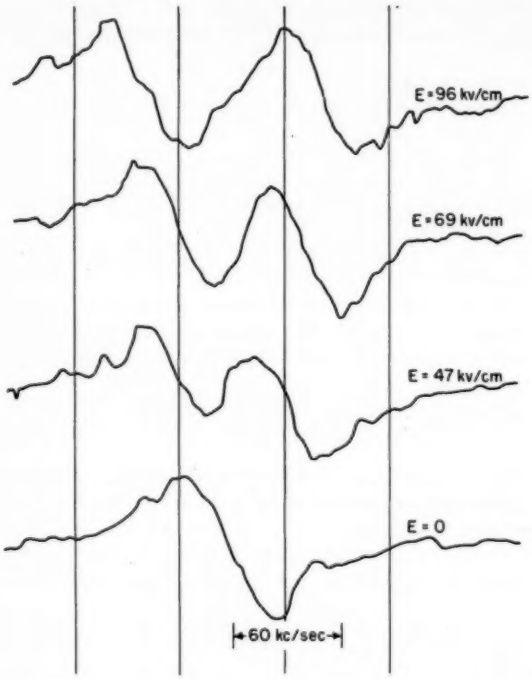

FIG. 1. The absorption derivation of the F^{19} resonance in MnF_2 at 4.2°K in zero magnetic field. An electric field of variable strength is applied along the [100] crystallographic axis.

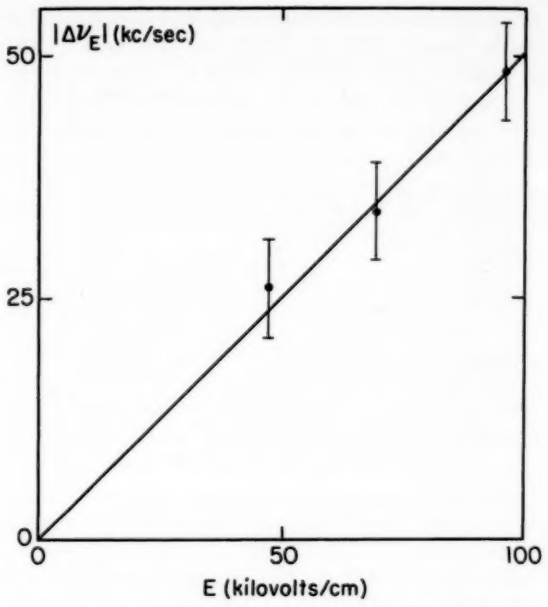

FIG. 2. The absolute shift of the F^{19} resonance versus applied electric field strength along [100]. The "electric doublet splitting" is twice the shift and amounts to 1 cps/(volt/cm).

This experimental result is an order of magnitude smaller than the admittedly crude theoretical estimate,[1] which was based on the assumption of an isotropic binding force of the F^- ion in the (001) plane. Inspection of the nuclear distances in MnF_2 and the ionic radii of F^- and Mn^{++} reveals that the F^- ion at the position $(u,u,0)$ is most tightly bound with the Mn^{++} ion at the origin, and somewhat weaker with the Mn^{++} ions at $(\frac{1}{2},\frac{1}{2},\pm\frac{1}{2})$. Its interaction with F^- ions and farther Mn^{++} ions should be much weaker. The binding is therefore highly anisotropic. When one uses the known force constants of the MnF and MnF_2 molecules,[5] the change in the nearest Mn-F distance Δr_{II} could be nearly an order of magnitude less than estimated earlier. The assumption that u does not change with hydrostatic pressure may also have to be revised. If the internuclear distance r_{II} is most difficult to change, u would increase somewhat under compression. This would make the values for $(\partial A/\partial r)_{I,II}$ quoted by Benedek and Kushida[4] too large. A revision of the covalent effects, utilizing the refinements pointed out by Freeman and Watson, and a determination of the internal electric field at the bond position, is also necessary to obtain agreement with experimental observation.

Finally it is pointed out that the observed effect may be used to study the presence or absence of antiferromagnetic domain walls. Néel introduced this concept, and several interesting theoretical discussions have appeared,[8,9] but experimental evidence is difficult to obtain. Consider a crystal of MnF_2 with an external magnetic field H_0 (>25 gauss) along the c axis, [001]. Two F^{19} magnetic resonance lines will be observed. Apply an electric field along the [110] direction. If the crystal is a single domain, only one component of the "magnetic doublet" will be split further. Work on this problem is in progress.

---

*Research was supported by the U. S. Joint Services.

[1]N. Bloembergen, Phys. Rev. Letters 7, 90 (1961).

[2]R. D. Haun and J. R. Zacharias, Phys. Rev. 107, 107 (1957).

[3]V. Jaccarino and R. G. Shulman, Phys. Rev. 107, 1196 (1957).

[4]G. B. Benedek and T. Kushida, Phys. Rev. 118, 46 (1960).

[5]G. D. Rochester and E. Olsson, Z. Physik 114, 495 (1939).
[6]A. J. Freeman and R. E. Watson, Phys. Rev. Letters 6, 343 (1961); also Phys. Rev. (to be published).
[7]L. Néel, Proceedings of the International Conference on Theoretical Physics, Kyoto, 1953 (Science Council of Japan, Tokyo, 1954), pp. 711-714.
[8]Y. Y. Li, Phys. Rev. 101, 1450 (1956).
[9]J. W. Cahn and R. Kikuchi, J. Phys. Chem. Solids 20, 94 (1961).

COMPARISON OF THE BETA SPECTRA OF B^{12} AND N^{12}†

T. Mayer-Kuckuk* and F. C. Michel
California Institute of Technology, Pasadena, California
(Received August 3, 1961)

The observed near equality of the vector beta coupling constant given by the decay of O^{14} and the muon decay coupling constant led Feynman and Gell-Mann[1] to postulate the conservation of the vector part of the beta-decay current. Gell-Mann[2] pointed out that a consequence of this conserved vector current (CVC) theory is an additional coupling in the beta interaction analogous to the anomalous magnetic moment of the nucleon ("weak magnetism"). The interference between this term and the Gamow-Teller transition amplitude for a $1^+ \rightarrow 0^+$, $\Delta T = 1$ beta transition then results in a deviation from the allowed shape of the B^{12} and N^{12} spectra. The magnitude of the effect can be calculated[2,3] from the rate of the analogous $M1$ gamma transition in C^{12}. If $S(E)$ is the spectrum of each transition, divided by the corresponding allowed Fermi spectrum, then the CVC theory predicts

$$S(E, B^{12})/S(E, N^{12}) = \text{const}[1 + (A + \delta A)E]f(E),$$

where the constant A arises from this interference term. The quantity $f(E)$ is the inner bremsstrahlung correction. The expected value for A is $(1.33 \pm 0.15)\%$ per Mev with an electromagnetic correction[4] δA of $(-0.25 \pm 0.15)\%$ per Mev. The uncertainty in A comes from the uncertainty in the C^{12} gamma-decay rate and the uncertainty in δA is an estimate of the error from using the shell model. Without the CVC theory hypothesis, A is estimated to be roughly 5 times smaller.[4,5]

The beta spectra of B^{12} ($E_{max} = 13.369$ Mev) and N^{12} ($E_{max} = 16.43$ Mev) were analyzed with the iron-free single-lens magnetic spectrometer described by Hornyak et al.[6] The baffle system was modified for the high electron energies involved. B^{12} (20.3 msec) was produced by bombarding targets of natural boron with 1.65-Mev deuterons, and N^{12} (12.5 msec) was produced by bombarding targets of enriched (96%) B^{10} with 2.75-Mev He^3 ions. Both beams were pulsed at 60 cps at the ion source of the electrostatic accelerator. The targets consisted of approximately 0.3 mg/cm^2 of boron deposited by cracking diborane on foils of thickness 0.5 mg/cm^2 and 3 mg/cm^2 for B^{12} and N^{12}, respectively. The beta rays were detected in a 10-mm thick anthracene scintillator. This is sufficiently thin (approximately 2.3-Mev range for electrons) to give nearly identical pulse-height spectra for all energies in the range studied (5-13 Mev). The use of a thin scintillator allows amplifier gain and discriminator settings to be left constant, reduces background as a result of its small volume, and produces a negligible small pulse tail extending into the noise background.[7] The activity produced on the target was monitored by the reaction protons from $B^{10}(d, p)B^{11}$ for B^{12} and $B^{10}(He^3, p)C^{12}$ for N^{12}. A silicon p-n junction counter mounted in the spectrometer near the target served as a proton detector.

The spectra were sampled at 0.5-Mev intervals in the range 5 to 10.5 Mev for B^{12} and 5 to 13 Mev for N^{12}, the data being collected at alternating high- and low-energy points to minimize effects of target deterioration and instrumental drifts. The lower limit of 5 Mev was dictated by uncertainties in the branching ratios to excited states of C^{12}; the upper limit was maintained well below the spectrum end points to minimize uncertainties arising from calibration errors and background subtraction. The background was studied at energies above the end points of the beta spectra, at zero field, and by using target backings without the boron. The neutron background was separately investigated with a beryllium target. Typical background corrections at 8 Mev amounted to about 1.7% for B^{12} and 4.2% for N^{12}. A B^{12} spectrum taken with the relatively thicker backing used for the N^{12} showed no deviation from the other B^{12} spectra.

The observed spectra are corrected for branching[8,9] to the 4.4- and 7.6-Mev excited states of C^{12} and for inner bremsstrahlung.[4] The N^{12} branch to the 7.6-Mev state is assumed to be 3.5%. The

small inner bremsstrahlung correction has been applied entirely to $S(E, B^{12})$. The Fermi plots, not corrected for branching, are given in Fig. 1. The B^{12} and N^{12} matrix elements, normalized to 1.00 at 8 Mev, are displayed in Fig. 2. The B^{12} plot represents one typical run, and the N^{12} plot is the data of 8 runs. We find the B^{12} matrix element has an energy dependence of $(1.30 \pm 0.10)\%$ per Mev and the N^{12} energy dependence is $(0.17 \pm 0.20)\%$ per Mev giving $(1.13 \pm 0.25)\%$ per Mev for $A + \delta A$.

This result appears to be in agreement with the CVC-theory prediction of $(1.08 \pm 0.22)\%$ per Mev. An important uncertainty is the 7.6-Mev branching ratio in the N^{12} decay. If, for example, we have overestimated this branching ratio by 10%,

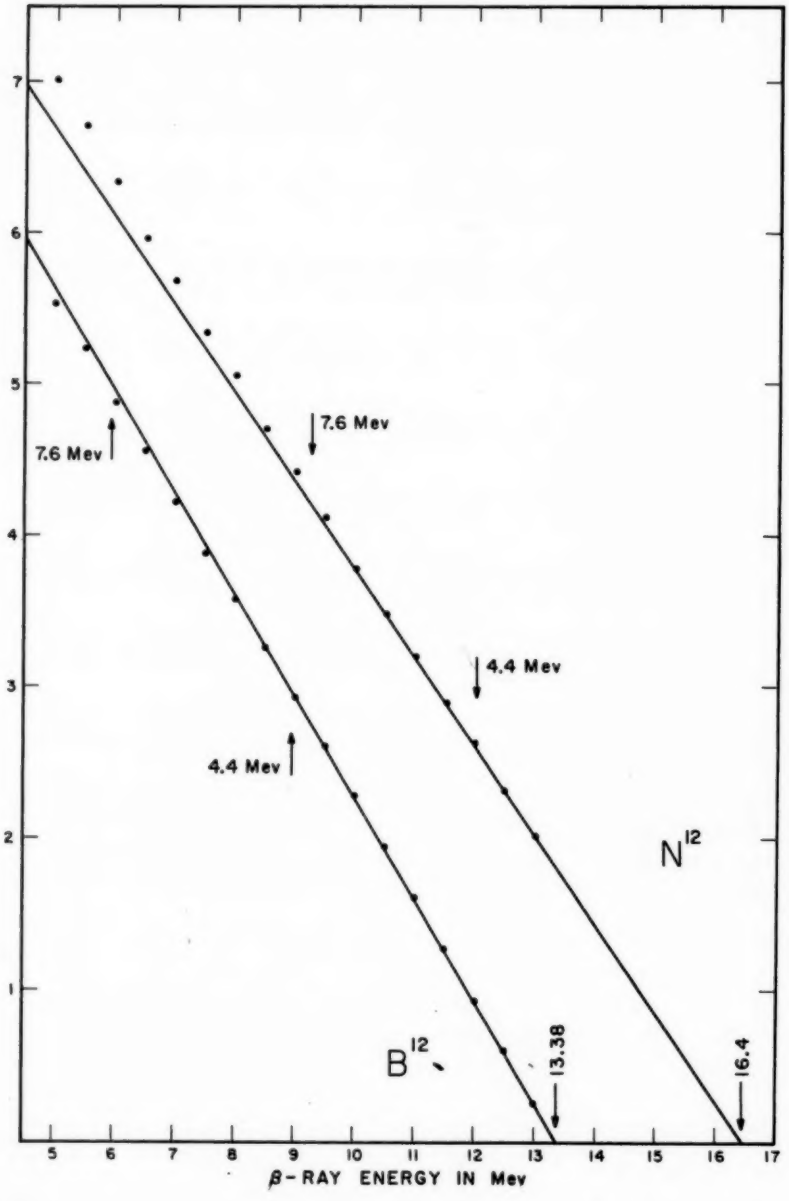

FIG. 1. Fermi plots for B^{12} and N^{12}. The observed end-point energies, indicated in the figure, are in agreement with the values from reaction data [F. Ajzenberg-Selove and T. Lauritsen, in Landolt-Börnstein Tables (to be published)] of 13.369 Mev for B^{12} and 16.43 for N^{12}. The curvature of the N^{12} plot due to branching can easily be seen. In the B^{12} plot this effect is overcompensated by the CVC shape factor. Branching end points are indicated by arrows.

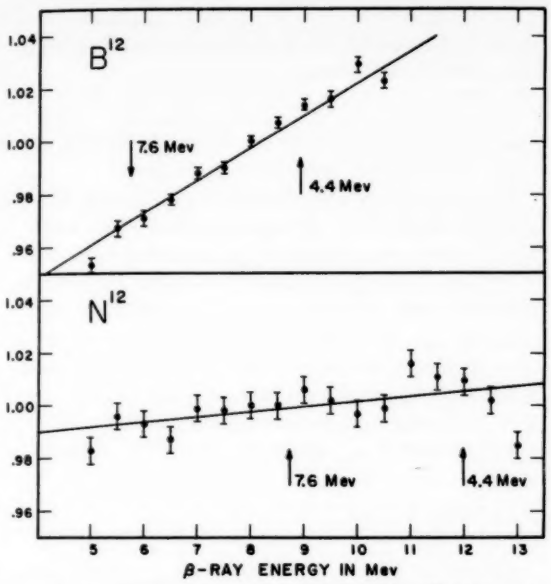

FIG. 2. Plots of the shape factors $S(E,B^{12})/f(E)$ and $S(E,N^{12})$ normalized to unity at 8 Mev. Statistical errors and least-squares fits are given. Branching end points are indicated by arrows. Slopes are 1.29 % per Mev for B^{12} and 0.17% per Mev for N^{12}.

our value for $A+\delta A$ should be increased by 0.12% per Mev. It is interesting that the relatively strong energy dependence of the B^{12} matrix element accounts for the failure of Hornyak et al.[10] to observe a B^{12} branch to the 4.4-Mev state of C^{12}, and in fact gives a Fermi plot that is slightly concave downwards.

Previously, Nordberg, Morinigo, and Barnes[11] compared the asymmetries of the beta-alpha angular correlation in the decays of Li^8 and B^8 and also found agreement with the CVC theory. A small discrepancy remains, however, between the muon lifetime and the Fermi coupling constant derived from the O^{14} decay.[12] Possibly this discrepancy is due to a charge dependence of the internucleon potential.[13]

The authors are indebted to Professor T. Lauritsen, Professor C. A. Barnes, Professor W. A. Fowler, Professor H. A. Weidenmüller, and Professor F. Boehm for valuable discussions. Two earlier experiments in this laboratory[14] by H. Hilton and V. Soergel, and H. Hilton and C. Van der Leun provided much of the groundwork which made the present experiment possible. One of us (Mayer-Kuckuk) was supported by Deutsches Bundesministerium für Atomkernenergie.

---

†Work supported in part by the joint program of the Office of Naval Research and the U. S. Atomic Energy Commission.

*On leave from Max Planck Institut für Kernphysik, Heidelberg, Germany.

[1]R. P. Feynman and M. Gell-Mann, Phys. Rev. 109, 193 (1958).

[2]M. Gell-Mann, Phys. Rev. 111, 362 (1958).

[3]H. A. Weidenmüller, Nuclear Phys. 21, 397 (1960).

[4]M. Gell-Mann and S. M. Berman, Phys. Rev. Letters 3, 99 (1959).

[5]M. L. Goldberger, Revs. Modern Phys. 31, 797 (1959).

[6]W. F. Hornyak, T. Lauritsen, and V. K. Rasmussen, Phys. Rev. 76, 731 (1949).

[7]Compare for example: F. T. Porter, M. S. Freedman, T. B. Novey, and F. Wagner, Phys. Rev. 103, 921 (1956).

[8]C. W. Cook, W. A. Fowler, C. C. Lauritsen, and T. Lauritsen, Phys . Rev. 111, 567 (1958).

[9]N. W. Glass, R. W. Peterson, and R. K. Smith, Bull. Am. Phys. Soc. 6, 49 (1961).

[10]W. F. Hornyak and T. Lauritsen, Phys. Rev. 77, 160 (1950).

[11]M. E. Nordberg, F. B. Morinigo, and C. A. Barnes, Phys. Rev. Letters 5, 321 (1960).

[12]R. K. Bardin, C. A. Barnes, and P. A. Seeger, Phys. Rev. Letters 5, 323 (1960).

[13]R. J. Blin-Stoyle and J. Le Tourneaux, Phys. Rev. 123, 627 (1961).

[14]H. Hilton, thesis, California Institute of Technology, 1960 (unpublished).

DOUBLE GAMMA EMISSION IN THE 6.06-Mev MONOPOLE TRANSITION OF O^{16}†

S. Gorodetzky, G. Sutter, R. Armbruster, P. Chevallier, P. Mennrath, F. Scheibling, and J. Yoccoz
Institut de Recherches Nucleaires, Strasbourg, France
(Received July 27, 1961)

In a continuation of our work on double gamma-ray emission in electric monopole transitions we have undertaken a study of the 6.06-Mev transition in O^{16}. This case was considered theoretically by Oppenheimer and Schwinger[1] in 1939, and then by Dalitz[2] and by Cameron.[3] Very recently, Yoccoz[4] has proposed a more complete theory of this problem and gives as preliminary result for the ratio of the probabilities of double gamma-ray emission and pair creation: $3\times10^{-3} \leq \Gamma_{\gamma\gamma}/\Gamma_{\pi} \leq 8\times10^{-3}$. At present, more detailed calculations are being undertaken.

The 6.06-Mev level was excited by the reaction $F^{19}(p,\alpha)O^{16}$, at the 1880-kev resonance. An excitation curve[5] for nuclear pair emission had shown that this resonance was the most advantageous one for a study of the monopole transition.

The method of summing the energies of the two gamma radiations, previously used in an attempt to detect double gamma-ray emission from the 1.75-Mev transition in Zr^{90},[6] was not suitable for the 6.06-Mev transition in O^{16}. Indeed for the gamma-ray energies occuring in O^{16} the total absorption rate in the crystals used is much lower than in Zr^{90}. We have thus been led to the use of $(\alpha-\gamma-\gamma)$ triple coincidence ($2\tau = 5\times10^{-9}$sec), gating a multichannel analyzer which records the energy spectrum of the alpha particles (Fig. 1). The gamma-rays were detected by two 4-in.×4-in. NaI crystals at 180°, and the alpha particles by a

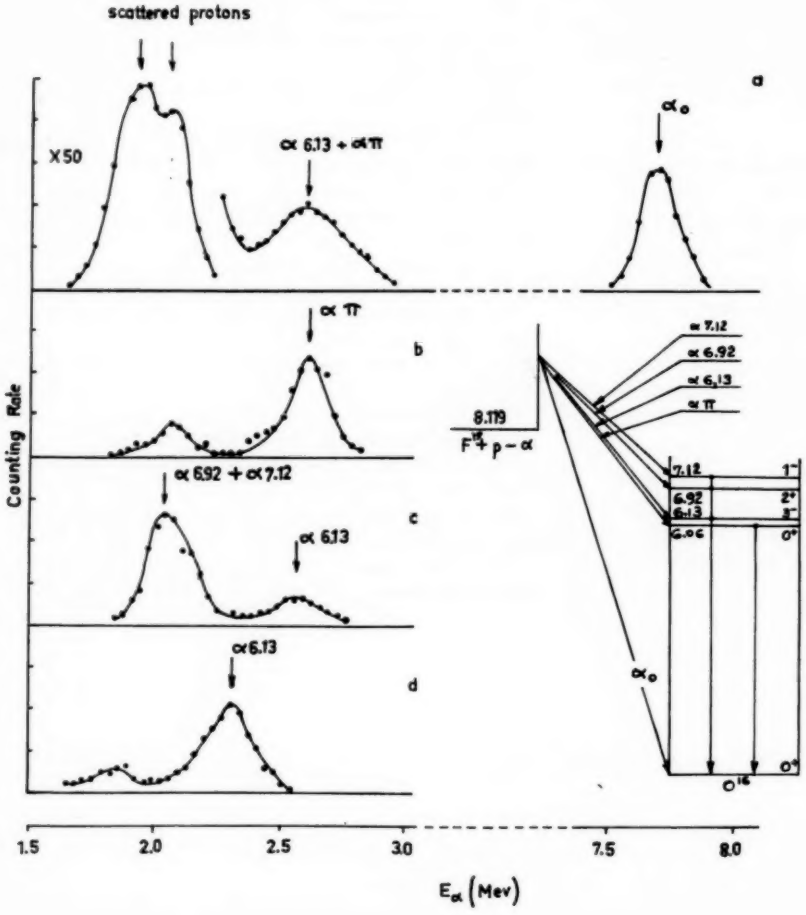

FIG. 1. (a) $E_p = 1880$ kev, direct alpha-particle spectrum. (b) $E_p = 1880$ kev, alpha-particle spectrum gated by alpha-gamma-gamma triple coincidences. Gamma-ray window at 0.511 Mev (annihilation radiation). Accidentals subtracted. (c) $E_p = 1880$ kev, alpha-particle spectrum gated by alpha-gamma double coincidences ($E_\gamma > 2$ Mev). Accidentals subtracted. (d) $E_p = 1375$ kev, alpha-particle spectrum gated by alpha-gamma double coincidences ($E_\gamma > 2$ Mev). Accidentals subtracted.

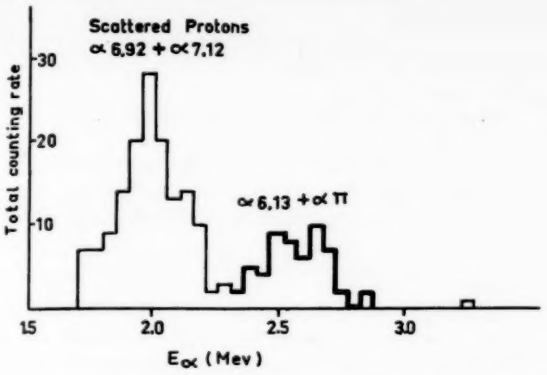

FIG. 2. $E_p = 1880$ kev, alpha-particle spectrum gated by alpha-gamma-gamma triple coincidences. Gamma-ray windows from 1.5 to 4.5 Mev. Accidentals not subtracted (see Table I).

20-mm² RCA junction detector at 150° to the direction of the incident beam.

A preliminary experiment[7] had given an upper limit: $\Gamma_{\gamma\gamma}/\Gamma_\pi \leq 6\times10^{-3}$.

Since this first experiment the apparatus has been improved by the use of a lead target chamber forming a conical diaphragm for the NaI crystals. Only gamma rays between 1.5 and 4.5 Mev were accepted by the circuit.

At $E_p = 1880$ kev a series of 166 measurements, each of 30 minutes duration, were made. Figure 2 shows the spectrum obtained. We have verified that the distribution of the coincidences in time follows the Poisson law.

Since the measurement of the accidental coincidence rate would be excessively time consuming because there are several possible kinds of such coincidences, we calculated[8] the rate from the various counting rates and the coincidence resolving time. Measurements made at the 1375-kev resonance [predominantly producing the 6.13-Mev level—see Fig. 1(d)] seem to show that the method is correct. The probability of double gamma-ray emission from this level is theoretically very small. Under the same experimental conditions as at 1880 kev (in particular, the same counting rate) no real events were observed; all the coincidences obtained could be attributed to accidentals. Furthermore, this method has been verified at the 1880-kev resonance by measuring the accidental coincidences of different kinds that occur with a greater beam intensity. We estimate that the maximum error in the calculation of accidentals is 20%.

Results obtained at the two resonances are shown in Table I.

The experimental results are related to the double gamma-ray emission probability by the following formula:

$$\frac{\Gamma_{\gamma\gamma}}{\Gamma_\pi} = \frac{1}{2}\frac{N_{\alpha_0}}{N_{\alpha_\pi}}\frac{N_{\alpha_{\gamma\gamma}}}{N_{\alpha_0}}\frac{C}{a^2\epsilon\langle\Omega\eta\rangle_{av}^2}\frac{E_0^7/140}{\int_{1.5\ \mathrm{Mev}}^{4.5\ \mathrm{Mev}}[Ep(E)]^3[(E_0-E)p(E_0-E)]^3dE}, \tag{1}$$

where $E_0 = 6.06$ Mev, $\langle\Omega\eta\rangle_{av}$ = the mean value of the product of the solid angle and the efficiency of a crystal, ϵ = the efficiency of the coincidence circuit (here $\epsilon = 1$), $C = 0.89$ = a factor due to the $(1+\cos^2\theta)$ correlation between the two $E1$ gamma rays detected, and $a = 0.87$ = the mean transmission of gamma rays by the absorber which stops the electrons from nuclear pair creation.

The product $\langle\Omega\eta\rangle_{av}$ was measured directly at the 1375-kev resonance from the ratio

$$N_{\mathrm{coinc}}{}^{(\alpha-\gamma)}{}_{6.13}/N_{\alpha 6.13},$$

Table I. Alpha-gamma-gamma measured coincidences and calculated accidentals.

		Scattered protons $+\alpha_{6.92}+\alpha_{7.12}$	$\alpha_{6.13}+\alpha_\pi$
1375 kev	Measured coincidences	40	55
	Calculated accidentals	43	52
1880 kev	Measured coincidences	146	55
	Calculated accidentals	147	15

taking into account the α-γ angular correlation. We obtained $\langle\Omega\eta\rangle_{av}\epsilon = 3.66\times10^{-2}$. This result was verified by a measurement made with a calibration source of Co^{60} corrected to our energy by the use of curves given by Wolicki et al.[9]

Using the energy spectrum of double gamma-ray emission, which has the form $E^3(E_0-E)^3$,[10-12,4] we have calculated the integral in the denominator of Eq. (1) and find

$$\frac{140}{E_0^{\ 7}}\int_{1.5\ \mathrm{Mev}}^{4.5\ \mathrm{Mev}} [Ep(E)]^3\,[(E_0-E)p(E_0-E)]^3dE = 0.24, \tag{2}$$

where $p(E)$ is the form factor of the energy spectrum of a gamma ray of energy E in a 4 in.×4 in. NaI crystal. The term $140/E_0^{\ 7}$ is the normalization factor. The number $N_{\alpha 0}$ is measured directly during the experiment. In a separate experiment the ratio $N_{\alpha 0}/N_{\alpha\pi}$ has been measured as 2.8. The factor 1/2 is due to the indistinguishibility of the two gamma rays.

Since approximate calculations have shown that the internal and external bremsstrahlung coming from the pairs are negligible,[13] we believe that the true coincidences observed can be attributed to double gamma-ray emission. Insofar as no unknown phenomena of the same order of magnitude are taking place, our experimental result leads to the value

$$\Gamma_{\gamma\gamma}/\Gamma_{\pi} = (2.5\pm1.1)\times10^{-8}.$$

In addition, the measurement made at 1375 kev allows us to give an upper limit for the double gamma-ray decay of the 6.13-Mev $E3$ transition of O^{16}:

$$\Gamma_{\gamma\gamma}/\Gamma_{\gamma} \leq 5\times10^{-4}.$$

†This work was supported in part by the U. S. Air Force Office of Scientific Research.

[1]J. R. Oppenheimer and J. S. Schwinger, Phys. Rev. 56, 1066 (1939).

[2]R. H. Dalitz, Proc. Roy. Soc. (London) 206, 521 (1951).

[3]A. G. W. Cameron, Bull. Am. Phys. Soc. 3, 269 (1958).

[4]J. Yoccoz, Comptes-Rendus du Colloque de Strasbourg, May, 1961 [J. phys. radium (to be published)].

[5]S. Gorodetzky, G. Sutter, P. Chevallier, F. Scheibling, and R. Armbruster, Compt. rend. 250, 1028 (1960).

[6]S. Gorodetzky, G. Sutter, R. Armbruster, P. Chevallier, P. Mennrath, F. Scheibling, and J. Yoccoz, Compt. rend. 252, 1132 (1961).

[7]S. Gorodetzky, G. Sutter, R. Armbruster, P. Chevallier, P. Mennrath, F. Scheibling, and J. Yoccoz, Comptes Rendus du Colloque de Strasbourg, May, 1961 [J. phys. radium (to be published)].

[8]We have evaluated in particular the triple accidental coincidences due to real double events. Concerning the impurities of the target, we have experimentally tested that they do not give any effect.

[9]E. A. Wolicki, R. Jastrow, and F. Brooks, Naval Research Laboratory Report NRL-4833 (unpublished).

[10]M. Goeppert, Naturwissenschaften 17, 932 (1929). M. Goeppert-Mayer, Ann. Physik 9, 273 (1931).

[11]R. G. Sachs, Phys. Rev. 57, 194 (1940).

[12]G. J. McCallum, D. A. Bromley, and J. A. Kuehner, Nuclear Phys. 20, 382 (1960).

[13]"Bremsstrahlung" (annihilation in flight of pair positrons) coincidences have also been evaluated; the value obtained gives a negligible contribution, that is $\leq 2\%$ of the observed effect, of the same order of magnitude as the contribution due to external bremsstrahlung.

MAGNETIC MOMENT OF N^{13}†

M. Posner, J. L. Snider, A. M. Bernstein, and D. R. Hamilton
Palmer Physical Laboratory, Princeton University, Princeton, New Jersey
(Received August 15, 1961)

Uncertainties in the form of the magnetic dipole moment operator and the exact structure of nuclear wave functions make the theoretical interpretation of nuclear magnetic moments difficult.[1] In addition to the usual orbital and spin contributions to the moment one must consider the effects of relativity[2] and of the currents due to the exchange of charged π mesons between nucleons (exchange moments).[3] As a consequence of the assumption of the charge independence of nuclear forces the wave functions of mirror nuclei are the same. A comparison of the magnetic moments of a mirror pair could, in principle, yield information about the structure of the operator. In particular, Sachs has pointed out that the sum of the moments of a pair of mirror nuclei should be independent of mesonic current contributions.[3]

With these ideas in mind we have measured the spin and magnetic moment of 10-minute N^{13} by the atomic beam magnetic resonance method. Because of the short half-life a continuous-flow source was used. The radioactivity was produced by the bombardment of N^{14}, in melamine powder, with 18-Mev protons. The resulting N^{13}, in gaseous molecular form, was flushed with neon from the cyclotron target to the atomic beam machine. There a microwave discharge dissociated the molecules to produce a beam of neutral N^{13} atoms. These atoms were then passed through a machine of a new design, consisting of a six-pole focusing A magnet,[4] a C magnet,[5] and a two-pole, constant-gradient, B magnet. The atoms were collected by means of a chemical reaction on titanium foils maintained at a temperature of 1050°C. After exposure to the beam these foils were removed from the apparatus and the positron activity was counted in standard scintillation counters.

The optics of the machine allowed us to place two collector foils at the B-magnet exit, one of which monitored the beam while the other collected primarily atoms which had undergone resonance transitions. The ratio of the count rates on these foils is low off resonance, increases at resonance, and is independent of the size of the beam. This technique enabled us to observe resonances with beams which were not completely steady.

The N^{13} atoms were produced mainly in the $^4S_{3/2}$ atomic ground state, but resonances were also seen in the metastable $^2D_{3/2}$ and $^2P_{3/2}$ states. A nuclear spin of $\frac{1}{2}$ was measured by observing resonances in the Zeeman region (where the resonance frequencies vary linearly with magnetic field) in the atomic states mentioned above.[6] Several resonances were observed at each of a number of magnetic fields, these being consistent only with a nuclear spin of $\frac{1}{2}$.

To measure the value of the hyperfine structure separation, $\Delta\nu$, the $^4S_{3/2}$, $F=2$, $m_F=1$ to $F=2$, $m_F=0$ transition (assuming $\mu<0$) was followed out of the Zeeman region to a field of 22 gauss. The shifts of the resonance frequency from linearity with field give

$$\Delta\nu = 33.2 \pm 0.3 \text{ Mc/sec.}$$

Combining this with the value of $\Delta\nu$ and μ for N^{15},[7] we obtain

$$|\mu(N^{13})| = 0.321 \pm 0.003 \text{ nm.}$$

One would assume that the sign of the moment is negative as in N^{15}.

In Table I we list the data now available on the magnetic moments of pairs of mirror nuclei. (This table does not include the neutron and proton whose moments are basic ingredients of the single-particle or Schmidt moments.) For both pairs of nuclei the moments lie "outside" the Schmidt moments by amounts which are approximately equal and opposite. From a careful consideration of the sum of the moments of the mass-three nuclei, Sachs has shown[3] that the moments

Table I. Magnetic moments of mirror pairs of nuclei. μ_E is the experimental moment, μ_S the Schmidt single-particle moment. The values of μ_S for He^3 and H^3 are the same as the free neutron and proton moments, upon which the Schmidt moments are based. All values of μ_E except that for N^{13} are taken from Strominger et al.[a]

Nucleus	μ_E	μ_S	$(\mu_E-\mu_S)$
He^3	-2.127	-1.913	-0.214
H^3	2.979	2.793	0.186
Sums	0.852	0.880	-0.028
C^{13}	0.702	0.638	0.064
N^{13}	(-)0.321	-0.264	-0.057
Sums	0.381	0.374	0.007

[a]D. Strominger, J. M. Hollander, and G. T. Seaborg, Revs. Modern Phys. 30, 585 (1958).

cannot be explained by any reasonable mixing of LS states and that therefore these results must be due to mesonic current contributions of 0.27 nm.

For the $A = 13$ mirror pair, calculations performed using the intermediate-coupling shell model and the usual magnetic moment operator show that if there is a sufficient deviation from jj coupling toward LS coupling, the magnetic moments can lie outside the Schmidt limits.[8-10] Analysis of the available experimental data, not including the magnetic moments or $M1$ transition rates, indicates that the coupling is intermediate between LS and jj, but is not of sufficient precision to determine the exact coupling.[10] Therefore, the prediction of the model for the magnetic moments cannot be precisely determined at present.

It should be pointed out that the Hamiltonian used in these calculations includes exchange and velocity-dependent (spin-orbit) interactions which change the form of the current operator. Since the proper form of this operator is not known, these terms have not been taken into account. Therefore, the calculation of the magnetic moments and magnetic transition rates is not self-consistent.[11]

The sum of the moments of N^{13} and C^{13} as calculated in intermediate coupling is independent of the coupling and is equal to the sum of the Schmidt moments to within 0.04 nm,[12] in agreement with the experimental results. From this agreement one can conclude that the mesonic current contributions in N^{13} and C^{13}, if they exist, obey the mirror principle (i.e., they are equal and opposite in a pair of mirror nuclei).[3,13]

A more detailed discussion of this work will be published subsequently.

---

†This work was supported by the U. S. Atomic Energy Commission and the Higgins Scientific Trust Fund.

[1]For a review of the subject see R. J. Blin-Stoyle, Theories of Nuclear Moments (Oxford University Press, New York, 1957).

[2]L. Rosenfeld, Nuclear Forces (North-Holland Publishing Company, Amsterdam, 1949), p. 417.

[3]R. G. Sachs, Nuclear Theory (Addison-Wesley Publishing Company, Inc., Reading, Massachusetts, 1953).

[4]R. L. Christensen and D. R. Hamilton, Rev. Sci. Instr. 30, 356 (1959).

[5]L. S. Goodman, Rev. Sci. Instr. 31, 1351 (1960).

[6]J. L. Snider, M. Posner, A. M. Berstein, and D. R. Hamilton, Bull. Am. Phys. Soc. 6, 224 (1961).

[7]L. W. Anderson, F. M. Pipkin, and J. C. Baird, Jr., Phys. Rev. 116, 87 (1959).

[8]For an introduction to the intermediate-coupling shell model see J. P. Elliot and A. M. Lane, Handbuch der Physik, edited by S. Flügge (Springer-Verlag, Berlin, 1957), Vol. 39, p. 241.

[9]D. Kurath, Phys. Rev. 101, 216 (1956).

[10]A. M. Lane, Proc. Phys. Soc. A68, 197 (1955), and earlier papers.

[11]In principle, it seems reasonable that these currents should be equivalent to the mesonic exchange currents since the nuclear force is believed to derive from the interchange of mesons.

[12]D. Kurath, Phys Rev. (to be published). We thank Dr. Kurath for sending us a preprint in advance of publication.

[13]We have not discussed the relativity contribution to the magnetic moment as it is expected to be small compared to the deviation from the Schmidt moment. See reference 2.

IDENTIFICATION OF DOUBLET STATES AT 5.16 Mev in B^{10}

E. L. Sprenkel, J. W. Olness, and R. E. Segel
Aeronautical Research Laboratory, Dayton, Ohio

(Received August 15, 1961)

The isotopic spin analog of the first excited states in Be^{10} and C^{10} should be located at an excitation energy of about 5.1 Mev[1] in the self-conjugate nucleus B^{10}. In this region three levels have been reported previously[2] at 4.77, 5.11, and 5.16 Mev, of which the first two levels may readily be eliminated as candidates for the $J^{\pi} = 2^{+}$, $T = 1$ isotopic spin analog. The energy displacement of the 4.77-Mev state, from the expected position at 5.1 Mev, would be exceptionally large and the broad width ($\Gamma_{c.m.} = 1.2$ kev) of the 5.11-Mev state makes an assignment of $T = 1$ very unlikely for that state. Recently Meads et al.[3] have shown, from a comparison of proton and deuteron (about 10-Mev incident energy) inelastic scattering by B^{10}, that the isotopic spin of both the 4.77- and 5.11-Mev states is $T = 0$.

The state at 5.16 Mev has presented a puzzle. Investigation of the 5.16-Mev level when fed by 2.40-Mev gamma-ray transitions from the 7.56-Mev level in B^{10} yields results which are not supported when the 5.16-Mev level is produced by

other means. From a study of the angular distributions of the gamma rays emitted from the 5.16-Mev level, produced in the $Li^6+\alpha$ reaction, Meyer-Schützmeister and Hanna[4] found that the possible J^π assignments were 1^+ or 2^+, the decay scheme favoring the latter assignment. The apparent absence of transitions to the $J^\pi=0^+$, $T=1$ state at 1.74 Mev would appear to rule out a $J^\pi=1^+$, $T=0$ assignment to the 5.16-Mev level on the basis of Morpurgo's rule.[5] Since a $J^\pi=1^+$, $T=1$ assignment cannot be reconciled with the $T=1$ system of levels in the mirror nuclei Be^{10} and C^{10}, the proper assignment for the 5.16-Mev level would be expected to be $J^\pi=2^+$, $T=1$. Recently the $T=1$ assignment has been supported by Meads et al.[3] as a result of their comparison of proton and deuteron inelastic scattering. On the other hand, the strong 2.40-Mev gamma ray emitted by the $J^\pi=0^+$ state at 7.56 Mev in B^{10} indicates that the assignment of the 5.16-Mev level[6] populated by this transition must be $J=1$.

The intrinsic c.m. width of the 5.16-Mev level of B^{10} formed in the $Li^6+\alpha$ reaction has been reported by Hanna[7] to be less than 500 ev. In a preliminary investigation of $Be^9(d,n)B^{10}$ reactions, Chase and Warburton[8] report both neutron and gamma-ray thresholds for the 5.16-Mev level with $\Gamma_\gamma > 0.1\Gamma$. For $Be^9(p,\gamma)B^{10}$ reactions, Meyerhof, Tanner, and Hudson[9] have shown, from the spectra in coincidence with capture gamma rays to the 5.16-Mev level, that $\Gamma_\gamma \approx 0.1\Gamma$ for this state. Similar results were obtained by Meyerhof and Chase[10] for the gamma rays emitted from the interaction of 2.8-Mev deuterons with a thick beryllium target. On the other hand, Sprenkel and Daughtry[11] did not observe gamma rays in coincidence with 2.40-Mev transitions from the 7.56-Mev level and placed a limit of $\Gamma_\gamma < 0.01\Gamma$ for the 5.16-Mev state. In order to explain the disagreement of their results with those presented above, Sprenkel and Daughtry[11] postulated the existence of doublet states at 5.16 Mev in B^{10}.

Since the doublet state that is fed by 2.40-Mev gamma rays is expected to have a $J=1$, $T=0$ assignment, the decay of this state should proceed mainly through the transition to the $J^\pi=0^+$, $T=1$ state at 1.74 Mev in B^{10}. The expected predominance of this transition (3.42 Mev) arises from the selection rules for the strong reduction in strength of $E1$ and $M1$ transitions between levels of the same isotopic spin in self-conjugate nuclei.[5,12] Accordingly a search was made for a 3.42-Mev gamma-ray transition that should result from the decay of a $J=1$ doublet member produced by bombarding Li^6 with alpha particles of about 1.17 Mev. Since the known member of the 5.16-Mev doublet decays by 3.01-Mev (64%), 4.44-Mev (29%), and 5.16-Mev (7%) transitions,[4] the detection of a peak corresponding to the full energy of a 3.42-Mev gamma ray is rendered difficult, because the peak lies in the same spectral region as the second escape peak of the 4.44-Mev transition. In order to increase the sensitivity for the detection of 3.42-Mev gamma rays, spectra were taken in coincidence with either of the other members of the 3.42-1.02-0.72 Mev cascade. Two NaI(Tl) crystals (8 in. diameter × 8 in. long and 5 in. diameter × 5 in. long) were placed at 90° with respect to the alpha beam and at a distance of about 3/4 in. from the Li^6 target. To minimize escape-peak formation, the larger NaI(Tl) crystal was used for the detection of the coincidence spectrum. The fixed channel, for the smaller crystal, extended from 0.6 to 1.2 Mev for selection of the 0.72- and 1.02-Mev cascade gamma rays. Coincidence spectra were obtained at alpha-energy inter-

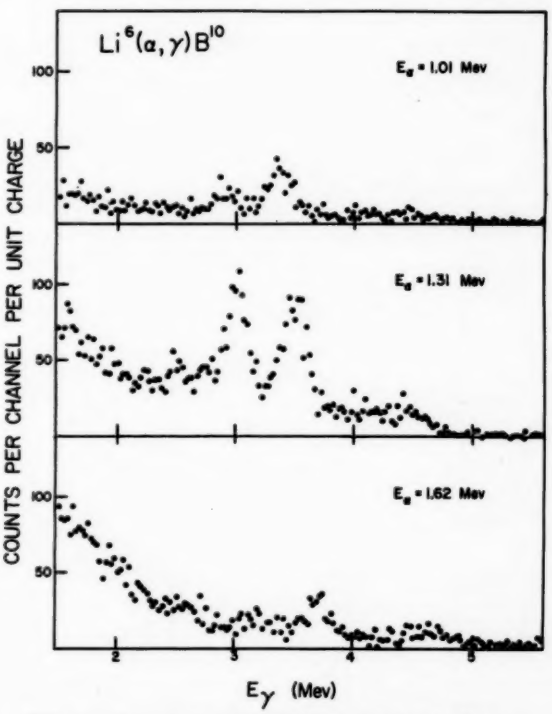

FIG. 1. Gamma-ray coincidence spectra in the region of the 1.20-Mev resonance in $Li^6(\alpha,\gamma_{3.42})B^{10}$. The middle spectrum also shows gamma rays from the previously known 1.175-Mev resonance.

vals of 75 kev using an enriched Li^6 target with an average thickness of 50 kev. A peak corresponding to a 3.42-Mev transition was seen to appear at about $E_\alpha = 1.0$ Mev, increase sharply in intensity to reach a maximum at about $E_\alpha = 1.2$ Mev, and then gradually decrease in intensity (Fig. 1 and Fig. 2). The position of the peak shifted in a regular manner (Fig. 1), showing a change in gamma-ray energy from 3.36 Mev at $E_\alpha = 1.0$ Mev to 3.70 Mev at $E_\alpha = 1.6$ Mev. Peaks corresponding to 3.01- and 4.44-Mev transitions from the previously known member of the doublet were found to be very intense in the coincidence spectrum taken at $E_\alpha = 1.19$ Mev. Because of the nonuniform thickness of the target, the 3.01-Mev peak is still apparent in the spectrum taken at $E_\alpha = 1.31$ Mev (Fig. 1). For positive identification of the 3.42-1.02-0.72 Mev cascade chain, a spectrum was taken in coincidence with the "3.42-Mev" gamma ray detected in the large crystal. The resultant spectrum showed the presence of only two gamma rays at 0.72 and 1.02 Mev, which provided identification of the expected cascade chain.

The "3.42-Mev" gamma-ray yield curve (Fig. 2) was fitted with the single-level expression:

$$\sigma_{\alpha\gamma} = \pi\lambda^2 g \frac{\Gamma_\alpha \Gamma_\lambda}{(E_\lambda + \Delta_\lambda - E_\alpha)^2 + (\Gamma_\lambda/2)^2}, \qquad (1)$$

where the energy dependence of the resonance

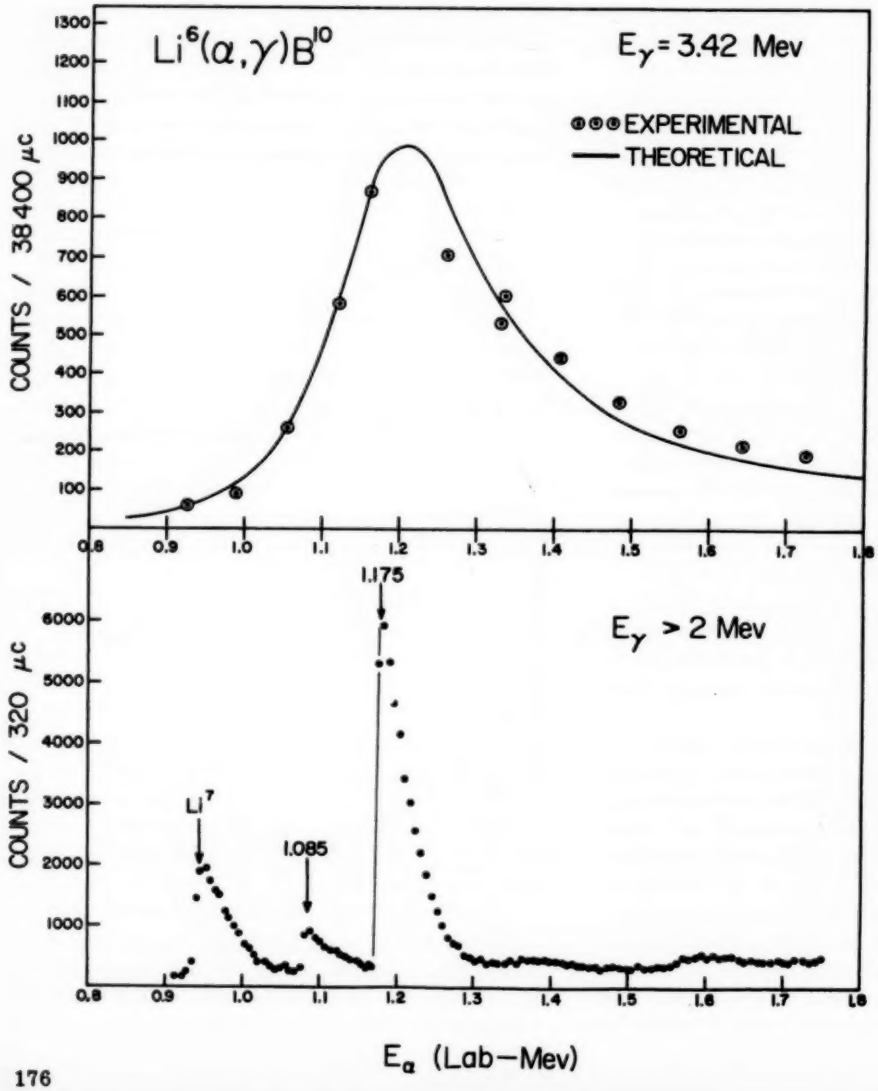

FIG. 2. Yield curves for $Li^6(\alpha,\gamma)B^{10}$. The upper graph shows the coincidence yield of the "3.42-Mev" gamma ray as a function of alpha-particle bombarding energy. The theoretical curve was calculated for the resonance assignments in the text. The lower graph shows the yield of gamma rays of energy greater than 2 Mev. The previously known resonances in $Li^6(\alpha,\gamma)B^{10}$ are indicated by their resonance energies, as is the $Li^7(\alpha,\gamma)B^{11}$ resonance, resulting from the presence of Li^7 in the target. The broad peaks at 1.4 and 1.6 Mev probably result from $C^{13}(\alpha,n)O^{16}$ reactions in carbon deposits on the analyzing slits of the accelerator system.

parameters is given by Sachs.[13] Using an interaction radius of 4.94×10^{-13} cm and assuming s-wave formation, the theoretical curve satisfactorily fit the experimental data when $E_\gamma(\text{lab}) = E_\lambda + \Delta_\lambda{}^0 = 1.210 \pm 0.035$ Mev ($B^{10*} = 5.18$ Mev) and $\Gamma_\lambda{}^0(\text{lab}) = 0.340 \pm 0.050$ Mev. The ~200-kev (c.m.) breadth of the state agrees with the report that the 2.40-Mev gamma ray feeding the state appears to have an observable energy spread.[11,14] The width corresponds to about 86% of the single-particle limit for s-wave (α) formation and 190% for p-wave formation. $Be^9(d,n)B^{10}$ angular distribution data[15] imply a negative-parity state in the 5.1-Mev region for which the newly found state offers the only possibility. However, the large width measured here favors s-wave formation although there is enough uncertainty in the resonance parameters to allow p-wave formation of approximately single-particle width.

Comparison of the thick-target yields for the 3.01- and 3.42-Mev gamma rays, using the previously determined[4] 3.01-Mev gamma-ray yield, provided the value $\Gamma_{\gamma\,3.42} = 0.06 \pm 0.03$ ev. This radiation width corresponds to $|M|^2 \sim 0.06$ which is well within the predicted[16] range of an allowed $M1$ transition. An upper limit of ~1/3 the intensity of the 3.42-Mev transition was placed on any other gamma ray emanating from this broad 5.18-Mev state. The branching ratio $\Gamma_\gamma/\Gamma \sim 3\times10^{-7}$ is consistent with the upper limit of 10^{-2} established by Sprenkel and Daughtry.[11]

The identification of another state in the 5.1-Mev region of B^{10} finally allows a solution of the puzzle regarding the isotopic spin analog of the first excited states in Be^{10} and C^{10}. The 7.56-Mev level decays by 2.40-Mev gamma rays to feed the $J=1$, $T=0$ broad level centered at 5.18 Mev, leaving the previously known narrow 5.16-Mev level for the long sought $J^\pi = 2^+$, $T=1$ state. These assignments allow reconciliation of all conflicting results from the previous experiments described above.

---

[1]G. A. Jones and D. H. Wilkinson, Phys. Rev. 90, 722 (1953).

[2]F. Ajzenberg-Selove and T. Lauritsen, Nuclear Phys. 11, 1 (1959).

[3]D. H. Wilkinson (private communication).

[4]L. Meyer-Schützmeister and S. S. Hanna, Phys. Rev. 108, 1506 (1957).

[5]G. Morpurgo, Phys. Rev. 110, 721 (1958).

[6]N. W. Tanner and S. S. Hanna, Nuclear Phys. 23, 319 (1961).

[7]Quoted in reference 10.

[8]L. F. Chase and E. K. Warburton (to be published).

[9]W. E. Meyerhof, N. W. Tanner, and C. M. Hudson, Phys. Rev. 115, 1227 (1959).

[10]W. E. Meyerhof and L. F. Chase, Phys. Rev. 111, 1348 (1958).

[11]E. L. Sprenkel and J. W. Daughtry, Phys. Rev. (to be published).

[12]L. A. Radicati, Proc. Phys. Soc. (London) A66, 139 (1953).

[13]R. G. Sachs, Nuclear Theory (Addison-Wesley Publishing Co., Inc., Reading, Massachusetts, 1953), p. 300.

[14]W. E. Meyerhof (private communication).

[15]F. Ajzenberg, Phys. Rev. 88, 298 (1952).

[16]D. H. Wilkinson, in Nuclear Spectroscopy, edited by F. Ajzenberg-Selove (Academic Press, Inc. New York, 1960), Chap. V F.

EVIDENCE FOR A $T=0$ THREE-PION RESONANCE*

B. C. Maglić, L. W. Alvarez, A. H. Rosenfeld, and M. L. Stevenson
Lawrence Radiation Laboratory and Department of Physics, University of California, Berkeley, California

(Received August 14, 1961)

The existence of a heavy neutral meson with $T=0$ and $J=1^-$ was predicted by Nambu[1] in an attempt to explain the electromagnetic form factors of the proton and neutron. Chew[2] has pointed out that such a vector meson should exist on dynamical grounds as a three-pion resonance or a bound state. Such a particle is also expected in the vector meson theory of Sakurai[3] and, as a member of an octet of mesons, according to the unitary symmetry theory[4]; and for other reasons.[5] We will refer to it as ω.

Previous searches[6] for ω have primarily been confined to the mass region $m_\omega < 3\mu$, with μ = the pion mass, where only the following radiative decay modes are allowed: $\omega \to \pi^0+\gamma$, $\omega \to 2\pi^0+\gamma$, and $\omega \to \pi^+ + \pi^- + \gamma$. The ω cannot decay into two pions.

The present search was made assuming $m_\omega > 3m_\pi$, where the decay

$$\omega \to \pi^+ + \pi^- + \pi^0 \qquad (1)$$

is possible.[7] We have searched for such a 3-pion decay mode by studying the effective mass distribution of triplets of pions in the reaction

$$\bar{p}+p \to \pi^+ + \pi^+ + \pi^- + \pi^- + \pi^0. \qquad (2)$$

We have measured 2500 four-prong events produced by antiprotons of 1.61 Bev/c in the 72-inch hydrogen bubble chamber.[8] The c.m. energy is 2.29 Bev. Upon fitting these 2500 four-prong events by using our kinematics program KICK, 800 four-prong events had a $\chi^2 \leq 6.5$ for hypothesis (2) and would not fit the hypothesis that no π^0 was produced (610 of these 800 had a $\chi^2 < 2.5$).

The 800 four-prong events must have some small contamination of events in which two π^0's were produced, but inspection of the "missing mass" distribution convinces us that it is <7%. Other tests confirm this low contamination. For example, the angular distribution of the π^0 is symmetric within statistics, and the momentum of the π^0 resembles the momentum distribution of the charged pions.

We have evaluated the 3-body effective mass,

$$M_3 = [(E_1+E_2+E_3)^2 - (\vec{P}_1+\vec{P}_2+\vec{P}_3)^2]^{1/2}, \qquad (3)$$

for each pion triplet in Reaction (2). Each of the 800 four-prong events yields ten such quantities corresponding to the following charge states:

$$|Q|=0: \ \pi^+\pi^-\pi^0 \ (800\times 4 \text{ combinations}), \qquad (4)$$

$$|Q|=1: \ \pi^\pm\pi^\pm\pi^\pm \ (800\times 4 \text{ combinations}), \qquad (4')$$

and

$$|Q|=2: \ \pi^\pm\pi^\pm\pi^0 \ (800\times 2 \text{ combinations}). \qquad (4'')$$

For each value of M_3 as given by Eq. (4) we can calculate an uncertainty δM_3, by using the variance-covariance matrix of the fitted track variables, which is evaluated by KICK. By using these δM_3 we have formed the resolution function of M_3, and find that it has a half-width at half-maximum, $\Gamma_{\text{resol}}/2$, equal to 8.7 Mev. However, our input errors to KICK allow only for Coulomb scattering and estimated measurement accuracy, and do not account for optical distortion and unknown systematic errors. For example, our distributions have the correct shape but are too wide by a scale factor of about 2. This suggests that our average input error is too small by about $\sqrt{2}$. Hence, our estimate of δM_3 must be increased by about $\sqrt{2}$, and of $\Gamma_{\text{resol}}/2$ to 12 Mev. We chose 20-Mev histogram intervals for plotting our M_3 distribution.

In Fig. 1 we have plotted the M_3 distributions for the 800 Reactions (2). Distributions 1(A) and 1(B) are for charge combinations $|Q|=1$ and 2, respectively. The solid curves are an approximation to phase space.

The neutral M_3 distribution, 1(C), shows a peak centered at 787 Mev that contains 93 pion triplets above the phase-space estimate of 98. To contrast the difference between the neutral M_3 distribution and that for $|Q|>1$, we have replotted at the bottom of Fig. 1 both the neutral distribution and $\frac{2}{3}$ the sum of the $|Q|=1$ and $|Q|=2$ distributions.

Figure 2 shows the M_3 spectra with phase space subtracted. The absence of the peak in the $|Q|>0$ distributions determines the isotopic spin of the resonance,

$$T_\omega = 0.$$

The χ^2 distribution of the events in the "peak region" was compared with the χ^2 distribution of the events in the adjacent "control region," ranging from $M_3 \geq 820$ to $M_3 < 900$ Mev. These distributions agree with each other, which indicates that the events in the peak are genuine, rather than being caused by some unknown background reaction which was misinterpreted as Reaction

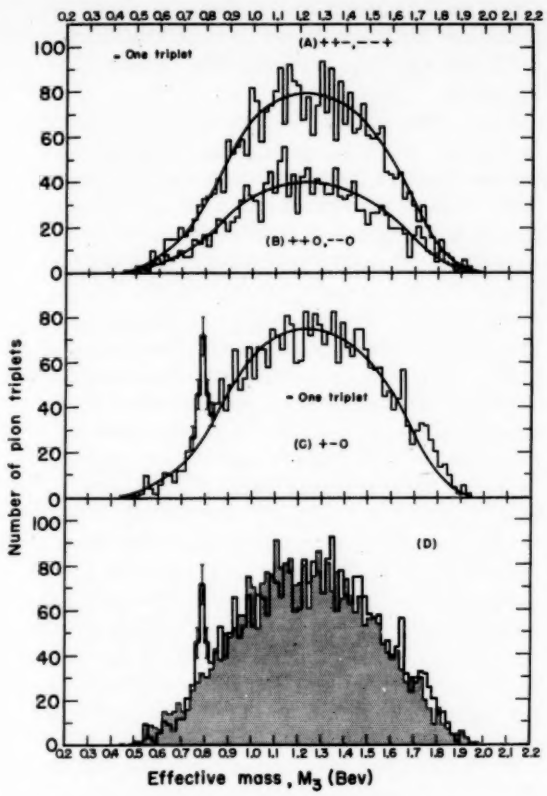

FIG. 1. Number of pion triplets versus effective mass (M_3) of the triplets for reaction $\bar{p}+p \to 2\pi^+ + 2\pi^- + \pi^0$. (A) is the distribution for the combination (4'), $|Q|=1$; (B) is for the combination (4''), $|Q|=2$; and (C) for (4), $Q=0$, with 3200, 1600, and 3200 triplets, respectively. Full width of one interval is 20 Mev. In (D), the combined distributions (A) and (B) (shaded area) are contrasted with distribution (C) (heavy line).

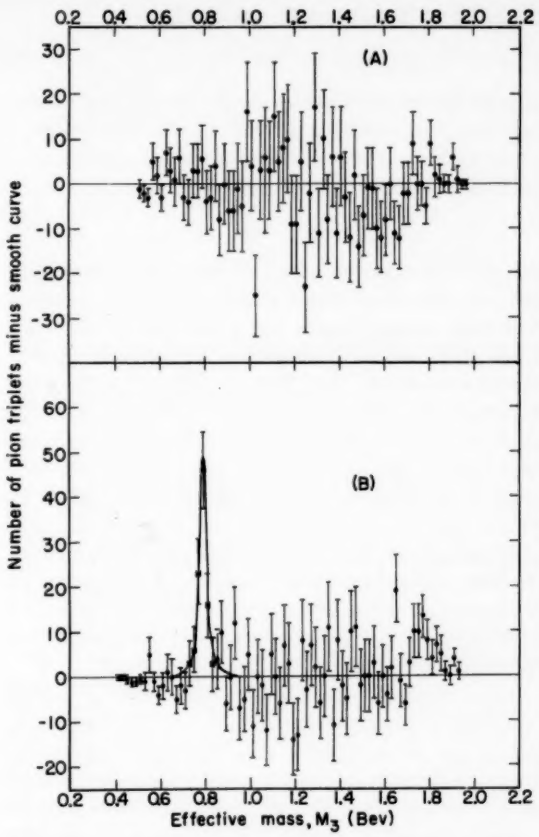

FIG. 2. (A) M_3 spectrum of the pion triplets in the combined distributions 1(A) and 1(B), with the smooth curve subtracted. (B) M_3 spectrum of the neutral pion triplets in distribution 1(C), again with the smooth background subtracted; a resonance curve is drawn through the peak at 787 Mev with $\Gamma/2=15$ Mev. The error flags are $\sqrt{N}$, where N is the total number of triplets per 20-Mev interval before subtraction of the smooth background curve.

(2). The missing-mass distributions in the two regions also agree with each other, thus supporting the above conclusion.

The peak in Fig. 2(B) appears to have a half-width $\Gamma/2<15$ Mev. This is so close to our resolution, $\Gamma_{\text{resol}}/2$, of 12 Mev that we cannot unfold it without further study and at present can only conclude that

$$M_\omega = 787 \text{ Mev},$$

and

$$\Gamma/2<15 \text{ Mev}. \qquad (5)$$

By using the uncertainty principle, we see that this half-width implies a mean life $\tau>4\times10^{-23}$ sec. Our ω's are produced with a typical c.m. momentum of 800 Mev/c, so that in a mean life they travel farther than 13 f.

We now assume that the ω peak is real, and want to estimate how many ω mesons it contains. As shown in Fig. 1(C), 191 triplets have M_3 values between 740 and 820 Mev. (We call this the "peak region.") However, these 191 triplets come from only 170 different four-prong events [i.e., 21 Reactions (2) have two values of M_3 in the peak region]. We use the charged M_3 distribution to estimate the background in the interval as 98 triplets, and then calculate a production of 83 ± 16 ω mesons out of 800 Reactions (2); i.e.,

$(10\pm 2)\%$ of Reactions (2) proceed via

$$\bar{p}+p\rightarrow\pi^{+}+\pi^{-}+\omega. \qquad (6)$$

Among the same 800 five-pion events, we have searched for—and found—the $T=J=1$ pion-pion resonance (ρ meson).[9] We found that approximately 30% of them proceed via

$$\bar{p}+p\rightarrow 2\pi+\rho. \qquad (7)$$

We have checked whether there is any correlation between the observed ρ mesons and the ω mesons. For each triplet inside the peak region, $740\leq M_3<820$ Mev, we have evaluated the effective mass of the remaining $\pi^{+}\pi^{-}$ doublet, M_2. The M_2 distribution is consistent with a continuum, starting from about 300 Mev, that has $(10\pm 2)\%$ of the doublets with values of M_2 in the region of ρ, which we took to be 750 ± 50 Mev. There is no evidence that the ω and the ρ are produced in association.

Although the masses of ω and ρ differ by only 35 Mev, we believe that they cannot be the same particle, because of their different widths (the $\Gamma/2$ for ρ being 40 Mev), isotopic spin, and G-conjugation parity—which forbids $2\pi\rightarrow 3\pi$.

In referring to the $T=0$ 3π resonance as ω, we have tacitly supposed that it is in fact a vector state with $J=1^{-}$. However, the spin and parity must be decided by experiment. Even if we assume the spin is <2, there are left three possibilities which are listed in Table I. A $T=0$ state of three pions must be antisymmetric in all pairs; hence all three pions must have different charges, i.e., $\pi^{0}\pi^{0}\pi^{0}$ is forbidden. The matrix element of the $\pi^{+}\pi^{-}\pi^{0}$ state is conveniently analyzed in terms of a single pion plus a di-pion. The pions of the di-pion are assigned momentum $\vec{P}$ and angular momentum $\vec{L}$ (in the di-pion rest frame). Then another pair of variables, $\vec{p}$ and $\vec{l}$, describe the remaining pion in the 3π rest frame. Because the state is antisymmetric in any pair, $\vec{L}$ must be odd; henceforth, we assume $L=1$. Then if $l=0$ we have a $J=1^{-}$ (i.e., vector) matrix element, as listed on the bottom line of Table I. Since three pions are involved, there is an intrinsic parity of $(-1)^{3}$, so that the corresponding "meson" is not V, but A.

If $l=1$, the matrix element can be 1+ (axial) or 0+ (scalar) corresponding, respectively, to a vector meson (ω) or a pseudoscalar (PS) meson.

Do we have enough data to distinguish between totally antisymmetric A vs S vs V matrix elements? It is convenient to make a Dalitz plot[10] [Fig. 3(D) for the peak region events, 3(A) for the control region events] that displays the threefold symmetry of three pions in an antisymmetric state. Unit area on a Dalitz plot is proportional to the corresponding Lorentz-invariant phase space, so that the density of plotted points is proportional to the square of the matrix element. It is easily shown that the size of the figure is proportional to $T_1+T_2+T_3=Q=m_{\omega}-(2m_{\pi^{\pm}}+m_{\pi^{0}})$.[11] Because of the finite width of the peak and the control regions, Q varies from event to event, so we use normalized variables, T_i/Q. The antisymmetry allows the plot to be folded about any median, so that in Figs. 3(C) and 3(B) all the data have been concentrated into $\frac{1}{6}$ of the plot area; the statistical distribution of the events is then more evident.

All three competing matrix elements, being antisymmetric, must vanish where any two pions "touch" in momentum space. If two pions touch, the third must have its maximum kinetic energy [regions (d), (f), and (b) on the plot]. The resonance region points [Figs. 3(C) and 3(D)] seem to show the required depopulation at points (d), (f), and (b).

More evident, however, on the plot is the fact that near $p=0$ [points (a), (c), and (e)] the density of peak-region points is only one half of that on the control plot. This is all the more suggestive when it is remembered that even the peak-region data contain only $(43\pm 7)\%$ resonance events. This depopulation at $p=0$ suggests an angular momen-

Table I. Possible three-pion resonances with $T=0$, $J\leq 1$.

"Meson" Type, $\vec{J}$	$\vec{l}$, $\vec{L}$	Matrix element Type, $\vec{J}$	Simple example	Vanishes at:
V, 1-	1, 1	A, 1+	$E_{-}(\vec{p}_0\times\vec{p}_{+})+E_0(\vec{p}_{+}\times\vec{p}_{-})+E_{+}(\vec{p}_{-}\times\vec{p}_0)$	whole boundary
PS, 0-	1, 1	S, 0+	$(E_{-}-E_0)(E_0-E_{+})(E_{+}-E_{-})$	$a,c,e+b,d,f$
A, 1+	0, 1	V, 1-	$E_{-}(\vec{p}_0-\vec{p}_{+})+E_0(\vec{p}_{+}-\vec{p}_{-})+E_{+}(\vec{p}_{-}-\vec{p}_0)$	b,d,f only

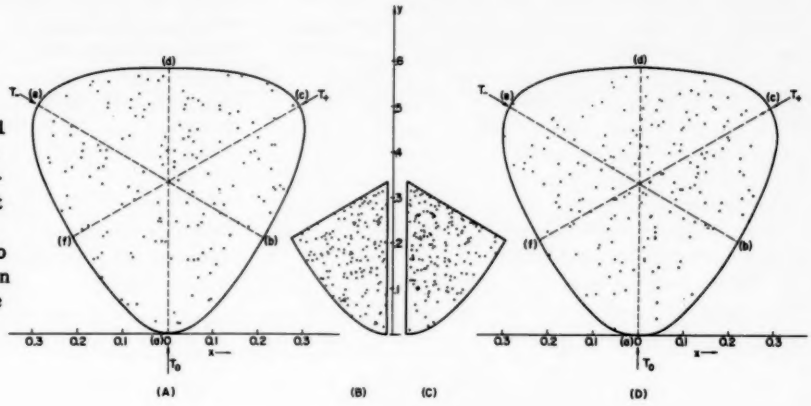

FIG. 3. (A): Dalitz plot of 171 triplets from the control region ($820 \leq M_3 < 900$); (B): folded control region plot; (D): Dalitz plot for 191 triplets in the peak region, $43 \pm 7\%$ of which are due to ω mesons; (C) folded peak region plot. T_+, T_-, and T_0 are kinetic energies of the π^+, π^-, and π^0, respectively.

tum barrier ($l > 0$) and constitutes mild evidence against a V matrix element (A meson).

The two stronger remaining candidates have A vs S matrix elements. The dashed lines in Fig. 3(D), as well as the two straight lines of the folded distribution in Fig. 3(C), correspond to equal energies of two pions. The scalar matrix element (S) of Table I vanishes when any two pions have the same energy, and therefore would require depopulation along these lines. This is not observed. An A matrix element has terms in $\vec{p}_i \times \vec{p}_j$, which vanish for collinear pions. The boundary of the plot represents collinearity, and seems indeed to be depopulated; although clearly more statistics and more detailed analysis such as investigation of polarization and alignment are needed.

We conclude that the data fit the qualitative criteria for an axial vector matrix element (ω meson); there is reasonable evidence against both an A meson and a PS meson.

The film used in this measurement was obtained in collaboration with J. Button, P. Eberhard, G. Kalbfleisch, J. Lannutti, G. Lynch, and N. H. Xuong; and this experiment would not have been possible without their help. It is a pleasure to thank Professor Murray Gell-Mann for his theoretical discussions. We wish to acknowledge the active participation of C. Tate, L. Champomier, A. Hussain, C. Rinfleisch, and F. Richards in the final stages of this experiment.

*Work done under the auspices of the U. S. Atomic Energy Commission.

[1]Y. Nambu, Phys. Rev. 106, 1366 (1957). See also S. Bergia, A. Stanghellini, S. Fubini, and C. Villi, Phys. Rev. Letters 6, 367 (1961); R. Blankenbecler and J. Tarski (to be published); G. Chew, R. Karplus S. Gasiorowicz, and F. Zachariasen, Phys. Rev. 110, 265 (1958); P. Federbush, M. Goldberger, and S. Treiman, Phys. Rev. 112, 642 (1958).

[2]G. F. Chew, Phys. Rev. Letters 4, 142 (1960). See also V. de Alfaro and B. Vitale, Phys. Rev. Letters 7, 72 (1961).

[3]J. Sakurai, Ann. Phys. 11, 1 (1960); Nuovo cimento 16, 388 (1960). See also V. I. Ogievetski and I. V. Polubarinov, Dubna Report D-676, 1961, submitted to J. Exptl. Theoret. Phys. (U.S.S.R.) for publication.

[4]M. Ikeda, S. Ogawa, and Y. Ohnuki, Progr. Theoret. Phys. (Kyoto) 22, 715 (1959); see also Y. Ohnuki, in Proceedings of the 1960 Annual International Conference on High-Energy Physics at Rochester (Interscience Publishers, Inc., New York, 1960); Y. Yamaguchi, Progr. Theoret. Phys. (Kyoto), Suppl. No. 11 (1959); J. Wess, Nuovo cimento 15, 52 (1960); Y. Neeman, Nuclear Phys. (to be published); A. Salam and J. C. Ward, Nuovo cimento (to be published); M. Gell-Mann (to be published); M. Gell-Mann and F. Zachariasen, Phys. Rev. (to be published).

[5]S. Sawada and M. Yonezawa, Progr. Theoret. Phys. (Kyoto) 22, 610 (1959). A somewhat similar particle was predicted by M. Johnson and E. Teller, Phys. Rev. 98, 783 (1955); H. Duerr and E. Teller, Phys. Rev. 101, 494 (1956); E. Teller, Proceedings of the Sixth Annual Rochester Conference on High-Energy Physics, 1956 (Interscience Publishers, New York, 1956); H. Duerr, Phys. Rev. 103, 469 (1956).

[6]A. Alberigi, C. Bernardini, R. Querzoli, G. Salvini, A. Silverman, and G. Stoppini (reported by G. Bernardini), in Ninth Annual International Conference on High-Energy Physics at Kiev, July, 1959 (Academy of Science U.S.S.R., Moscow, 1960), Vol. 1, p. 42; R. Gomez, H. Burkhardt, M. Daybell, H. Ruderman, M. Sands, and R. Talman, Phys. Rev. Letters 5, 170 (1960). A. Abashian, N. Booth, and K. Crowe, Phys. Rev. Letters 5, 258 (1960); 7, 35 (1961). J. Button, P. Eberhard, G. R. Kalbfleisch, J. Lannutti, S. Limentani, G. Lynch, B. Maglić, M. L. Stevenson, and N. H. Xuong (reported by F. Solmitz), in Proceedings of the 1960 Annual International Conference on High-Energy Physics at Rochester (Interscience Publishers, Inc., New York, 1960), p. 166; K. Berkelman, G. Cortellessa, and A. Reale, Phys. Rev. Letters 6, 234 (1961).

E. Pickup, F. Ayer, and E. O. Salant, Phys. Rev. Letters 5, 161 (1960); J. G. Rushbrooke and D. Radojčić, Phys. Rev. Letters 5, 567 (1960); J. Anderson, V. Bang, P. Burke, D. Carmony, and N. Schmitz, Phys. Rev. Letters 6, 365 (1961); A. R. Erwin, R. March, W. D. Walker, and E. West, Phys. Rev. Letters 6, 628 (1961); D. Stonehill, C. Baltay, H. Courant, and N. H. Xuong, Phys. Rev. 121, 1788 (1961).

[7]According to G. Sudarshan (University of Rochester, private communication) m_ω is expected to be within the limits $m_\rho < m_\omega < m_\rho + m_\pi$, where $m_\rho = 750$ Mev is the mass of the $T=J=1$ $\pi\pi$ resonance.

[8]J. Button, P. Eberhard, G. R. Kalbfleisch, J. E. Lannutti, G. R. Lynch, B. C. Maglić, M. L. Stevenson, and N. H. Xuong, Phys. Rev. 121, 1788 (1961).

[9]M. L. Stevenson, G. R. Kalbfleisch, B. C. Maglić, and A. H. Rosenfeld, Lawrence Radiation Laboratory Report UCRL-9814 (to be published). For previous evidence see: I. Derado, Nuovo cimento 15, 853 (1961); W. Fickinger, E. C. Fowler, H. Kraybill, J. Sandweiss, J. Sanford, and H. Taft, Phys. Rev. Letters 6, 624 (1961).

[10]R. Dalitz, Phil. Mag. 44, 1068 (1953). See also E. Fabri, Nuovo cimento 11, 479 (1954).

[11]Specifically, Q equals the height of the exscribed triangle.

TOTAL CROSS-SECTION MEASUREMENTS OF K^+-p AND K^+-n INTERACTIONS IN THE MOMENTUM REGION 0.77 TO 2.83 Bev/c*

V. Cook, D. Keefe, L. T. Kerth, P. G. Murphy,† W. A. Wenzel, and T. F. Zipf
Lawrence Radiation Laboratory, University of California, Berkeley, California
(Received July 31, 1961)

Total K^+-p and K^+-n cross-section measurements have been made previously up to 0.8 Bev/c with emulsions,[1] counters,[2] and bubble chambers,[3] in the region 0.8 to 2.4 Bev/c by the M.I.T. group,[4] and at momenta above 2.7 Bev/c by the CERN[5] and Dubna[6] groups. From the data of the M.I.T., Dubna, and CERN experiments, it is difficult to arrive at a satisfactory description of the K^+-p cross section, σ_p, in the region of a few Bev/c. At the highest momentum measured by the M.I.T. group (2.4 Bev/c), σ_p was found to be 12.9 ± 1.0 mb, whereas at 2.9 Bev/c, the CERN group found $\sigma_p = 24.5 \pm 2.5$ mb. The present experiment was undertaken partly for the purpose of resolving this difficulty.

The experimental technique was similar to that used by Cook et al. to measure K^--p total cross sections.[7] The beam is illustrated in Fig. 1. A feature of the present beam not encountered in the K^- beam described in reference 7 was that the high proton counting rate (approx 2×10^6/sec) could cause accidental background. This source of accidentals was eliminated with an anticoincidence circuit designed to reject any K^+ meson that was accompanied by another beam particle within a time of ± 50 mμsec.

The hydrogen-deuterium target was 4 ft long, 6 in. in diameter, made of 0.007-in. stainless steel, and was vacuum insulated. Two transmission counters, T_1 and T_2, were used. The T_1 counter was a 12-in. $\times$12-in. $\times\frac{1}{4}$-in. scintillator, and T_2 was a circular scintillator 9 in. in diameter and $\frac{1}{4}$

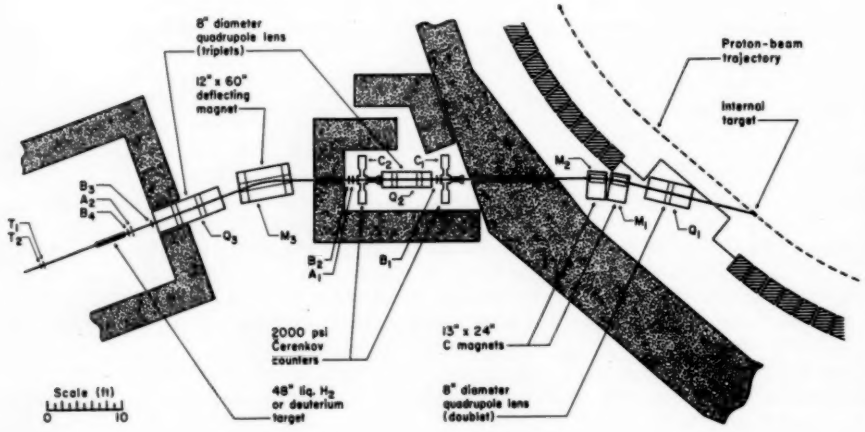

FIG. 1. Arrangement of the variable-momentum K^+ beam. M_1, M_2, and M_3 are bending magnets; Q_1, Q_2 and Q_3 are magnetic quadrupole lenses; B_1, B_2, B_3, and B_4 are coincidence counters; A_1 and A_2 anticoincidence counters; and C_1 and C_2 are gas Čerenkov counters. The transmission of the hydrogen target was measured by the scintillation counters T_1 and T_2.

Table I. Total cross sections: K^+-p, K^+-d, and K^+-n. The corrections that have been included are described in the text. The quoted errors include all known random uncertainties; in addition, there may be a systematic error of—at most—±0.3 mb, which would translate all values together. The σ_n has not been corrected for Pauli principle effects in the deuteron. The $\Delta\Omega_1$ is the solid angle subtended by T_1 at the center of the hydrogen target.

Momentum (Bev/c)	0.77	0.97	1.17	1.30	1.44	1.69	1.97	2.26	2.55	2.83
σ_p(mb)	13.0 ±0.9	15.4 ±0.6	18.1 ±0.6	17.9 ±0.9	18.1 ±0.7	17.5 ±0.6	16.9 ±0.4	17.1 ±0.5	17.1 ±0.6	16.7 ±0.5
σ_d(mb)	27.3 ±0.6	32.4 ±0.5	35.4 ±0.5	35.6 ±0.6	35.4 ±0.5	35.1 ±0.5	34.6 ±0.5	33.9 ±0.6	33.4 ±0.5	33.4 ±0.7
σ_n(mb)	15.5 ±1.1	17.8 ±0.8	18.2 ±0.8	18.5 ±1.1	18.1 ±0.9	18.5 ±0.8	18.6 ±0.6	17.7 ±0.8	17.1 ±0.8	17.5 ±0.9
$\Delta\Omega_1$(msr)	40.0	22.5	19.8	17.8	15.9	13.6	11.9	10.0	10.0	8.6

in. thick. The distance of T_1 and T_2 from the target was varied between 5 ft and 10 ft, depending on the momentum, to minimize the corrections for Coulomb scattering, decay in flight, etc. Several alternate "target full" and "target empty" runs were made at each momentum. The results are shown in Table I and are plotted in Figs. 2(a) and 2(b), together with data from other experiments.

Corrections have been included for the following: (a) There is a change in the decay-in-flight rate due to energy loss in the full target—this is largest at low momenta (approx 3 mb) but can be calculated reliably. (b) Forward scattering and forward recoil corrections to the hydrogen data were calculated using values for the 0-deg and 180-deg cross sections obtained by interpolation from angular-distribution measurements at 1.0, 1.2, and 2.0 Bev/c.[8] For the larger counter this correction amounted, at most, to 0.4 mb. The forward scattering corrections to the deuterium data were calculated using optical theorem values for the forward scattering cross sections. For the larger counter this correction varied from 0.5 mb to a maximum of 1.3 mb at the highest momentum. (c) Multiple scattering in the target introduced a correction to the smaller counter results at 770 Mev/c (0.7 mb) and 970 Mev/c (0.1 mb). (d) The Glauber screening correction,[9] used to derive σ_n from $\sigma_d - \sigma_p$, amounted to about 5% at all energies. In arriving at σ_n from $(\sigma_d - \sigma_p)$, a further correction should be applied for the effect of

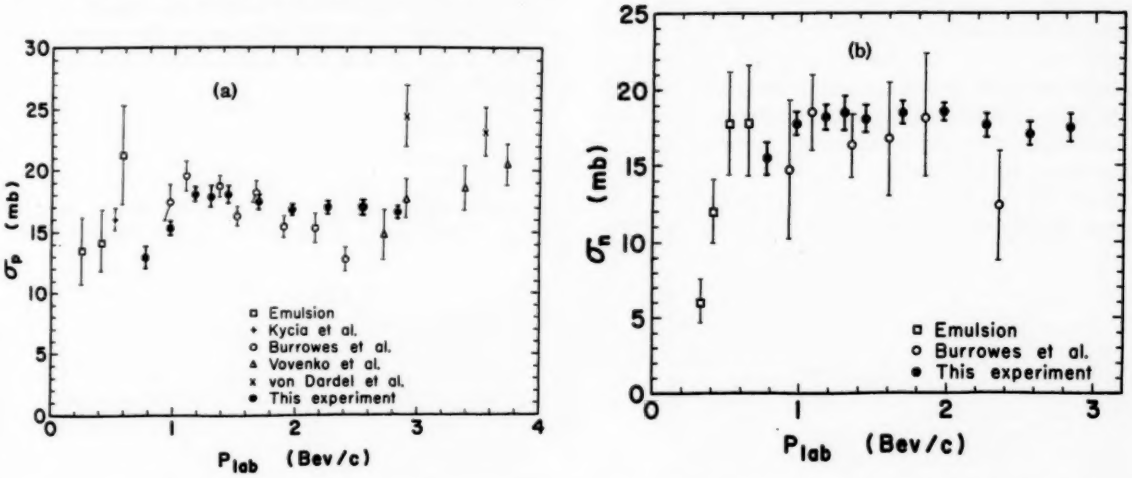

FIG. 2. The K^+ total cross sections as a function of momentum: (a) K^+-p cross section, σ_p, and (b) K^+-n cross section, σ_n.

the Pauli exclusion principle in suppressing forward charge-exchange scattering in deuterium. Until relevant data becomes available this correction cannot be estimated accurately, and therefore no correction was included.

There is a small systematic difference between the cross sections measured by the counters T_1 and T_2, the former giving a smaller value at each energy. The results given in Table I are averages of the corrected cross sections obtained from the two counters, and may therefore contain a systematic error of – at most – ±0.3 mb, affecting all the values equally.

Both σ_p and σ_n appear to remain remarkably constant at about 17 to 18 mb in the momentum range 1 to 3 Bev/c, implying that the $I=0$ and $I=1$ interactions are of approximately equal strength. The present measurements give a value of σ_p above that for the highest energy point of the M.I.T. group, below that for the lowest energy point of the CERN group, and in good agreement with the points of the Dubna group. At lower energies the present results are in good agreement with those of the M.I.T. group. The K^+-p cross section at 0.77 Bev/c is significantly below the value at higher energies, in agreement with recent bubble chamber measurements.[10]

The K^+-p interaction up to 0.8 Bev/c has been explained almost exclusively in terms of an S-wave interaction,[1-3] but it is clear that the approximately constant value of σ_p persisting to higher energies cannot be due to $I=0$ contributions alone, since $4\pi\lambda^2$ is 18 mb at 1.0 Bev/c and 10 mb at 1.5 Bev/c. The results of reference 8 show that there is a rapidly developing anisotropy in the elastic angular distribution at 1 Bev/c and above, indicating that higher angular momentum states contribute strongly to the elastic scattering at these energies. Furthermore, the K^+-p interaction shows an increasing contribution from inelastic processes above 1 Bev/c.

We wish to thank Dr. E. J. Lofgren and the Bevatron Operations Group. We are grateful to William Holley and Carl M. Noble, Jr., for their assistance in setting up and running the experiment and to C. Burton, R. Duncan, D. Linn, and G. Schnurmacher who contributed to the construction and assembly of the experimental apparatus.

---

*Work was done under the auspices of the U. S. Atomic Energy Commission.

†On leave from the Rutherford High-Energy Laboratory, Harwell, England.

[1]For summary, see D. Keefe, A. Kernan, A. Montwill, M. Grilli, L. Guerriero, and G. A. Salandin, Nuovo cimento 12, 241 (1959).

[2]T. F. Kycia, L. T. Kerth, and R. G. Baender, Phys. Rev. 118, 553 (1960).

[3]W. Chinowsky, G. Goldhaber, S. Goldhaber, W. Lee, T. O'Halloran, T. Stubbs, W. E. Slater, D. H. Stork, and H. K. Ticho, in Proceedings of the 1960 Annual International Conference on High-Energy Physics at Rochester (Interscience Publishers, Inc., New York, 1960), p. 451.

[4]H. C. Burrowes, D. O. Caldwell, D. H. Frisch, D. A. Hill, D. M. Ritson, and R. A. Schluter, Phys. Rev. Letters 2, 117 (1959).

[5]G. von Dardel, D. H. Frisch, D. Mermod, R. H. Milburn, P. A. Piroue, M. Vivargent, G. Weber, and K. Winter, Phys. Rev. Letters 5, 333 (1960).

[6]Chzan Nai-sen, Sui Yuin-chan, M. F. Lykhachev, and V. S. Stavinsky, in Proceedings of the 1960 Annual International Conference on High-Energy Physics at Rochester (Interscience Publishers, Inc., New York, 1960), p. 444; A. S. Vovenko, B. A. Kulakov, M. F. Lykhachev, A. L. Ljubimov, Ju. A. Matulenko, I. A. Savin, Ye. V. Smirnov, V. S. Stavinsky, Sui Yuin-chan, and Shzan Nai-sen, The Joint Institute for Nuclear Research, Dubna Report D721, May, 1961 (unpublished).

[7]V. Cook, B. Cork, T. F. Hoang, D. Keefe, L. T. Kerth, W. A. Wenzel, and T. F. Zipf, Phys. Rev. 123, 320 (1961).

[8]V. Cook, D. Keefe, L. T. Kerth, P. G. Murphy, W. A. Wenzel, and T. F. Zipf (to be published).

[9]R. J. Glauber, Phys. Rev. 100, 242 (1955).

[10]T. Stubbs, H. Bradner, W. Chinowsky, G. Goldhaber, S. Goldhaber, W. Slater, D. M. Stork, and H. K. Ticho, Phys. Rev. Letters 7, 188 (1961).

ANTIPROTON-PROTON AND PROTON-PROTON TOTAL CROSS SECTIONS FROM 4 TO 20 Bev/c*

S. J. Lindenbaum, W. A. Love, J. A. Niederer, S. Ozaki, J. J. Russell, and L. C. L. Yuan
Brookhaven National Laboratory, Upton, New York
(Received August 16, 1961)

Previous experiments have observed and compared the behavior of the $\bar{p}$-p total cross section[1,2] and the p-p total cross section[3,4] from low incident momenta (~3 Bev/c) to 10 Bev/c. Although the p-p cross section was slowly decreasing with increasing momentum from ≈44 mb to 40 mb, the $\bar{p}$-p cross section fell rapidly from ≈80 mb at 3 Bev/c to ≈50 mb at 10 Bev/c. The detailed behavior of the $\bar{p}$-p total cross section at even higher energies and comparison to the p-p total cross section was thought to be of considerable general interest, and also of specific interest due to a theorem of Pomeranchuk[5] which can be stated as follows: If one assumes that the total cross section of a particle β for a particle α becomes constant beyond an incident energy ϵ such that

$$\sigma_{\text{total}}(\alpha+\beta) = \text{const for energies} > \epsilon_1, \quad (1)$$

$$\sigma_{\text{total}}(\bar{\alpha}+\beta) = \text{const for energies} > \epsilon_2, \quad (2)$$

where $\bar{\alpha}$ is the antiparticle of α, then one can demonstrate on the basis of the forward dispersion relations that

$$\sigma_{\text{total}}(\bar{\alpha}+\beta) = \sigma_{\text{total}}(\alpha+\beta) \text{ for energies} > \epsilon, \quad (3)$$

where $\epsilon >$ both ϵ_1 and ϵ_2. Although the basic assumption of constant total cross sections at high energy which is made by Pomeranchuk's theorem represents reasonable physical intuition, there is of course no compelling reason to believe that this is necessarily so, and of course no good reason to believe that, even if an ϵ exists, it is in the 10-20 Bev energy region.

The p-p total cross section has previously been shown to be constant within the errors (~5%) from 10 to 28 Bev/c and appears to satisfy the basic assumption of Pomeranchuk's theorem provided it remains constant at higher energies. As previously mentioned, the $\bar{p}$-p total cross section was still decreasing up to 10.5 Bev/c, the highest momentum previously reported, where $\sigma_{\text{total}}(\bar{p}$-$p) - \sigma_{\text{total}}(p$-$p) \approx 10 \pm 3$ mb, so that Pomeranchuk's assumption was not yet satisfied.

Using the Brookhaven 33-Bev alternating gradient synchrotron the present investigation has determined the $\bar{p}$-p and p-p total cross sections at ~1-Bev/c intervals (except for two points) from 4 Bev/c to 20.3 Bev/c. It is found that Pomeranchuk's theorem is still not verified.

The experimental arrangement used for momenta above 9 Bev/c is shown in Fig. 1. Except for small corrections to the angle due to the synchrotron fringing field, the beam consists of particles emitted from the synchrotron target at 4.5°. The magnets Q_1, Q_2, B, Q_3, and Q_4 focus a beam of the desired momentum on scintillator S_3, 1 in. in diameter. The momentum of the system is defined to ~±2.5% by the proton beam size on the synchrotron target and S_3; the absolute scale of the momentum is uncertain by 2%. The particle compositions of these beams are given in a previous publication.[6] Typical $\bar{p}/\pi^-$ ratios were ~1% at low momenta, dropping to 0.2% at 20.3 Bev/c. Particles in the beam are identified by the focussing gas Čerenkov counter $\check{C}$. A schematic diagram of the optics of the counter is shown in Fig.

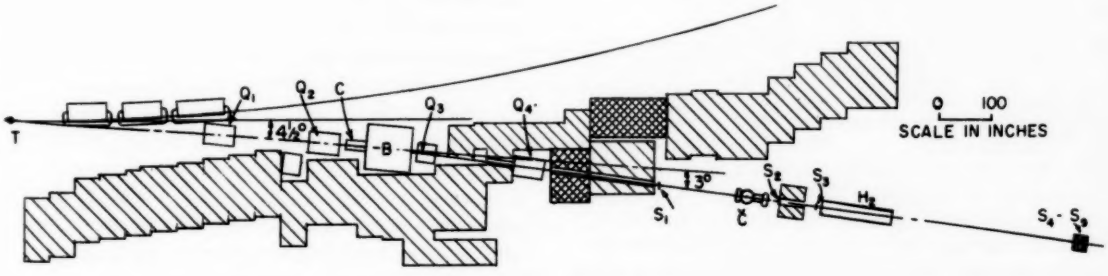

FIG. 1. Experimental arrangement. T, internal target; Q_{1-4}, Focussing magnets; C, collimator; B, analyzing magnet; S_{1-3}, beam-defining scintillators; $\check{C}$, velocity-selecting Čerenkov counter; H_2, liquid hydrogen target; S_{4-9}, scintillators for transmission measurement.

2(a). In Fig. 2(b) is shown a curve of the ratio $S_1S_2S_3\check{C}\bar{A}/S_1S_2S_3$ in the region of pressure corresponding to antiprotons at 16 Bev/c. As can be seen, there is a small background (~4%) at pressures at which the counter should not respond. It has been verified that these counts are due to incomplete rejection of pions and K mesons, and a correction of ~2% was made to the cross section for this effect. To measure the cross section alternate runs are made with a 10-foot long liquid-H_2-filled target and two Al plates which simulated the empty target. By requiring, in addition to the $(S_1S_2S_3\check{C}\bar{A})$ identification, a coincidence with one of the counters S_4-S_9, ranging from 4 to 12 in. in diameter (see Fig. 1), simultaneous measurements are made of the transmission of the hydrogen for six different geometries. A seventh channel measured accidental coincidences with the 12-in. counter delayed. The transmissions thus measured, of course, include particles scattered through small angles as well as secondaries produced in inelastic collisions in the target.

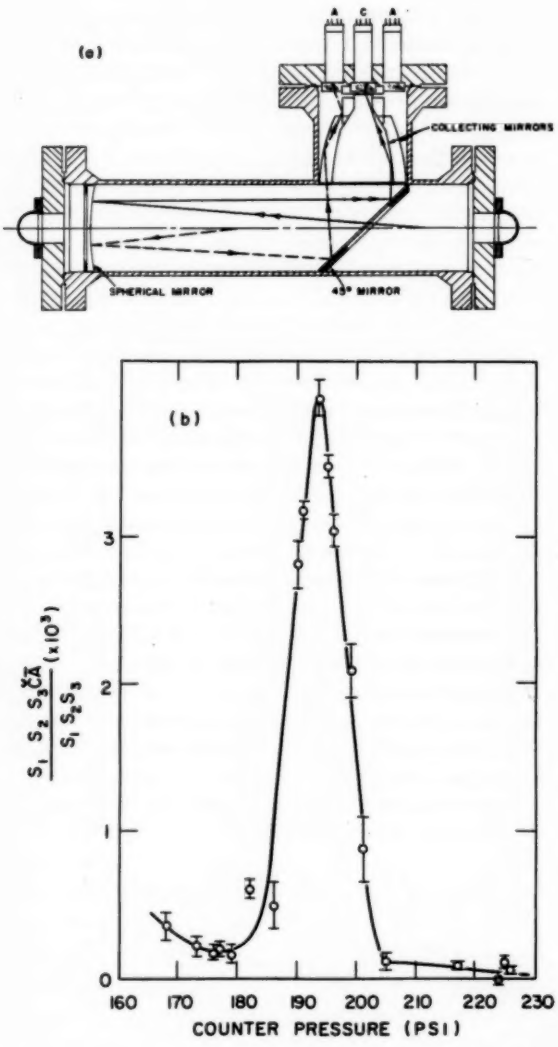

FIG. 2. (a) Velocity-selection Čerenkov counter. The solid ray is a typical ray from a particle with the desired velocity, and the broken ray is that from a particle with higher velocity. The first is counted in channel C, the second in channel A. (b) Čerenkov counter response in the region where 16-Bev/c antiprotons are expected to be detected.

By plotting the transmissions of the various counters S_4-S_9 against their respective areas and extrapolating to zero area, one obtains the proper transmission which should result from an experiment having an ideal "good geometry."

Cross sections at 4-10 Bev/c were obtained with an arrangement similar to that shown in Fig. 1 except that the beam used leaves the synchrotron target at 9° and the angle of bending in magnet B is 5.5°. The momentum resolution of this beam is ±1.5%. The Čerenkov counter described above was used to measure 6-10 Bev/c while at 4, 5, and 6 Bev/c a pair of smaller counters capable of withstanding higher gas pressures were used in tandem in order to obtain a high rejection ratio for pions.

At the lower momenta the effects of multiple Coulomb scattering in the hydrogen target are not negligible. Sternheimer's method[7] of correcting for this effect was used. The smallest counter at low momenta requires an appreciable correction and was used only as a monitor on the beam size during runs with the hydrogen removed.

The cross sections shown in Fig. 3 were obtained by plotting the ratio of transmission with hydrogen in to transmission with hydrogen out versus counter area; each transmission was corrected for accidental coincidences first. These were small for the $\bar{p}$-p but were as much as a few percent for some cases of p-p at low momenta where the proton beam rates were high. The corrected ratios, as is expected, lie on a linear plot since the angles subtended by the counters S_4-S_9 are small enough to be within the isotropic portion of the diffraction scattering peak. The smallest counter used in the extrapolation contains all but a negligible number of the singly Coulomb-scattered particles and hence no correction is required for this effect.

In Fig. 3 the errors shown are a combination of statistical errors and an estimated error on

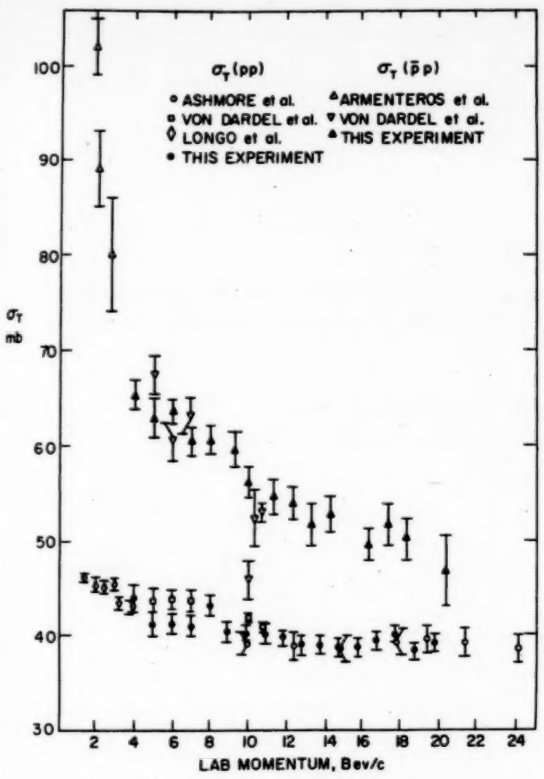

FIG. 3. Total $\bar{p}$-p and p-p cross sections.

the extrapolation to zero solid angle, an error associated with the multiple Coulomb scattering correction, and background errors.

It is clear that our results generally agree with the early measurements[2] of $\sigma_{total}(\bar{p}$-$p)$ up to 10.5 Bev/c, and with the earlier $\sigma_{total}(p$-$p)$ up to 28 Bev/c[4] which used a C-CH_2 difference instead of a liquid hydrogen target. There is no evidence from our measurements for any appreciable structure in either $\sigma_{total}(\bar{p}$-$p)$ or $\sigma_{total}(p$-$p)$. In fact, we also find that $\sigma_{total}(p$-$p)$ is constant within the errors from 10-12 Bev/c to 20 Bev/c with a value $\sigma_{total}(p$-$p) = 39.5 \pm 1$ mb. On the other hand, $\sigma_{total}(\bar{p}$-$p)$ appears to decrease monotonically from 10 Bev/c [where $\sigma_{total}(\bar{p}$-$p) = 58 \pm 4$ mb] to 20.3 Bev/c [where $\sigma_{total}(\bar{p}$-$p) = 48 \pm 4$ mb].

Amati, Fierz, and Glaser have shown[5] that in order to assure constancy of the cross sections at high energies and convergence of the integral

$$\int^{t=\infty} \frac{\sigma^-(E) - \sigma^+(E)}{E} dE, \qquad (4)$$

in which the particle cross section is $\sigma^+(E)$ and the antiparticle cross section is $\sigma^-(E)$, one must require that

$$[\sigma^-(E) - \sigma^+(E)] \to 0 \qquad (5)$$

faster than $1/\ln E$ as $E \to \infty$. The convergence of the above integral is necessary to give meaningful results for many dispersion relation treatments.

If we assume that the $\bar{p}$-p and p-p cross sections above 10 Bev/c have reached their limiting energy-dependence region, and if we assume the dependence to be $[\sigma^-(E) - \sigma^+(E)] \propto 1/\ln E$, then a fit of our data implies that $\sigma^-(E) - \sigma^+(E)$ may still be greater than 1 mb even for energies of several hundred Bev. Even if $\sigma^-(E) - \sigma^+(E)$ were to approach zero as fast as linearly with energy, it would appear from our data that the difference would not become zero before 35 Bev.

Von Dardel et al.[2] showed that $\sigma(K^-$-$p)$ was substantially larger than $\sigma(K^+$-$p)$ up to 8 Bev/c, where $\sigma_{total}(K^-$-$p) - \sigma_{total}(K^+$-$p) \approx 5 \pm 2$ mb. The results of their experiments as to whether $\sigma_{total}(\pi^-$-$p)$ and $\sigma_{total}(\pi^+$-$p)$ were the same or different up to 10 Bev/c were inconclusive due to possible experimental uncertainties. It was also not clear in these experiments that the cross sections at the higher energies were energy independent, but at least their energy variation appeared to be slow. Therefore, to date there has not been a clear demonstration of even a single case where Pomeranchuk's theorem was apparently applicable and verified.

The authors wish to acknowledge the cooperation of the AGS staff and the operating crew during these experiments. The authors also wish to acknowledge the assistance of J. Elias and C. Sinclair during these experiments.

---

*This work was performed under the auspicies of the U. S. Atomic Energy Commission.

[1]R. Armenteros, C. A. Coombes, B. Cook, G. R. Lambertson, and W. A. Wenzel, Phys. Rev. 119, 2068 (1960).

[2]G. von Dardel, D. H. Frisch, R. Mermod, R. H. Milburn, P. A. Piroue, M. Vivargent, G. Weber, and K. Winter, Phys. Rev. Letters 5, 333 (1960).

[3]M. J. Longo, J. A. Helland, W. N. Hess, B. J. Moyer, and V. Perez-Mendez, Phys. Rev. Letters 3, 568 (1959).

[4]A. Ashmore, G. Cocconi, A. M. Diddens, and A. M. Wetherell, Phys. Rev. Letters 5, 576 (1960).

[5]I. Pomeranchuk, J. Exptl. Theoret. Phys. (U.S.S.R.)

34, 725 (1958) [translation: Soviet Phys.-JETP 34, (7) 499 (1958)].

[6]W. F. Baker, R. L. Cool, E. W. Jenkins, T. F. Kycia, S. J. Lindenbaum, W. A. Love, D. Lüers, J. A. Niederer, S. Ozaki, A. L. Read, J. J. Russell, and L. C. L. Yuan, Phys. Rev. Letters 7, 101, (1961).

[7]R. M. Sternheimer, Rev. Sci. Instr. 25, 1070 (1954).

[8]D. Amati, M. Fierz, and V. Glaser, Phys. Rev. Letters 4, 89 (1960).

K^+-p INTERACTION AT 455 Mev*

Theodore F. Stubbs, Hugh Bradner, William Chinowsky, Gerson Goldhaber, and Sulamith Goldhaber
Lawrence Radiation Laboratory and Department of Physics, University of California, Berkeley, California

and

William Slater, Donald M. Stork, and Harold K. Ticho
Department of Physics, University of California, Los Angeles, California
(Received July 31, 1961)

We have undertaken a systematic study of the interaction of positive K mesons with hydrogen and deuterium in the energy interval from 0 to 455 Mev. Some preliminary results have already been reported.[1] In this note we present the results obtained for the elastic and inelastic K^+-p interaction at 455 Mev.

Previous investigations of K^+ interactions in nuclear emulsion[2] and propane[3] have yielded measurements of differential and total cross sections for the process $K^+ + p \rightarrow K^+ + p$ in the energy interval 40 to 300 Mev. The differential cross section at 225 Mev,[4] as well as the total cross sections in the range 175 Mev$< E_K <$8 Bev, have been measured by counter techniques.[5,6] The features of the K^+-p scattering from 80 to 300 Mev are that (a) the total cross section is approximately 14 mb, varying little, if at all, with energy; and (b) the angular distribution is isotropic.

The Lawrence Radiation Laboratory 15-inch hydrogen bubble chamber was exposed to a separated beam of K^+ mesons produced by the 6-Bev circulating protons of the Bevatron (Fig. 1). The system was designed for a momentum of 645 Mev/c. With adjustment of the magnet parameters it was possible to obtain the higher momentum of 810 Mev/c ($T_K \approx 455$ Mev). A mass-resolution curve at 810 Mev/c for the separation system is shown in Fig. 2. The background of light particles (pions, muons, and electrons) was approximately 10%; the pion component is analyzed in more detail below.

The initial sample of events, chosen to satisfy geometric and incident-momentum criteria, contained both inelastic and elastic K^+ interactions and also a background of π^+ interactions. Kine-

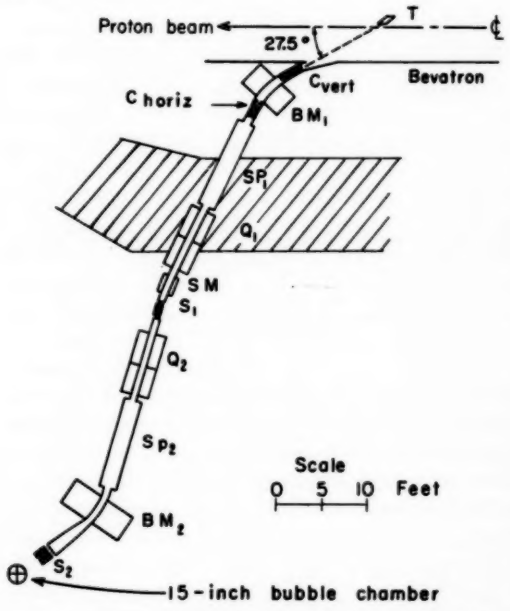

FIG. 1. Layout of the separated K^+ beam. The beam design was similar to a separated K^- beam designed earlier [P. Eberhard, M. Good, and H. K. Ticho, Rev. Sci. Instr. 31, 1054 (1960)], and is described in detail in G. Goldhaber, S. Goldhaber, J. Kadyk, T. Stubbs, D. H. Stork, and H. K. Ticho, Lawrence Radiation Laboratory Internal Report Bev-483, February 26, 1960 (unpublished). The K^+ beam from the target (T) is focused by the quadrupole Q_1 onto slit S_1. The momentum selection is effected by bending magnet BM_1, and the subsequent mass separation by the crossed electric and magnetic field in spectrometer Sp_1. The second state is essentially a mirror image of the first. The steering magnet SM was introduced for additional freedom in the horizontal plane. C_{horiz} and C_{vert} are horizontal and vertical collimators, respectively.

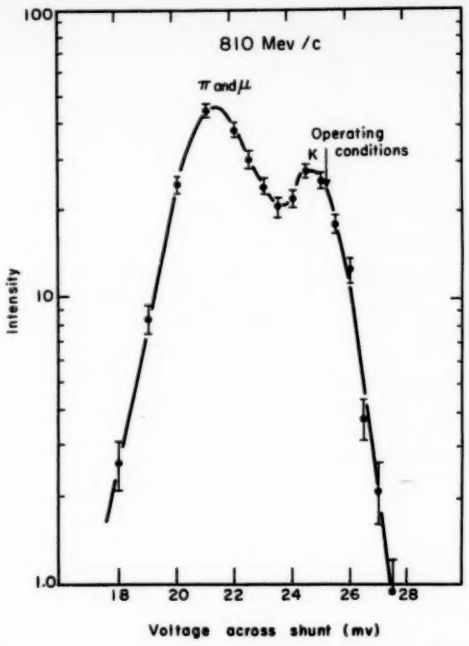

FIG. 2. Mass analysis of particles emerging from slot S_1 in Fig. 1. This curve was obtained by setting spectrometer Sp_1 to transmit K mesons and varying the magnetic field in spectrometer Sp_2. One thus obtains a mass analysis of particles leaving slit S_1. The final operating conditions for Sp_2 are indicated by the arrow.

matical fitting procedure (with further evidence from estimates of bubble density of the secondary tracks) provides means of separating the elastic from inelastic interactions with essentially complete certainty. The pion elastic scatterings are distinguishable from K^+ elastic scatterings for $\cos\theta_\pi^{\text{c.m.}} < 0.4$. To determine the total number of pion scatterings, we use the π^+-p angular distribution[7] to evaluate the number of such events in the remaining angular interval $0.4 < \cos\theta_\pi^{\text{c.m.}} < 0.96$. This number (i.e., 31 events) is then subtracted from the group consistent with K^+-p elastic scatterings. The observed number of π^+ inelastic interactions (i.e., 29 events) is in agreement with the sum of observed and inferred numbers of π^+ elastic interactions. The contamination of pion inelastic scatterings in the sample of K^+-p elastic scatterings is thus negligible. We accepted only those scatterings with $\cos\theta_K^{\text{c.m.}} < 0.96$ in order to preclude any effects of low efficiency for detecting small-angle scattering. We find, then, a total of 1330 elastic K^+-p scatterings satisfying the above conditions. The total K^+ path length was determined by three independent methods:

(a) From K^+ decays into three charged secondaries (316 decays) and the known branching ratio,[8] $b_1 = 0.061 \pm 0.002$ for these decay modes; this yields a total path length of $(3.12 \pm 0.25) \times 10^6$ cm.

(b) From K^+ decays into one charged secondary with projected angle $\theta_{\text{lab}} > 27.5$ deg. This cutoff angle was introduced in order to avoid possible confusion with K^+-p scatterings without observable recoil. The decays included in this sample correspond to a fraction $b_2 = 0.29 \pm 0.01$ of all K^+ decays. A total path length of $(2.93 \pm 0.14) \times 10^6$ cm is obtained by this method.

(c) From a direct count of tracks passing through the chamber. After corrections for light-particle contamination, decays, and interactions, we obtain a total path length of[9] $(2.96 \pm 0.16) \times 10^6$ cm. The weighted average of the path lengths obtained by the above three methods is $L_{\text{total}} = (2.97 \pm 0.09) \times 10^6$ cm. Correcting for the scanning efficiency for elastic scattering, $\epsilon_s = 0.997$, and decays, $\epsilon_d = 0.994$, and extrapolating the angular distribution (considered as flat) to $\cos\theta_{\text{c.m.}} = 1.0$, we obtain the total elastic-scattering cross section, at 455 ± 5 Mev, $\sigma_{\text{el}} = 13.0 \pm 0.7$ mb. This cross section contains some Coulomb effects below $\cos\theta_K^{\text{c.m.}} = 0.96$, and is to be compared with the purely nuclear cross sections as deduced from the phase-shift analyses below. The error includes the uncertainties in the path-length determinations and statistical error in the number of scatterings. For the inelastic K^+-p interactions, discussed below, we obtain a cross section $\sigma_{\text{inel}} = 1.0 \pm 0.2$ mb.

The differential cross section plotted in Fig. 3 shows only a small angular dependence. We analyzed the data in terms of s- and p-wave scattering for the elastic and inelastic interaction.

We can thus write the differential cross section as

$$\left(\frac{d\sigma}{d\Omega}\right)_{\text{el}} = \frac{1}{4k^2}\left\{\left|\frac{-i\alpha}{\sin^2(\theta/2)}\exp[-i\alpha\ln\sin^2(\theta/2)] + \eta_1 e^{2i\delta_1} - 1 + \frac{1+i\alpha}{1-i\alpha}(\eta_{11}e^{2i\delta_{11}} + 2\eta_{13}e^{2i\delta_{13}} - 3)\cos\theta\right|^2 + |\eta_{11}e^{2i\delta_{11}} - \eta_{13}e^{2i\delta_{13}}|^2 \sin^2\theta\right\}, \quad (1)$$

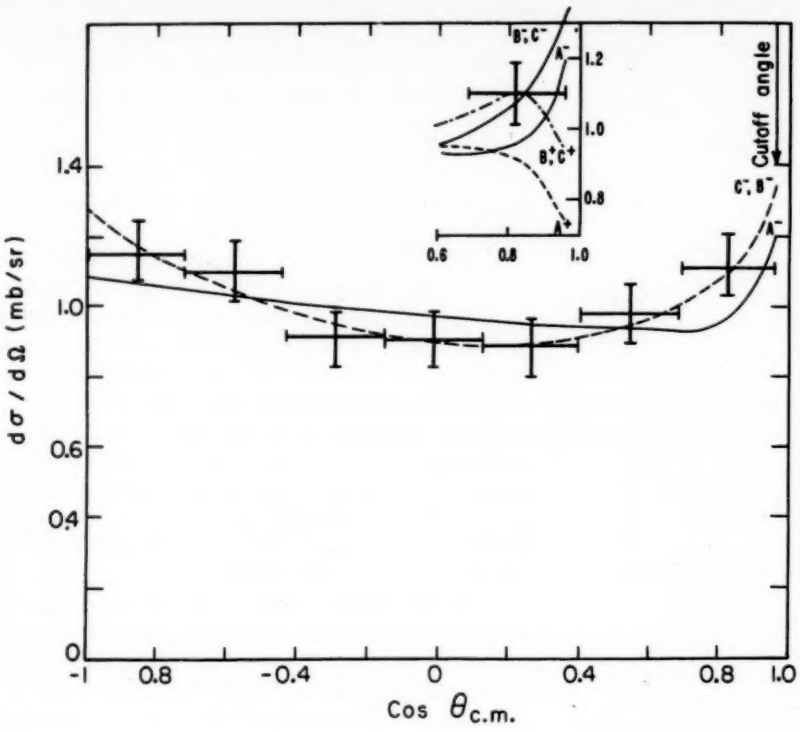

FIG. 3. The $K^+ + H$ elastic differential cross section at 455 Mev. The results correspond to 1320 scattering events. The curves are computed from the various "best fit" phase shifts as given in Table I. Sets B^-, C^-, and B^+C^+ give essentially identical differential cross-section curves. For clarity, only Set A^- and Set B^- and C^- are shown in the main figure. The inset shows the small-angle behavior of all the phase-shift solutions.

and the inelastic cross section as

$$\sigma_{\text{inel}} = \frac{\pi}{k^2}[(1-\eta_1^2)+(1-\eta_{11}^2)+2(1-\eta_{13}^2)]. \qquad (2)$$

Here $\alpha = e^2/\hbar v_{\text{rel}}$, θ is the c.m. scattering angle, $\hbar k$ the c.m. momentum, and v_{rel} the relative velocity[10]; δ_1, δ_{11}, and δ_{13} are the $s_{1/2}$, $p_{1/2}$, and $p_{3/2}$ $T=1$ phase shifts, respectively, and η_1, η_{11}, and η_{13} correspond to the imaginary part of these phase shifts. For simplicity we have assumed that the inelastic scattering occurs principally in one of the three scattering amplitudes. Solutions for the phase shifts were obtained by setting two of the absorbitive amplitudes η, equal to unity and obtaining the third one from (2). The solutions are rather insensitive as to which phase shift was chosen as complex. In Table I and Fig. 3 we give the solutions corresponding to $\eta_1 = 0.92 \pm 0.2$ and $\eta_{11} = \eta_{13} \equiv 1$.

There are three sets of phase-shift solutions.

Set A: A dominant s-wave solution. The sign of the $s_{1/2}$ phase shift can be seen to be most probably negative in agreement with earlier results at lower energy.[4,11]

Set B: A dominant $p_{1/2}$ solution which is the Minami ambiguity corresponding to Set A. A unique determination of the sign of δ_{11} from our data is not possible because Coulomb interference here occurs at smaller angles than for solution A.

Set C: A combination of $p_{1/2}$ and $p_{3/2}$ amplitudes such as to reproduce near isotropy with an ambiguity in sign. This is the Fermi-Yang ambiguity corresponding to solution B. If we consider the evidence for a repulsive (i.e., positive) nuclear potential from the emulsion data[2,11] whose largest contribution comes from the forward scattering amplitude in the $T=1$ state; viz., $V \sim -\mathrm{Re}[0.75 f_1(0) + 0.25 f_0(0)]$, we can infer the sign of the dominant phase shifts. For reasonable values of $f_0(0)$ this would rule out solutions A^+, B^+, and C^+.

Isotropy and little variation of the scattering cross section dominate the K^+-p interaction throughout the energy interval up to 455 Mev. To ascribe the scattering to predominant repulsive s-wave interaction even at 455 Mev (Set A^-) does imply an anomalously low p-wave interaction. A $p_{1/2}$ solution (Minami ambiguity) can clearly fit an isotropic distribution at any energy. The near constancy of the cross section, however, over the large energy interval makes a dominant $p_{1/2}$ (Set B) or $p_{1/2}$-$p_{3/2}$ mixture (Set C) solution rather unlikely. At this point we would

Table I. Phase shifts for K^+-nucleon scattering at 455 Mev in the $T=1$ state.[a]

Solution	Phase shifts (deg) δ_1	δ_{11}	δ_{13}	Probability from a χ^2 fit	σ_{el}[b] (mb)
A^-	-47 ±1	0.5 ±4.5	1.5 ±2.5	0.15	12.2 ±0.4
A^+	49 ±1	- 0.5 ±4	0 ±2	0.01	13.0 ±0.4
B^-	4.5 ±2	-45.5 ±1	- 2.5 ±1	0.92	12.6 ±0.5
B^+	- 1.5 ±1.5	46.5 ±1	4 ±1	0.73	13.0 ±0.5
C^-	4.5 ±2	14.5 ±1.5	-28 ±1	0.92	12.5 ±0.5
C^+	- 1.5 ±2	-13.5 ±1.5	29 ±1	0.73	13.0 ±0.5

[a]The solutions given here are computed for $\eta_1=0.92$, $\eta_{11}=\eta_{13}\equiv 1$. If we take $\eta_{11}=0.92$ and $\eta_1=\eta_{13}\equiv 11$, for example, Solution A^- becomes $\delta_1=-45°$, $\delta_{11}=3.5°$, $\delta_{13}=1.5°$.

[b]This is the nuclear elastic cross section computed from the respective phase shifts leaving out the Coulomb terms. The errors reflect the errors on the respective phase shifts.

like to emphasize that we have not explored combinations of s, p, and d waves, which will, of course, also reproduce the K^+-p scattering process. As is well known from the proton-proton interaction, certain combinations of several angular momentum states can reproduce isotropic and energy-independent differential cross sections over appreciable energy intervals.

As can be seen from the inset in Fig. 3, a precise measurement of the scattering at small angles can distinguish between dominant s and dominant p solutions because of the difference in the respective Coulomb interference. Similarly, polarization measurements of the recoil proton could determine the presence of a mixture of $p_{1/2}$ and $p_{3/2}$ amplitudes or possibly higher partial waves. Scattering in the $s_{1/2}$ and in the pure $p_{1/2}$ states, respectively, does not give rise to polarization.

Inelastic interactions of positive K mesons with single pion production can proceed via three possible channels. Among the 102 inelastic scatterings recorded in the chamber, we observed examples of all three modes of pion production. Table II summarizes the results.

Those examples of Reaction I with subsequent K_1^0 decay are readily identifiable; 25 were observed. For a K_1^0 branching of $\frac{2}{3}$ into charged pions, these events should represent $\frac{1}{3}$ of all K^0 mesons produced in Reaction I. If all ambiguous inelastic scatterings belong to channel I(b), the observed ratio is consistent with that expected. In any event it is clear that Reaction I dominates strongly. It is interesting to note that if the K and π mesons were produced in a total isotopic spin state of $T=\frac{1}{2}$, the ratio of the rates of Reactions I, II, and III would be 2:1:0, while production of the π meson and nucleon in the $T=\frac{3}{2}$ state would yield at ratio 9:2:1. The data are suggestive of a dynamical effect which may be due to an enhancement in the production in one of these isotopic spin states.

We wish to thank Professor Luis W. Alvarez and many members of his group for making the 15-inch bubble chamber and analyzing facilities available to us. We are very grateful for the tireless efforts of the bubble chamber crew and the Bevatron crew as well as our own scanning

Table II. Pion production in K^+-p collisions.

	Channel	Number of events
I	(a) $K^+ + p \to K_1^0 + \pi^+ + p$, $K_1^0 \to \pi^+ + \pi^-$	25
	(b) $K^+ + p \to K^0 + \pi^+ + p$, $K^0 \to K_2^0$ or neutral decay of K_1^0	35
II	$K^+ + p \to K^+ + \pi^0 + p$	24
III	$K^+ + p \to K^+ + \pi^+ + n$	8
	Ambiguous—I(b) or III	10
	Total[a]	102

[a]Included in this number are nine events also consistent with π-p inelastic scatterings.

and measuring group, without whose assistance this experiment would not have been possible. We would also like to acknowledge the important contributions of Thomas O'Halloran and Dr. Won-yong Lee.

---

*This work was done under the auspices of the U. S. Atomic Energy Commission.

[1]W. Chinowsky, G. Goldhaber, S. Goldhaber, W. Lee, T. O'Halloran, T. F. Stubbs, W. Slater, D. H. Stork, and H. K. Ticho, in Proceedings of the 1960 Annual International Conference on High-Energy Physics at Rochester (Interscience Publishers, New York, 1960), p. 451.

[2]See, for instance, J. E. Lannutti, G. Goldhaber, S. Goldhaber, W. W. Chupp, S. Giambuzzi, C. Marchi, G. Quareni, and A. Wataghin, Phys. Rev. 109, 2121 (1958); D. Keefe, A. Kernan, A. Montwill, M. Grilli, L. Guerriero, and G. A. Salandin, Nuovo cimento 12, 241 (1959).

[3]D. I. Meyer, M. L. Perl, and D. A. Glaser, Phys. Rev. 107, 279 (1957).

[4]T. F. Kycia, L. T. Kerth, and R. G. Baender, Phys. Rev. 118, 553 (1960).

[5]H. C. Burrowes, D. O. Caldwell, D. H. Frisch, D. A. Hill, D. M. Ritson, and R. A. Schluter, Phys. Rev. Letters 2, 117 (1959).

[6]G. Von Dardel, D. H. Frisch, R. Mermod, R. H. Milburn, P. A. Piroué, M. Vivargent, G. Weber, and K. Winter, Phys. Rev. Letters 5, 333 (1960).

[7]We have used unpublished data of Peter Newcomb and Wilson F. Powell (Lawrence Radiation Laboratory), on π^+ interactions at 740 Mev/c, it being assumed that this angular distribution is not significantly different from that at 812 Mev/c. These data indicate an inelastic cross section approximately 25% of the total. We are grateful to the above authors for permission to use their data in advance of publication.

[8]This number is a weighted average of results quoted by L. B. Okun, Ann. Rev. Nuclear Sci. 9, 61 (1959), and our own measurements on stopping K^+ mesons. In both cases the branching ratio obtained for these decay modes was $b_1 = 0.061 \pm 0.003$.

[9]The uncertainty in the path length by this method comes from the reproducibility of the count, the determination of the contamination, and the statistics of the number of tracks.

[10]Here $v_{rel} = v_{lab}$ of the K meson. This is essentially the relativistic form given by F. Solmitz [Phys. Rev. 94, 1799 (1954)] in the small-angle region.

[11]See, for instance, G. Igo, D. G. Ravenhall, J. J. Tiemann, W. W. Chupp, G. Goldhaber, S. Goldhaber, J. E. Lannutti, and R. M. Thaler, Phys. Rev. 109, 2133 (1958); M. A. Melkanoff, O. R. Price, D. H. Stork, and H. K. Ticho, Phys. Rev. 113, 1303 (1959); B. Sechi-Zorn and G. T. Zorn, Phys. Rev. 120, 1898 (1960).

π-π RESONANCE IN π^--p INTERACTIONS AT 1.25 Bev*

E. Pickup,† D. K. Robinson, and E. O. Salant
Brookhaven National Laboratory, Upton, New York
(Received August 14, 1961)

It has become apparent that π-π interactions are important in π-p collisions in the Bev region. Several experiments on single-pion production[1-6] have shown that there is an excess of nucleons at low laboratory kinetic energies over that which would be expected on a statistical or isobar theory. Goebel[7] has pointed out that such an excess would be indicative of a π-π interaction. Fraser and Fulco[8] showed that a π-π resonance in an $I=1$, $J=1$ state could explain features of electron-nucleon scattering, and suggested a resonance at $w^2 \simeq 10\mu^2$, where w is the total energy of the two pions in the π-π rest frame, and μ is the pion rest mass ($w = Q + 2\mu$). Later calculations[9] suggested that the resonance was at $w^2 \simeq 22\mu^2$. Indications of a π-π resonance in π-p interactions have been obtained in several experiments,[5,6,10-12] but the results were limited by low incident pion energies, or by statistics. With the higher statistics available in the present work, strong evidence is obtained for a π-π resonance in an $I=1$ state.

As part of a study of π-p interactions, using the bubble chamber technique, we have measured 4000 π^--p events at 1.25-Bev incident pion energy. 968 events of the type

$$\pi^- + p \rightarrow \pi^- + \pi^+ + n, \tag{1}$$

and 566 of the type

$$\pi^- + p \rightarrow \pi^- + \pi^0 + p, \tag{2}$$

have been identified using the GUTS kinematic fitting program, and ionization density measurements.

Comparison of the pion momentum spectra with the predictions of the extended isobar model[13] indicate that pion production through isobar formation is not the dominant process at this energy.

The nucleons from both reactions are produced predominantly backward in the c.m. system, and thus are peaked at low laboratory kinetic energies. Figures 1(a) and (b) show the nucleon laboratory kinetic energy, T, for reactions (1) and (2), respectively. The curves in Fig. 1 were computed assuming a constant π-π cross section, $\sigma_{\pi-\pi}$, from the equation given by Chew and Low[14]:

$$\frac{\partial^2\sigma}{\partial\Delta^2\partial w^2} \xrightarrow[\Delta^2\to-\mu^2]{} \frac{f^2}{2\pi}\frac{\Delta^2/\mu^2}{(\Delta^2+\mu^2)^2}\frac{w}{q_{1L}}(\tfrac{1}{4}w^2-\mu^2)^{1/2}\sigma_{\pi-\pi}, \quad (3)$$

where Δ is the four-momentum transfer to the nucleon ($\Delta^2 = 2MT$), f^2 is the renormalized pion coupling constant and q_{1L} is the laboratory momentum of the incident pion. The theoretical curves are normalized to the total numbers of events in the histograms. The theoretical and experimental distributions seem to agree at low momentum transfers, but the histograms are more sharply peaked than would be expected.[15]

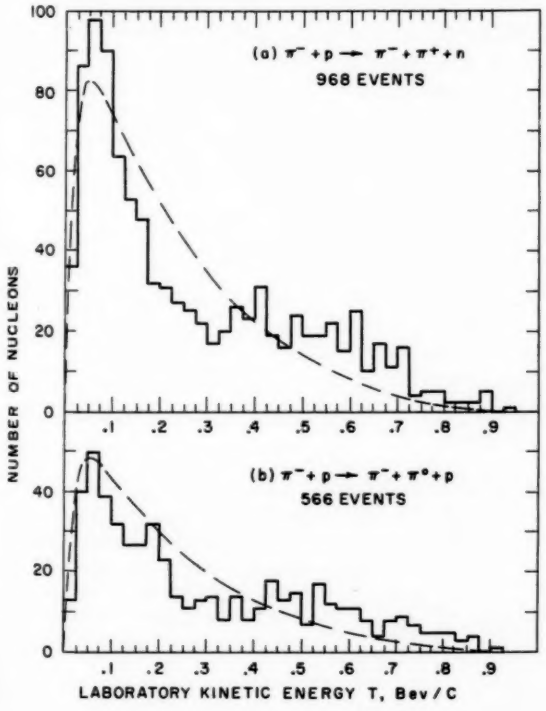

FIG. 1. Histogram of nucleon laboratory kinetic energies. The curve was calculated from the Chew-Low equation, for constant $\sigma_{\pi-\pi}$.

There is also a group of high-momentum-transfer events, not expected on a one-pion exchange model.

Figure 2 shows Q values for π^--π^+ and π^--π^0 systems, and also the prediction of the statistical model. The isobar prediction is similar to the latter. Both histograms exhibit well-defined peaks at the same Q value. The agreement in position of the two Q peaks suggests that the same π-π resonance state is dominant in both reactions. It follows, therefore, that isotopic spin $I = 0$ is excluded for this state.

The branching ratio for reactions (1) and (2), $R = \sigma(2)/\sigma(1) = 0.585 \pm 0.031$, and the ratio, $R_{\pi-\pi}$, for events in the $Q_{\pi-\pi}$ peaks (400 Mev < $Q_{\pi-\pi}$ < 550 Mev), is 0.50 ± 0.04. The one-pion exchange model predicts that $R_{\pi-\pi} = \frac{1}{2}$ for a π-π interaction

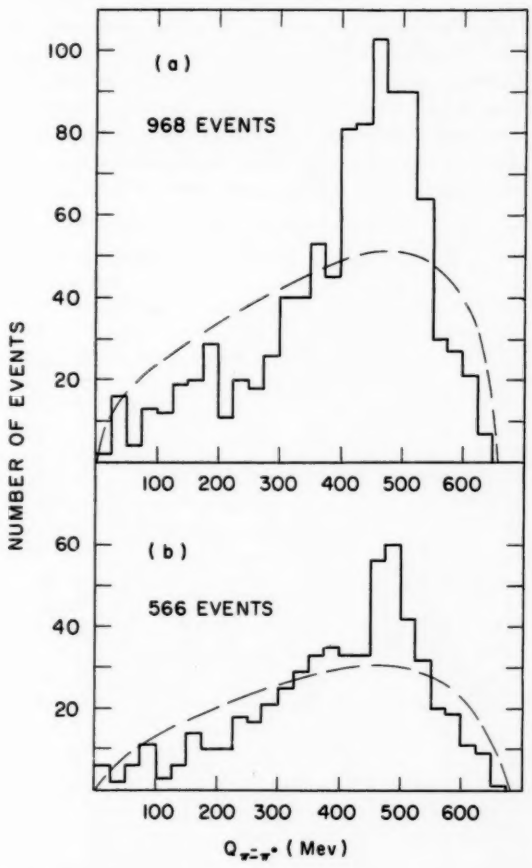

FIG. 2. Q-value distributions for π-π system for all events, for (a) $\pi^- + p \to \pi^- + \pi^+ + n$, (b) $\pi^- + p \to \pi^- + \pi^0 + p$; the dashed curves are from statistical theory.

in a pure $I=1$ state, and $\frac{8}{5}$ for $I=2$. The model is more likely to be valid if we select events with small Δ^2. Restricting the selection of events in the Q peak to those with $\Delta^2<10\mu^2$, or $T<104$ Mev, we obtain $R_{\pi-\pi}=0.42\pm0.06$. The data are in agreement with the predictions of the model for $I=1$. This state is further suggested by the Yale π^+-p experiment at 1.26 Bev,[11] by comparing the π^+-π^0 and π^+-π^+ Q distributions.

The π-π cross section, as a function of w^2, was calculated by integrating Eq. (3) up to $\Delta^2=10\mu^2$, assuming this equation to be valid in the physical region. Comparison of the experimental and theoretical distributions in Fig. 1 indicates that this may be a reliable procedure for small Δ^2.[16] Figure 3 shows $\sigma_{\pi-\pi}$ obtained in this way, for the combined events from reactions (1) and (2). The background on the low-energy side of the resonance is associated with both reactions. This would seem to eliminate a pure $I=0$ low-energy effect. We obtain $\sigma_{\pi-\pi}=95$ mb at the peak, $w^2=29\mu^2$ ($Q=475\pm10$ Mev). The full width at half maximum is 130 Mev. These values, and the values determined at 1.74 Bev by Erwin et al.[12] agree within statistics. This agreement between results at two quite different energies implies that there is, indeed, a resonance, π^*, in the π-π system.

The decay angle, δ, between the direction of the π^- in the rest frame of π^* and the c.m. direction of π^*, was calculated. In Figs. 4(a) and (b) the distributions of events in the Q peaks show backward-forward symmetry, but a marked departure from isotropy. Restricting the selection to events with small Δ^2 shows that the anisotropy is mainly associated with such events. For events outside the Q peak, the asymmetries observed in both reactions (1) and (2) are consistent with some $(\frac{3}{2},\frac{3}{2})$ π-p isobar formation.

To investigate angular momentum states involved in the π^* resonance, the angle, α, between the direction of the π^- in the rest frame of π^* and the direction of the incident pion, was calculated. Events were selected in which π^* was emitted closely parallel or antiparallel to the incident pion direction ($|\cos\theta|\geq0.9$).[17] Provided that the Adair analysis[18] holds for this selection, and for a short-lived resonant state, the π^- angular distribution is expected to be a relatively simple function of the angular momentum state J ($a+b\cos^2\alpha$ for $J=1$). The distributions are shown in Figs. 4(c) and (d). That in 4(c), at least, is suggestive of $J=1$, rather than larger J values which would give higher powers of $\cos^2\alpha$. The distribution in 4(c)

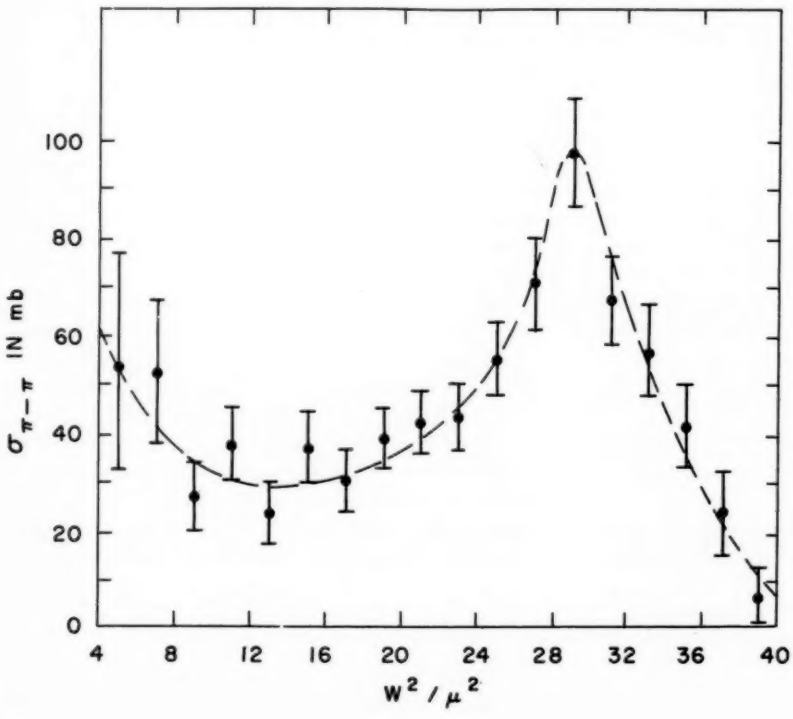

FIG. 3. Variation of cross section, $\sigma_{\pi-\pi}$ with energy, w, for the π-π system for events with $\Delta^2<10\mu^2$. The dashed curve is a free curve drawn through the points. μ = rest mass of charged pion.

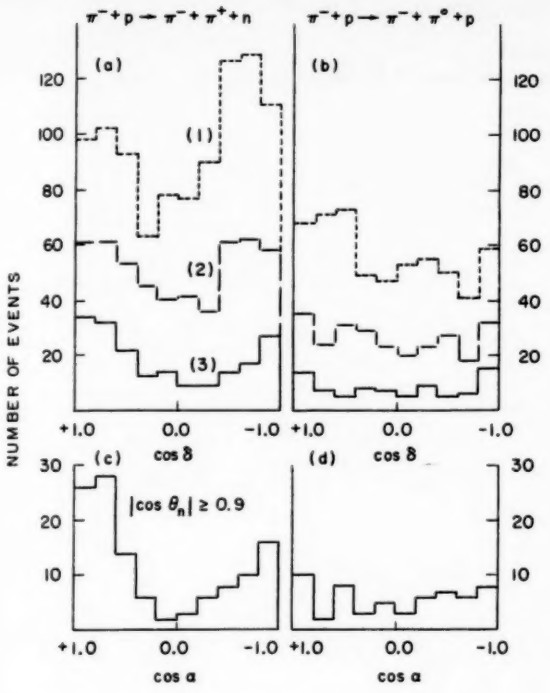

FIG. 4. Angular distributions for the π-π system. (a) and (b) show decay angles δ of π^- in π^* rest frame, relative to c.m. direction of π^*: (1) All events (dotted); (2) events with 400 Mev $\leq Q_{\pi-\pi} \leq$ 550 Mev (dashed); (3) events from (2) with $\Delta^2 < 10\mu^2$ (solid). (c) and (d) show decay angles α of π^- in π^* rest frame, relative to incident pion direction, for events with $|\cos\theta| \geq 0.9$, where θ = c.m. angle of π^*.

shows some asymmetry (backward/forward ratio =43/76), which may indicate interference from another state.

We wish to thank the BNL bubble chamber group, the Yale group who set up the beam, and our efficient team of scanners.

---

*Work was performed under the auspices of the U. S. Atomic Energy Commission.

†On leave of absence from the National Research Council, Ottawa, Ontario, Canada.

[1]F. Bonsignori and F. Selleri, Nuovo cimento 15, 465 (1960).

[2]I. Derado, Nuovo cimento 15, 853 (1960).

[3]E. Pickup, D. K. Robinson, and E. O. Salant, Proceedings of the Tenth Annual International Rochester Conference on High-Energy Physics (Interscience Publishers, Inc., New York, 1960), p. 72.

[4]J. G. Rushbrooke and D. Radojičić, Phys. Rev. Letters 5, 567 (1960).

[5]D. K. Robinson, B. Munir, E. Pickup, and E. O. Salant, Bull. Am. Phys. Soc. 6, 301 (1961).

[6]E. Pickup, F. Ayer, and E. O. Salant, Phys. Rev. Letters 4, 474 (1960).

[7]C. Goebel, Phys. Rev. Letters 1, 337 (1958).

[8]W. R. Frazer and J. R. Fulco, Phys. Rev. Letters 2, 365 (1959); Phys. Rev. 117, 1609 (1960).

[9]J. Bowcock, W. N. Cottingham, and D. Lurié, Phys. Rev. Letters 5, 386 (1960).

[10]J. A. Anderson, V. X. Bang, P. G. Burke, D. D. Carmony, and N. Schmitz, Phys. Rev. Letters 6, 365 (1961).

[11]D. Stonehill, C. Baltay, H. Courant, W. Fickinger, E. C. Fowler, H. Kraybill, J. Sandweiss, J. Sanford, and H. Taft, Phys. Rev. Letters 6, 624 (1961).

[12]A. R. Erwin, R. March, W. D. Walker, and E. West, Phys. Rev. Letters 6, 628 (1961).

[13]R. M. Sternheimer and S. J. Lindenbaum, Phys. Rev. 123, 333 (1961).

[14]G. F. Chew and F. E. Low, Phys. Rev. 113, 1640 (1959).

[15]Substitution of a resonant form for $\sigma_{\pi-\pi}$ in Eq. (3) would not significantly change the shape of the theoretical curve.

[16]Similar calculations for pion production in p-p collisions at 2 Bev give absolute $np\pi^+$ cross sections in approximate agreement with experiment for small momentum transfers [W. J. Fickinger, E. Pickup, D. K. Robinson, and E. O. Salant, following Letter, Phys. Rev. Letters 7, 196 (1961)]. Also, in p-p collisions at 2 Bev, a test of the Chew-Low method by extrapolation into the unphysical region [similar to the test made at 3 Bev by G. A. Smith, H. Courant, E. Fowler, H. Kraybill, J. Sandweiss, and H. Taft, Phys. Rev. Letters 5, 571 (1961)] gave good results [W. J. Fickinger, E. Pickup, D. K. Robinson, and E. O. Salant (to be published)].

[17]It should be noted that this selection of events is approximately equivalent to selecting events with very small Δ^2 [Figs. 4(a), (b)].

[18]R. K. Adair, Phys. Rev. 100, 1540 (1955).

ONE-PION EXCHANGE IN p-p COLLISIONS AT 2 Bev*

W. J. Fickinger†
Yale University, New Haven, Connecticut and Brookhaven National Laboratory, Upton, New York

and

E. Pickup,‡ D. K. Robinson, and E. O. Salant
Brookhaven National Laboratory, Upton, New York

(Received August 14, 1961)

Recently several authors[1-4] have proposed the use of the one-pion exchange model to describe the mechanism of pion production in p-p collisions. It is assumed that the dominant process is the exchange of a single pion between nucleons, with scattering of the virtual pion on one nucleon. The model then allows the calculation of the nucleon angular and momentum distributions, and predicts the absolute pion production cross sections, using the known π-p elastic scattering cross sections and the renormalized pion coupling constant. Experimental results of Batson et al.[5] and Fowler et al.[6] have been compared with the predictions of the model by Kobayashi,[1] Selleri,[2] and Iizuka and Klein.[4] However, the limited statistics in these experiments do not provide an adequate test of the model.

In a recent experiment at the Cosmotron, proton-proton interactions at 2 Bev were observed in the 20-inch hydrogen bubble chamber. The results of a complete analysis of this experiment are being prepared for publication.[7] From the measurement of about 4000 two-prong events, 1300 events of the type

$$p+p \rightarrow p+n+\pi^+$$

were identified, using digitized equipment and the GUTS kinematic fitting program, together with ionization density measurements. The results have been compared with the theory presented by Selleri. In general the agreement between theory and experiment is remarkable, but there are significant deviations.

The histogram in Fig. 1 shows the experimental c.m. momentum distribution of the neutrons. The dashed curve, normalized to the number of events, gives the prediction of the statistical theory, while the solid curve was computed by numerical integration of Selleri's equation,[8] using the experimental π^+-p elastic scattering cross sections. The contribution from π^0-p charge exchange scattering has been neglected in the calculation. For a pure $T=3/2$ state, this is 1/9 the contribution from π-p scattering. It should be noted that, since absolute cross sections are given by the theory, this latter curve is not normalized to the data. The sharp peak at 800 Mev/c in the theoretical neutron momentum spectrum is a consequence of the (3/2, 3/2) pion-proton resonance. A similar peak is also predicted by the isobar model of Lindenbaum and Sternheimer,[9] although this model does not give absolute cross sections or production angular distributions.

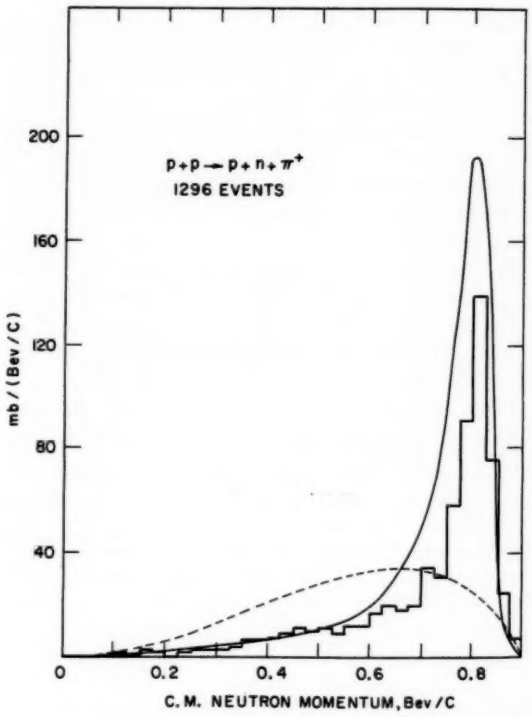

FIG. 1. Variation of partial cross section with neutron c.m. momentum for the reaction. The histogram is the experimental distribution; the dashed curve is from statistical theory (normalized); the solid curve is calculated from the equation of Selleri.

The c.m. angular distribution of the neutrons (folded about 90°) is shown by the histograms in Fig. 2. The dashed curves were computed from

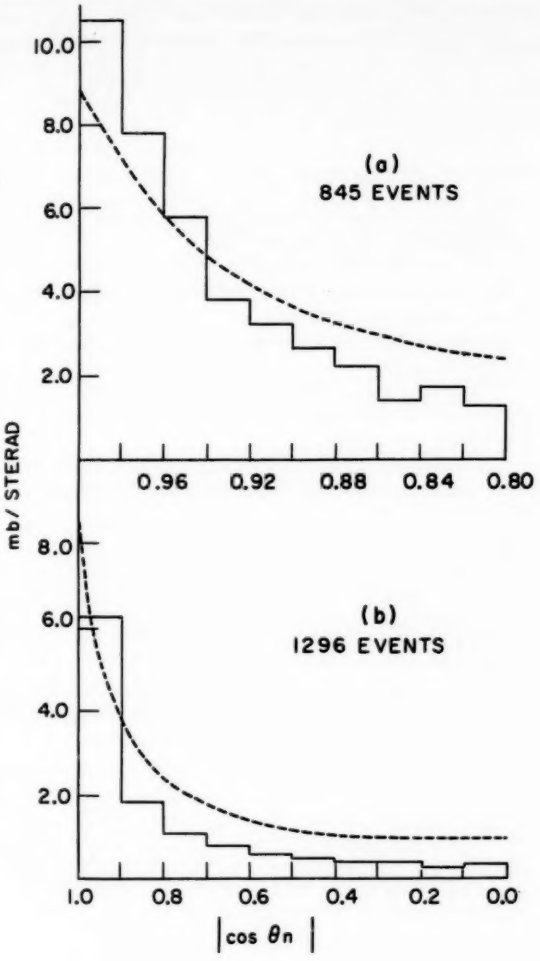

FIG. 2. Variation of cross section with c.m. angle of the neutron compared with the prediction from Selleri's equation. (a) shows the distribution for $|\cos\theta| \geq 0.8$; (b) shows the distribution for all angles, folded about 90°.

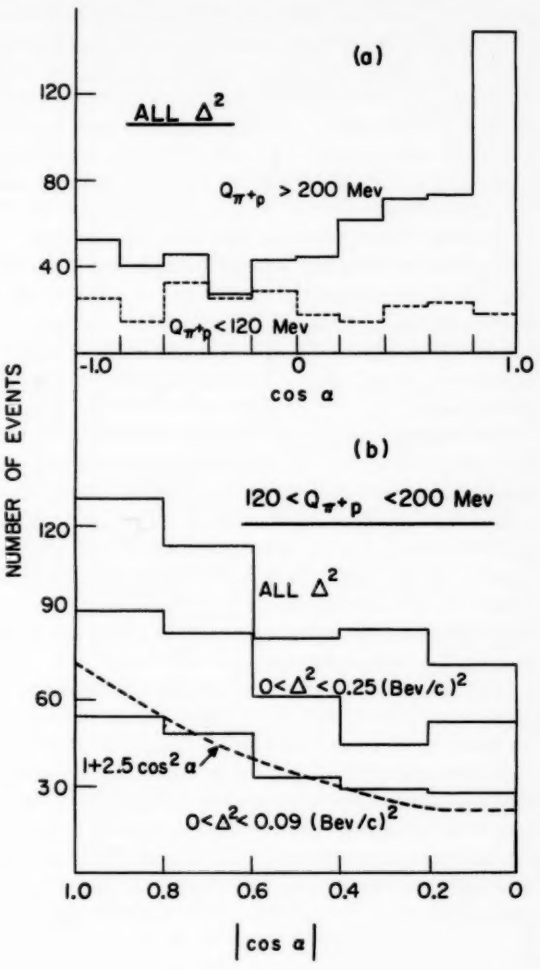

FIG. 3. Scattering angle of the virtual pion in the π^+-p c.m. system. (a) Events outside (3/2, 3/2) resonant peak; (b) events in resonant peak.

Selleri's equation, thus giving the absolute differential cross sections. The model gives a reasonable fit to the data at small angles, although the predicted differential cross section drops off less rapidly than the observed distribution. At large angles the theoretical cross sections are about twice those observed experimentally. Thus, the total cross section predicted was 23.4 mb, compared with our experimentally determined value of 16.06 ± 0.44 mb for this reaction. However, events with large recoil angles involve large momentum transfers, i.e., collisions with small impact parameters. Consequently, the concept of real scattering of an intermediate virtual pion is unlikely to be valid in such collisions.

An independent test of this concept might be given by considering the angular distribution of scattering of the virtual pion. If these can be considered to behave as real pions the characteristic $(1 + 3\cos^2\alpha)$ distribution, associated with π-p scattering in the angular momentum state $J = 3/2$, should be observed for those events for which the total kinetic energy of the pion and proton in their c.m. system, $Q_{\pi p}$, is in the region of the (3/2, 3/2) resonance. The direction and momentum of the incident virtual pion were assumed to be given by

the resultant of the laboratory momenta of the final-state pion and proton. The angle, α, of the final-state pion in the π-p center-of-mass system, relative to this virtual pion direction, was calculated for each event. Of two possible rest frames (incident proton and target proton) for each event, that one was chosen in which the neutron retained the higher momentum, so that the virtual pion production was more probably associated with a peripheral collision. Events were selected from the resonant region with 120 Mev $\leq Q_{\pi p} <$ 200 Mev. An examination of the experimental π^+-p scattering data[10] showed that the mean angular distribution through this region is approximately $(1+2.5\cos^2\alpha)$.

The results are shown in Fig. 3. Events in the selected Q interval were approximately symmetric about 90° (forward/backward = 254/227). The folded distribution shows partial agreement with a $(1+2.5\cos^2\alpha)$ distribution. Events with $Q<120$ Mev give isotropy within statistics, and for those with $Q \geq 200$ Mev the distribution is peaked strongly forward in qualitative agreement with π^+-p scattering above the resonance.

The shape of the neutron momentum distribution predicted by the one-pion exchange model is in good agreement with experiment. The theoretical differential cross section is too high at large neutron angles, so that the total cross section is about 50% higher than that observed. At small angles (small momentum transfers) the mean differential cross section observed is in good agreement with theory, but the cross section changes more rapidly than the theory predicts.

We wish to thank the BNL bubble chamber group, our capable scanners, and Dr. Philip Duke for discussion and for information on π^+-p scattering cross sections.

---

*Work performed under the auspices of the U. S. Atomic Energy Commission.

†Now at University of Kentucky, Lexington, Kentucky.

‡On leave of absence from National Research Council, Ottawa, Ontario, Canada.

[1]T. Kobayashi, Progr. Theoret. Phys. (Kyoto) 18, 318 (1957).

[2]F. Selleri, Phys. Rev. Letters 6, 64 (1960).

[3]See also F. Salzman and G. Salzman, Phys. Rev. Letters 5, 377 (1960).

[4]J. Iizuka and A. Klein, Phys. Rev. 123, 669 (1961).

[5]A. P. Batson, B. B. Culwick, J. G. Hill, and L. Riddiford, Proc. Roy. Soc. (London) 251, 218 (1959).

[6]W. B. Fowler, R. P. Shutt, A. M. Thorndike, W. L. Whittemore, W. T. Cocconi, E. Hart, M. M. Block, and E. M. Harth, Phys. Rev. 103, 1484 (1956).

[7]W. J. Fickinger, E. Pickup, D. K. Robinson, and E. O. Salant (to be published).

[8]Selleri's equation has been multiplied by a factor of 2 to correct an error pointed out to us by F. Salzman (private communication).

[9]S. J. Lindenbaum and R. M. Sternheimer, Phys. Rev. 105, 1874 (1957).

[10]J. Ashkin, J. P. Blaser, F. Feiner, and M. O. Stern, Proceedings of the CERN Symposium on High-Energy Accelerators and Pion Physics, Geneva, 1956 (European Organization of Nuclear Research, Geneva, 1956), p. 225.

QUASI-ELASTIC PEAK IN HIGH-ENERGY NUCLEON-NUCLEON SCATTERING*

S. D. Drell and K. Hiida†

Institute of Theoretical Physics, Department of Physics, Stanford University, Stanford, California

(Received August 4, 1961)

A bump in the energy spectrum of inelastically scattered protons emerging from proton-nucleus collisions for incident energies in the range 9-25 Bev, and for 20-60 milliradians (mr) scattering angles has been reported by Cocconi et al.[1] at CERN. Characteristic feature of this bump are:

1. The energy difference between the inelastic peak and the peak corresponding to elastic scattering at the same angle is $\approx 0.8 - 1.1$ Bev and is roughly independent of the scattering energy and angle.

2. The height of the inelastic peak falls off with increasing momentum transfer as does the elastic cross section, in a manner suggestive of diffraction scattering.

It is the purpose of this Letter to suggest a mechanism giving rise to a bump with these characteristics. This mechanism is the diffraction scattering of a pion in the cloud of the target nucleon from the incident projectile nucleon. It leads to a simple physical picture with an apparently general application. We wish to discuss this here, and to give the main results of calculations for the conditions of observation at CERN. A detailed report of the calculations and especially of the relevant, and somewhat involved, relativistic kinematics is in preparation.[2]

Consider the Feynman diagram of Fig. 1 which introduces the notation q_i, p_i, and p_f for the four-momenta of a target, incident, and observed final nucleon, respectively; $q_i^2 = p_i^2 = p_f^2 = m^2$; ($\hbar = c = 1$). q is the recoil nucleon four-momentum and $\Delta \equiv q_i - q$ is the transferred momentum; $\Delta^2 < 0$. The meson produced in the collision carries off k, with $k^2 = \mu^2$. In the following, the binding of the target nucleon in the target nucleus is neglected and the mass ratio $\mu/m - 0$.

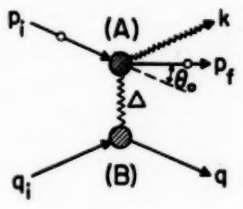

FIG. 1. Feynman diagram for scattering of a pion in the cloud of the target nucleon from the incident projectile nucleon. The circle o on the nucleon line denotes the high-energy incident and observed final nucleon.

We are interested only in a very restricted region of scattering through a laboratory angle $\theta_0 \leq 60$ mr and with small energy loss $\epsilon \equiv \delta + t/2m \approx 1$ Bev $\ll E_i$, where $t \equiv (p_i - p_f)^2 < 0$ is the invariant momentum transfer between the incident and observed nucleons of energy E_i and E_f, respectively, in the lab system, and $\delta \equiv E_i - E_f$; $\epsilon = 0$ for elastic scattering. For such events the magnitude of the momentum transferred between the two vertices A and B can be small [$|\Delta|^2_{\min} \simeq (2.4\,\mu)^2$ for $E_i = 25$ Bev, $\theta_0 = 40$ mr, and $\epsilon = 1$ Bev] and we approximate the scattering amplitude to the pole term shown in Fig. 1.

This approximation has been widely discussed recently[3] and is applied here with optimism in its at least qualitative validity since there is an enhancement factor at vertex A which we discuss in the following paragraph. We neglect contributions from graphs of the types in Fig. 2. Figure 2(a) is an exchange contribution and is unimportant when one of the two nucleons has almost all of the energy. Figure 2(b) was discussed previously[4] and is discarded here for two reasons: The momentum transfer between vertices is ≈ 1 Bev and far from the peripheral condition of an almost real pion being exchanged. If, nevertheless, the pole approximation is applied, its contribution to the inelastic peak is smaller than the observed cross section as well as smaller than

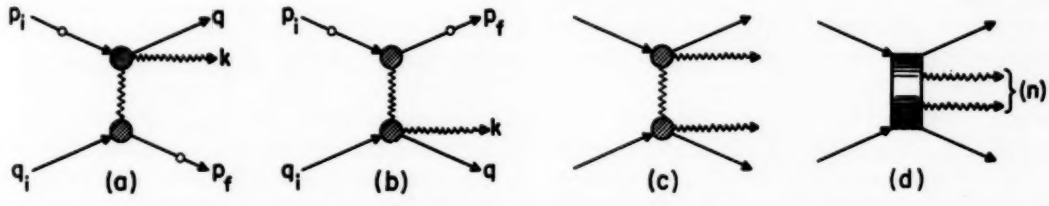

FIG. 2. Feynman diagrams for contributions neglected in the present calculation.

the contribution calculated from Fig. 1. (For $E_i = 16$ Bev, $\theta_0 = 40$ mr, and $\epsilon = 1$ Bev, it is smaller by a factor ≈ 4; see also footnote 10.) Feld and Iso[5] have shown that the inelastic bump occurs at an energy corresponding to a mean of the second and third resonances in pion-nucleon scattering and suggest this isobar formation as the cause of the observed inelastic bump. Their argument is kinematical, without reference to specific (poor) field-theoretic approximations. However, it is difficult to reconcile with the absence of an inelastic bump at $\epsilon \approx 300$ Mev corresponding to the large 3-3 resonance in pion-nucleon scattering. Figure 2(c)[6] can be shown[2] to contribute insignificantly for the small values of $\epsilon \approx 1$ Bev of interest here, primarily due to phase-space limitations. Figure 2(d) for more than a single-pion exchange between A and B is not calculable and its neglect can be defended only by measuring the ability of Fig. 1 in reproducing the observed cross sections.

An inelastic bump at the observed ϵ and of the observed magnitude emerges from Fig. 1 in the following way. The interaction at vertex A is treated as physical pion-nucleon scattering for small values of $|\Delta^2| < M^2$. The spin average of the square of the invariant matrix element for the pion-nucleon scattering, $\frac{1}{2}\sum_{\text{spins}} |M_A|^2 \equiv X_A$, can thus be related to experimental cross sections.

In the rest system of the incident nucleon we can write

$$X_A = 4(2\pi)^2 \left(1 - \frac{t}{s_1 - m^2 + t}\right)^2 \frac{d\sigma_{A,\,\text{lab}}(s_1, t)}{d\Omega}, \qquad (1)$$

in terms of the invariant total energy $s_1 \equiv (p_f + k)^2 > 0$ and momentum transfer $t = (p_i - p_f)^2 < 0$. We are interested in the experimental conditions at CERN which limit momentum transfers to $|t| \lesssim 2$ (Bev)^2. On the other hand, the scattering energy, s_1, can be much larger for inelasticities $\epsilon \approx 1$ Bev. It is this possibility that leads to the enhancement at the vertex A: For very large energies s_1, the pion-nucleon differential cross section develops a large forward diffraction peak. For forward scattering, $t = 0$, and we have in the approximation that there is mainly diffraction scattering at high energies:

$$\frac{d\sigma_{A,\,\text{lab}}(s_1, 0)}{d\Omega} \simeq \frac{\sigma_{\text{tot}}^2(s_1)}{4(4\pi)^2} \frac{(s_1 - m^2)^2}{m^2}. \qquad (2)$$

Here $\sigma_{\text{tot}}(s_1)$ is the total cross section for the pion-nucleon cross section and is nearly constant[7] [$\sigma_{\text{tot}} \approx 25$-$30$ mb at high energies, $s_1 \gtrsim (2$ Bev$)^2$]. The observed diffraction peak in high-energy π-N scattering suggests that we put in (1)

$$\frac{d\sigma_{A,\,\text{lab}}(s_1, t)}{d\Omega} = \frac{d\sigma_{A,\,\text{lab}}(s_1, 0)}{d\Omega} g(t). \qquad (3)$$

$g(t)$ must fall off faster than t^{-1} at large space-like t so that $\sigma_{A,\,\text{lab}}(s_1)$ remains constant as observed[7] in the several-Bev region, ≈ 5-8 mb. We choose

$$g(t) = 1 \Big/ \left(1 - \frac{t}{10\mu^2}\right)^2, \qquad (4)$$

for simplicity.[8] The results are insensitive to the specific form assumed here.[2] Inserting (2), (3), and (4) into (1) and approximating $|s_1/t| \gg 1$, since the second factor (2) weights heavily to high scattering energies, we obtain

$$X_A \cong \tfrac{1}{4}\sigma_{\text{tot}}^2(s_1) \frac{(s_1 - m^2)^2}{m^2} \Big/ \left(1 - \frac{t}{10\mu^2}\right)^2. \qquad (5)$$

This strong weighting of the amplitude at A to large energies s_1 is what leads to a bump as observed in the CERN experiments. Of the nine final momentum components $\vec{p}_f$, $\vec{q}$, and $\vec{k}$, only five are kinematically independent. If we observe a final nucleon at fixed $\vec{p}_f$ this leaves a two-dimensional integral,

$$\int d^3q\, d^3k\, \delta^4(q + k + p_f - p_i - q_i) = \int d^3\Delta\, d^3k\, \delta^4(k + p_f - p_i - \Delta),$$

to be carried out. What (5) tells us is that the contribution from large values of $s_1 = (p_f + k)^2 = (p_i + \Delta)^2$ is greatly enhanced in the phase-space integrals. This means that $\vec{p}_i$ and $\vec{\Delta}$ tend to be antiparallel, and the dominant contribution to the observed inelastic scattering comes when the target nucleon is hit head-on in the lab system. If the angles of $\vec{\Delta}$ are constrained in this way, we are then led to a unique relation between the magnitude of the momentum transfer $\Delta^2 \approx -|\vec{\Delta}|^2$ for $|\Delta^2| < M^2$, and the final nucleon energy E_f, or inelasticity,[9] ϵ:

$$\epsilon = \frac{|\vec{\Delta}|}{2} - \frac{t}{2}\left(\frac{1}{|\vec{\Delta}|} - \frac{1}{m}\right). \qquad (6)$$

Integrating over the range of possible $|\vec{\Delta}|$ for a given E_i and θ_0 leads to a corresponding range of preferred ϵ values according to (6). For the conditions of the CERN experiments these preferred inelasticities occur at $\frac{1}{2}$ Bev $\lesssim \epsilon \lesssim 2$ Bev and in the range of the observed quasi-elastic peaks.

The more accurate results of detailed calcula-

tions reproduce these general features. Inserting (5) into the calculation of the differential cross section for Fig. 1 gives

$$\frac{d^2\sigma}{dE_f d\Omega_f} \simeq \frac{3}{8}\frac{1}{(2\pi)^4}\frac{f^2}{\mu^2}\sigma_{\mathrm{tot}}^2(s_1)g(t)\frac{E_f}{E_i}\frac{1}{|\vec{p}_i - \vec{p}_f|}\int_{a-b}^{a+b} d(-\Delta^2)\frac{(-\Delta^2)}{(-\Delta^2+\mu^2)^2}F^4(\Delta^2)\int_0^{2\pi} d\varphi(s_1 - m^2)^2, \qquad (7)$$

where

$$a \approx \frac{2m^2 - (m+\epsilon)t}{m+2\epsilon} \text{ and } b \simeq |\vec{p}_i - \vec{p}_f|\frac{2m\epsilon}{m+2\epsilon}, \qquad (8)$$

and φ is the azimuthal angle of $\vec{q}$ relative to the plane of $\vec{p}_i$ and $\vec{q}_i$, which determines the polar axis. The integral $d\varphi$ is best carried out in the system in which the pion and recoil nucleon come off back to back; i.e., $\vec{k}+\vec{q}=0$. The form factor $F(\Delta^2)$ is introduced at each vertex to cut off the integral $d(-\Delta^2)$ at maximum values of $-\Delta^2 \approx (3\mu$ to $4\mu)^2$ compatible with the peripheral collision assumption of one-pion exchange with a physical amplitude inserted at vertex A. The observed quasi-elastic bump comes about because the emerging nucleon wants to steal most of the energy as indicated by (6). On the other hand, the integration interval in (7) vanishes when $b \propto \epsilon \to 0$ and this leads to a very sharp dropoff of the cross section at the inelastic threshold $\epsilon = 0$.

The second characteristic feature, of a decrease in peak height with increasing momentum transfer, is assured both by the diffraction factor $g(t)$ in (7) and by the integration limits, (8). As $-t$ increases, so does a and, therefore, $(-\Delta^2)_{\min}$; this reduces the integral $d(-\Delta^2)$ and further decreases $d^2\sigma/dE_f d\Omega_f$. The first characteristic feature, that the quasi-elastic peak is separated from the elastic one by a constant ϵ independent of momentum transfer t in the range $\frac{1}{2}$ (Bev)$^2 \lesssim -t \lesssim 2$ (Bev)^2, is also established. In order to understand this result, note that, according to (8), $(-\Delta^2)_{\min}$ increases with $-t$; this leads to a corresponding increase in the mean value of $|\vec{\Delta}|$ contributing to (7). As suggested by (6), an appropriate increase of $|\vec{\Delta}|$ with $-t$ can lead to a constant ϵ independent of t. This is what we find to occur to a good approximation.

Calculated curves are shown in Fig. 3 together with the data. The calculated numbers correspond to a cutoff in the integral $\int d(-\Delta^2)$ at a maximum[10] of $(4\mu)^2$. Were we to run the integrals out to the limits with $F(\Delta^2) \to 1$, the characteristic bump would remain but its height increases by a factor ≈ 6 for the 40-mr points and for the calculations at $E = 16.0$ Bev and $\theta_0 = 56$ mr. For the points with the largest momentum transfers, at $E_i = 26.10$ Bev and $\theta_0 = 56$ mr where $-t \approx 2$ (Bev)^2, the calculations are much less reliable. We are farther from the one-pion exchange pole, since, for $\epsilon \approx 1$ Bev, $|\Delta_{\min}| \approx 4\mu$ and the calculated cross sections are cutoff-sensitive and reduced by an order of magnitude. The neglected processes of Fig. 2 may then be relatively important and not negligible.

From the above arguments it appears that the process of Fig. 1 is the dominant peripheral contribution to quasi-elastic small-angle nucleon-nucleon scattering at high energies. The contribution of Fig. 2(b), which was discussed as a

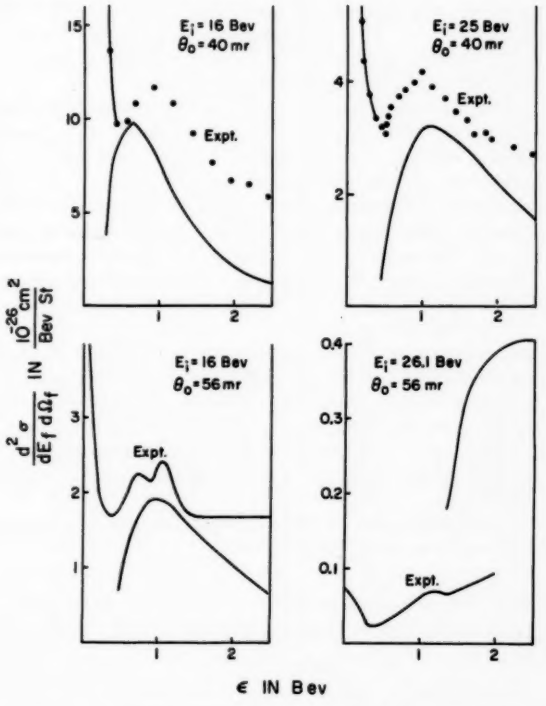

FIG. 3. Comparison of observed[1] cross sections in the region of the quasi-elastic bump for different values of the experimental parameters with calculations from Eq. (7).

test of the peripheral approximations,[4] is less important for the very small inelasticities, ϵ, considered here. This conclusion is also true as $\theta_0 \to 0$ and we approach the one-pion exchange pole.[2] It wins out only for larger ϵ which keep the amplitude of Fig. 1 from developing its diffraction peak. In an interesting letter which helped motivate this work, Selleri[11] has shown that at much lower energies both processes are important.

Our model offers no explanation of the camel's hump structure suggested in the recent experiments in progress at CERN.[1] Its existence, if confirmed, may indicate final-state interactions or other effects not included in the simple picture.

Finally we note that similar considerations apply to high-energy π-N scattering cross sections. For the same kinematics as in the CERN measurements, there should be a quasi-elastic diffraction peak in the process $\pi + N \to \pi + \pi + N$, whose height measures the square of the total π-π cross section in place of the π-N cross section $\sigma_{\text{tot}}^2(s_1)$, in (7).

---

*Supported in part by the U. S. Air Force through the Air Force Office of Scientific Research.

†On leave of absence from the Research Institute for Fundamental Physics, Kyoto University, Kyoto, Japan.

[1]G. Cocconi, A. N. Diddens, E. Lillethun, and A. M. Wetherell, Phys. Rev. Letters 6, 231 (1961). We wish to thank Dr. Wetherell for sending us results of further experiments on C and CH_2 targets carried out with higher resolution by Cocconi, Diddens, Lillethun, Manning, Taylor, Walker, and Wetherell. The same general features are observed with the added suggestion of a possible structure in the inelastic peak in the form of camel humps. The results of this study were presented at the CERN Conference on High-Energy Processes, Geneva, Switzerland, June, 1961 (unpublished) by Professor Marshall Baker of Stanford to whom we are grateful for a valuable report and discussion of the proceedings of the Conference especially as relevant to this work.

[2]K. Hiida and S. D. Drell (to be published). A similar mechanism was considered by D. Amati and J. Prentky (private communication).

[3]For a general discussion as well as detailed references to the literature contributed by many authors, see S. D. Drell, Revs. Modern Phys. 33, 458 (1961).

[4]S. D. Drell, Phys. Rev. Letters 5, 342 (1960).

[5]B. T. Feld and C. Iso, Nuovo cimento (to be published). We wish to thank these authors for a copy of their paper. Feld has also shown (to be published) that this isobar model leads to a diffraction angular distribution also in accord with the observed general features.

[6]I. M. Dremin and D. S. Chernavskii, J. Exptl. Theoret. Phys. (U.S.S.R.) 38, 229 (1960) [translation: Soviet Phys. – JETP 11, 167 (1960)]; D. S. Chernavski, I. M. Dremin, I. M. Gramenitski, and V. M. Maksimenko, Report A-27, and D. S. Chernavski and I. M. Dremin, Report A-28 of the Lebedev Physical Institute, Academy of Sciences of the U.S.S.R., Moscow, 1960 (unpublished); F. Salzman and G. Salzman, Phys. Rev. Letters 5, 377 (1960), and Phys. Rev. 121, 1541 (1961).

[7]O. Piccioni, Proceedings of the 1958 Annual International Conference on High-Energy Physics at CERN (CERN Scientific Information Service, Geneva, 1958); P. Falk-Vairant, G. Valladas, and G. Cocconi, Proceedings of the 1960 Annual International Conference on High-Energy Physics at Rochester (Interscience Publishers, New York, 1960).

[8]In the region of t values of interest this is numerically similar to the dependence deduced by Amati (report to La Jolla Conference) from the Mandelstam representation by considering the two-pion exchange contribution to elastic π-N scattering. This matches the data at several Bev.

[9]Equation (6) is insensitive to a variation in angle between $\vec{\Delta}$ and $-\vec{p}_1$ such that $(S_1 - m^2)^2$ falls to $\frac{1}{2}$ maximum value.

[10]Very similar numbers are obtained if we use a smooth cutoff such that $F^4(\Delta^2 = (3.5\mu)^2) \approx \frac{1}{2}$. The effect of such a cutoff on the isobar excitation calculation for Fig. 2(b) is to reduce the computed cross section to less than 4% of the observed value in typical parameters $E_i = 25$ Bev, $\theta_0 = 40$ mr.

[11]F. Selleri, Phys. Rev. Letters 6, 64 (1961). We find that the numerical results of this calculation should be multiplied by a factor of two due to an incorrect normalization procedure in computing the incident flux. See also T. Kobayashi, Progr. Theoret. Phys. (Kyoto) 18, 318 (1957); F. Bonsignori and F. Selleri, Nuovo cimento 15, 465 (1960).

K_{e3} DECAY AS A TEST OF UNIVERSAL V-A LEPTON COUPLING*

M. Bolsterli† and D. A. Geffen
School of Physics, University of Minnesota, Minneapolis, Minnesota
(Received July 28, 1961)

In this note, we show that the experimental spectrum of electrons from K_{e3} decay provides a direct test of universal vector-axial vector lepton coupling. The test is independent of the K-π form factor. We also discuss briefly the best way of treating the data so as to obtain information about the form factor itself.

K_{e3} decay has been treated extensively in the literature.[1] With the usual V-A lepton current, the matrix element for the decay is

$$T=(2\pi)^4(G/\sqrt{2})\delta^4(K-p-k-q)(4K_0q_0)^{-1/2}\bar{u}(k)\{\tfrac{1}{2}(\gamma\cdot K+\gamma\cdot q)f_+(Q^2)+\tfrac{1}{2}(\gamma\cdot K-\gamma\cdot q)f_-(Q^2)\}(1+\gamma_5)v(p). \quad (1)$$

We use units in which $\hbar=c=m_\pi=1$. The mass and four-momentum of K, π, e, ν are (M,K), $(1,q)$, (m_e,p), and $(0,k)$, respectively;

$$Q^2=(K-q)^2=(K-q)_0^2-(\vec{K}-\vec{q})^2; \quad (2)$$

f_+ and f_-, the K-π form factors, are analytic except for a branch on the real axis for $Q^2>(M+1)^2$; they are real in the range of Q^2 which occurs in K_{e3} decay: $(M^2-1)/2M<Q<M$. The equations

$$\bar{u}(k)\gamma\cdot k=0, \quad \gamma\cdot pv(p)=m_e v(p) \quad (3)$$

can be used to write Eq. (1) in the form

$$T=(2\pi)^4(G/\sqrt{2})(4K_0q_0)^{-1/2}f_+(Q^2)\delta^4(K-p-q-k) \times \bar{u}(k)\gamma\cdot K(1+\gamma_5)v(p). \quad (4)$$

In Eq. (4) and in the following, we set $m_e=0$. This neglect of m_e is justified as long as $|f_-/f_+| \ll M/m_e\sim 10^3$; the near equality of the K_{e3} and $K_{\mu3}$ rates[2] shows that this latter condition is satisfied.

We find for the number of electrons per unit time in the energy interval dp emitted by K's decaying at rest

$$N(p)dp=dp[G^2/2(2\pi)^3]M(M-2p)F(x), \quad (5)$$

where

$$x=\frac{2p(p_{\max}-p)}{M-2p}, \quad p_{\max}=\frac{M^2-1}{2M}, \quad (6)$$

$$F(x)=\int_0^x dy\,(x-y)f_+^2(2My). \quad (7)$$

This energy distribution for the electrons occurs (with different normalization) for any combination of vector and axial vector in the lepton current.

Note that p is a double-valued function of x. Therefore, $N(p)/(M-2p)\propto F(x)$ must have the same value for the two values of p corresponding to each value of x. This is, therefore, a simple condition that the electron spectrum must satisfy if leptons are universally coupled via a vector-axial vector current. This condition is independent of the form factor which occurs in $F(x)$ and depends only on the assumption of V-A lepton coupling. The data available at present are not sufficiently accurate to allow any conclusion as to whether or not this condition is satisfied.

$F(x)$ also has the properties

$$F(x)>0,$$
$$F'(x)>0, \quad F'(x)\geq x^{-1}F(x),$$
$$F''(x)=f_+^2(2Mx). \quad (8)$$

From these properties, it follows that $N(p)$ cannot have minima or maxima unless

$$p=0, \quad p=p_{\max}, \text{ or } (M^2-1)/4M\leq p\leq(M-1)/2. \quad (9)$$

Thus, except for the end points, maxima and minima must lie in the range

$$114 \text{ Mev}<p<180 \text{ Mev}. \quad (10)$$

The histogram given by Furuichi et al.[3] does not appear to satisfy this last condition, although improved statistics are needed before a definite conclusion can be drawn.

With sufficient data, it will be possible to determine $F(x)\propto N(p)/(M-2p)$. Besides the single-valuedness of $F(x)$, the conditions (7) can be verified and, in principle, $f_+^2(2Mx)$ can be determined from the curvature of $F(x)$. Note that $F(x)$ can be determined more accurately than $N(p)$, since each value of $F(x)$ comes from both values of p corresponding to that x and therefore has an accuracy

greater than either of the corresponding values of $N(p)$.

---

*Work supported in part by the U. S. Atomic Energy Commission.

†Present address: Institute for Theoretical Physics, Copenhagen, Denmark.

[1]See N. Brene, L. Egardt, and B. Qvist, Nuclear Phys. 22, 553 (1961) for a complete list of references.

[2]K. Bøggild, K. H. Hansen, J. E. Hooper, M. Scharff, and P. K. Aditya, Nuovo cimento 19, 621 (1961).

[3]S. Furuichi, S. Sawada, and M. Yonezawa, Nuovo cimento 10, 541 (1958).

POSSIBLE EXPLANATION OF THE HIGHER PION-NUCLEON AND K^--p RESONANCES IN TERMS OF INELASTIC THRESHOLDS

James S. Ball and William R. Frazer
University of California, San Diego, La Jolla, California

(Received July 31, 1961)

We have found by means of partial-wave dispersion relations that a large, rapidly rising inelastic cross section, such as is observed in the vicinity of the second and third pion-nucleon resonances,[1] can account for a sharp peak in the elastic scattering. We have calculated the inelastic contribution to the higher partial waves by means of the strip approximation to the Mandelstam representation,[2,3] in which the principal mechanism is the production of the $J=1$, $I=1$ pion-pion resonance. Assigning to this resonance a position and width in accord with recent experimental evidence,[4] we find strong inelastic scattering in angular momentum and isotopic spin states which phenomenological analyses have suggested as accounting for the resonances.[5,6] Moreover, resonances seem to be implied in approximately the correct positions, although we are unable at this stage to make really quantitative calculations. The same strip approximation calculation seems to imply a K^--p resonance, primarily in the $D_{3/2}$ state, at the observed energy,[7] provided the recently observed K^* has $J=1$ and $I=\frac{1}{2}$.[8]

In order to find the effect of strong, rapidly rising inelastic scattering in a given partial wave, consider the amplitude $f(\nu)$, which assumes the following form in the physical region:

$$f(\nu)=(e^{2i\delta}-1)/2i. \tag{1}$$

Above the inelastic threshold ν_i, $\delta=\delta_R+i\delta_I$, with $\delta_I>0$ according to unitarity. The variable ν is chosen appropriate to each particular reaction; for equal-mass scattering $\nu=k^2$, the square of the momentum in the center-of-mass system. Note that

$$\mathrm{Im}f=|f|^2+(1-\eta^2)/4, \tag{2}$$

where $\eta=e^{-2\delta_I}$. Thus the inelastic contribution to the cross section is proportional to $(1-\eta^2)/4$, so that δ_I is determined if the inelastic scattering in the partial wave is known. Let us assume for the moment that this is the case.

In order to keep the argument from being obscured by inessential complications, we shall now make two simplifying assumptions which could be relaxed without difficulty. We assume that $A(\nu)=f(\nu)/k$ is the function which is analytic in the ν plane except for the singularities given by the Mandelstam representation, thereby neglecting some relativistic effects. Since the point we wish to make concerns the effect of the inelastic scattering on the elastic at rather high energies, we also neglect the unphysical cuts.

We now have the following mathematical problem: Find a function $A=f/k$ with the properties: (a) It is analytic in the entire ν plane, except for a cut along the positive real axis. (b) It is real on the negative real axis. (c) The function $f(\nu)$ assumes the form of Eq. (1), with given δ_I, when the positive real axis is approached from above.

The solution is remarkably simple; construct

$$\delta(\nu)=\frac{k}{\pi}\int_{\nu_i}^{\infty}d\nu'\frac{\delta_I(\nu')}{k'(\nu'-\nu)}. \tag{3}$$

Using this formula to define δ in the entire ν plane, we assert that Eq. (1) provides a solution to the problem posed.[9,10] It can easily be verified that $A(\nu)$ has only the desired branch cuts, provided k is defined to have its cut along the positive real axis.

Let us now consider the effect upon the elastic amplitude of a rapidly rising inelastic cross section which rises to a value near its unitarity limit, such as is shown by the solid line in Fig. 1. Equation (3) implies that δ_R will be a sharply peaked function in the neighborhood of the rise

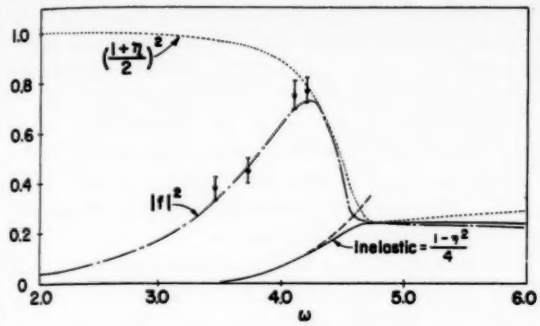

FIG. 1. A fit to the $D_{3/2}$ pion-nucleon resonance. The dashed line is the calculated $\sigma_I(D_{3/2})$. The dash-dot line is the absolute square of the elastic amplitude calculated from the inelastic cross section shown by the solid line. This inelastic cross section, which joins smoothly with our calculated values, has been chosen arbitrarily to produce a fit to the observed elastic scattering.[1] The dotted line is the unitarity limit for the absolute square of the elastic amplitude. The variable ω is defined as $\omega = W - m$, where W is the c.m. total energy and m is the nucleon mass.

in the inelastic cross section. The resulting elastic amplitude for a particular choice of δ_I is shown in Fig. 1. Note that the trailing edge of the peak is controlled mainly by the unitarity limit. The height and exact shape of the peak depend not only upon the rate of rise of the inelastic cross section, but also on its behavior at higher energies. It is possible, as illustrated in Fig. 1, to find reasonable inelastic cross sections which imply elastic peaks sharp enough to fit the higher resonances in pion-nucleon scattering.[11] The inelastic cross section itself need not be sharply peaked to produce a sharp, sizeable peak in the elastic amplitude. This statement is in principle subject to experimental verification; for example, by measuring the absorption in the $D_{3/2}$, $I = \frac{1}{2}$, pion-nucleon state above the second resonance. Note that our results do not imply a large elastic peak at all inelastic thresholds; the condition of a rapid rise to near-total absorption must be satisfied.

We turn now to the second part of the problem; namely, to calculate the inelastic cross section in each pion-nucleon partial wave and thereby obtain a value for δ_I to substitute in Eq. (3). As a first approximation to the problem, we use the "strip approximation" to the Mandelstam representation, in which only those parts of the double spectral functions corresponding to the lowest values of the momentum transfer are calculated.[2,3]

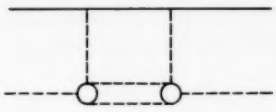

FIG. 2. Diagram giving rise to the pion-nucleon spectral function in the strip approximation.

The formulas, which are obtained by applying unitarity to the Mandelstam representation,[12] correspond to the process shown in Fig. 2. For the π-π amplitude we use a $J = 1$, $I = 1$ resonance formula.[13,14] Having calculated the double spectral functions for low momentum transfer, we substitute them into the equation for the imaginary part of the scattering amplitude,

$$\mathrm{Im}A(s,t) = \frac{1}{\pi}\int_{t_0}^{\infty} dt' \frac{a(s,t)}{t'-t}, \qquad (4)$$

where the lower limit t_0 is given by the Mandelstam boundary curve. We calculate the spectral function $a(s,t)$ correctly out to the boundary curve corresponding to four-pion exchange. The effect of neglecting these higher-mass-exchange contributions will be small for a sufficiently high partial wave. The $J = \frac{1}{2}$ states will certainly be unreliable, since the integral in Eq. (4) diverges logarithmically if we approximate the pion-pion amplitude by the P wave alone. For these states the contributions we have neglected, such as the contribution of the (3, 3) resonance, will surely be important. Therefore our calculation has some chance of reliability only for $J \geq \frac{3}{2}$. We project out partial waves from Eq. (4) and equate our calculated value of $\mathrm{Im}f_l$ with $(1-\eta^2)/4$, since the scattering via intermediate two-pion state is inelastic. Let us introduce the notation $\sigma_I(D_{3/2})$, for example, for the quantity $(1-\eta^2)/4$ in the $D_{3/2}$ state. Note that this quantity differs from the actual inelastic cross section by a factor $4\pi(J+\frac{1}{2})/k^2$.

Our results for these states are as follows: $\sigma_I(D_{3/2})$ rises rapidly in the region of the "threshold" for production of a π-π resonance, but rises to a height exceeding the unitarity limit by almost an order of magnitude. Our approximation has broken down because we have not taken unitarity into account for the processes $\pi + N \to \pi + \pi + N$ and $\pi + \pi + N \to \pi + \pi + N$. It may be possible to remedy this defect by means of an approximate treatment of these processes in which the particles are allowed to interact only in pairs. Such a calculation is now in progress. If we make the plausible conjecture that in a correctly unitarized calculation our large $\sigma_I(D_{3/2})$ will remain sizeable and will con-

tinue to rise rapidly, we can make a rough calculation of the position of a peak in the elastic $D_{3/2}$ amplitude. With a π-π resonance energy around $5m_\pi$, this peak coincides with the second resonance. Moreover, the effect of unitarity should not affect the results of our present calculation greatly as long as the result is well below the unitarity limit. Hence we can calculate the inelastic cross section in the region where it is beginning to rise and therefore, according to the arguments above, we can roughly predict the steepness of the trailing edge of the elastic peak. In Fig. 3 these results are compared with experiment. Also shown is the inelastic contribution to the only other state with $J \geq \frac{3}{2}$ which is sizeable in our model, the $F_{5/2}$ state. It rises rapidly at an energy coinciding with the third resonance. These angular momentum assignments seem to be consistent with experiment.[5] The way they arise in our model can be understood quite easily: Just above the "threshold" for production of a π-π resonance, the state in which the nucleon and the π-π resonance are in a relative S wave dominates. This state couples with the pion-nucleon system in the $D_{3/2}$ and $S_{1/2}$ states. We are unable to calculate $\sigma_I(S_{1/2})$ reliably, but we do expect $\sigma_I(D_{3/2})$ to rise rapidly in this region.[15] At a higher energy (thus explaining the separation between the two resonances),

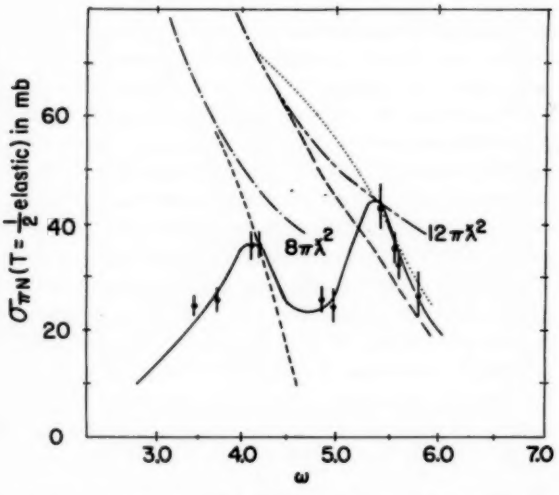

FIG. 3. The second and third pion-nucleon resonances. The dashed lines are the unitarity limits for elastic scattering in the $D_{3/2}$ and $F_{5/2}$ states calculated from the double spectral functions. The dotted line is the unitarity limit if a background of a saturated $\sigma_I(D_{3/2})$ is added. The points are from Falk-Vairant and Valladas.[1]

the relative P wave of the nucleon and π-π system will become important. This couples to the pion-nucleon $P_{1/2}$, $P_{3/2}$, and $F_{5/2}$ states. Again we cannot calculate $\sigma_I(P_{1/2})$. We find that $\sigma_I(F_{5/2})$ does indeed become important in our calculation, but $\sigma_I(P_{3/2})$ does not seem to attain a sufficiently high value to produce a large effect on the elastic scattering. This numerical result could be changed by a more definitive calculation.

The isotopic spin dependence of the diagram in Fig. 2 is such that the $I=\frac{1}{2}$ state is favored over the $I=\frac{3}{2}$ by a factor of four to one. This factor reduces $\sigma_I(F_{5/2})$ sufficiently that no analog of the third resonance is expected in π^+-p scattering. However, $\sigma_I(D_{3/2})$ is still large enough that the elastic amplitude in this state should show a peak around 800 Mev in π^+-p scattering. This may be the knee in the cross section which Carruthers has identified with the $D_{3/2}$ state.[6]

We have made a similar calculation for K^--p scattering around 1 Bev/c lab momentum, where a peak in the cross section has recently been found.[7] Again we calculate the diagram in Fig. 2, but now the incident and final mesons are K^-, and the intermediate resonance is the K^* resonance found by Alston et al.[8,16] If we assume that the K^* has $J=1$ (experiments have not yet distinguished between $J=0$ and $J=1$), then we again find a strong, rapidly rising $\sigma_I(D_{3/2})$ at just the right position to correspond to the observed peak (see Fig. 4). This implies a nearly saturated $D_{3/2}$ contribution to K^* production at 1.15 Bev/c, the energy in the experiment of Alston et al. Such a contribution to the process $K^- + p \to \bar{K}^0 + \pi^- + p$ turns out to be only 1.0 mb, however, which is not in disagreement with the experimental value which is of the order of 1 mb. In this process $\sigma_I(F_{5/2})$ does not come out to be strong, largely because of the narrowness of the K^* resonance as compared to the π-π resonance. We see from Fig. 4 that with a reasonable background the $D_{3/2}$ state does not seem to be able to account for the entire peak. The difference is probably due to the $S_{1/2}$ state which we are unable to calculate reliably.

If we assume the K^* has $J=0$, we find no large amplitudes with $J \geq \frac{3}{2}$, because a nucleon and K^* in a relative S state can then couple only to $J=\frac{1}{2}$ (which is clearly ruled out by the height of the observed peak). The relative P state does not contribute strongly for this process. Thus we definitely require the K^* to have $J=1$ if our model is to be valid. If we further assume $I=\frac{1}{2}$, as indicated by the K^* experiment, we find that in K-N scattering the $I=0$ state is favored over $I=1$ by a

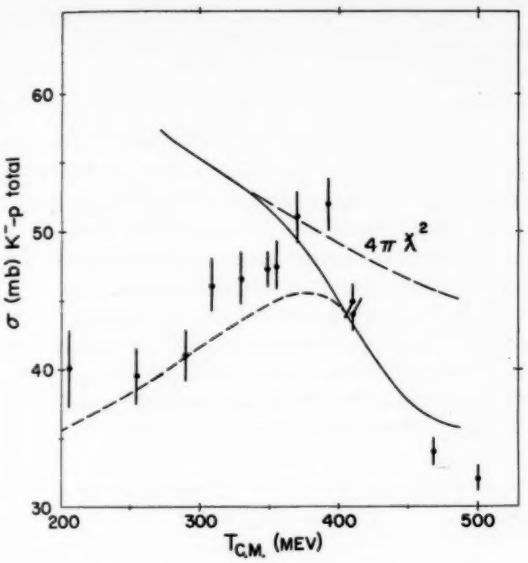

FIG. 4. The K^--p total cross section.[7] The solid line is the calculated unitarity limit for elastic scattering in the $D_{3/2}$ state, plus a constant background of 30 mb. The dashed line is a "fit" to the data, obtained by a suitable continuation of the calculated inelastic cross section.

ratio of 9/1. This agrees with the fact that no large peak is seen in the K^--n cross section. Our model implies that there should also be a peak in the K^+-n cross section, but it is impossible to predict its height from the present crude calculation. It is probably considerably smaller than the K^--p peak, because there are more inelastic channels open in the latter process, which may help to raise $\sigma_I(D_{3/2})$ close to the unitarity limit.

Additional resonances are probably implied in π-Y and K-Y systems, although detailed calculations must be carried out, which will depend upon assumptions about strange-particle couplings. The positions of these resonances will be around center-of-mass total energy $m_{\pi-\pi}+m_Y$ and $m_{K^*}+m_Y$, respectively.

---

[1]P. Falk-Vairant and G. Valladas, Proceedings of the 1960 Annual International Conference on High-Energy Physics at Rochester (Interscience Publishers, Inc., New York, 1960), p. 43.

[2]R. E. Cutkosky, Phys. Rev. Letters 4, 624 (1960).

[3]G. F. Chew and S. C. Frautschi, Phys. Rev. Letters 5, 580 (1960).

[4]J. A. Anderson, V. X. Bang, P. G. Burke, D. D. Carmony, and N. Schmitz, Phys. Rev. Letters 6, 365 (1961); D. Stonehill, C. Baltay, H. Courant, W. Fickinger, E. C. Fowler, H. Kraybill, J. Sandweiss, J. Sanford, and H. Taft, Phys. Rev. Letters 6, 624 (1960); A. R. Erwin, R. March, W. D. Walker, and E. West, Phys. Rev. Letters 6, 628 (1960); J. G. Rushbrooke and D. Radojičić, Phys. Rev. Letters 5, 567 (1960); E. Pickup, F. Ayer, and E. O. Salant, Phys. Rev. Letters 5, 161 (1960).

[5]Ronald F. Peierls, Phys. Rev. 118, 325 (1960).

[6]Peter Carruthers, Phys. Rev. Letters 4, 303 (1960).

[7]V. Cook, B. Cork, T. F. Hoang, D. Keefe, L. T. Kerth, W. A. Wenzel, and T. F. Zipf (to be published); O. Chamberlain, K. M. Crowe, D. Keefe, L. T. Kerth, A. Lemonick, T. Maung, and T. F. Zipf (to be published); Leroy T. Kerth, Revs. Modern Phys. 33, 389 (1961).

[8]M. H. Alston, L. W. Alvarez, P. Eberhard, M. L. Good, W. Graziano, H. D. Ticho, and S. G. Wojcicki, Phys. Rev. Letters 6, 300 (1961).

[9]We are indebted to Dr. Kenneth R. Greider for helping us to find this solution. The same solution, generalized to include a left cut, has also been found by Marcel Froissart (to be published). We are indebted to Dr. Froissart for advance communication of his results.

[10]Another method of solution is to set $A=N/D$, but giving N, in addition to the usual left cut, another cut beginning at the inelastic threshold with discontinuity $\mathrm{Im}N=(1-\eta)\,\mathrm{Re}D/2k$. The imaginary part of D is then $\mathrm{Im}D=-2k\,\mathrm{Re}N/(1+\eta)$. The resulting integral equations have been solved numerically, and it has been verified that the results coincide with Eq. (3).

[11]We continue to use the conventional term "resonance" for lack of a word more descriptive of the mechanism we propose.

[12]S. Mandelstam, Phys. Rev. 112, 1344 (1958).

[13]A model in which the higher resonances are explained in terms of a pion-pion resonance has been considered by many authors; most recently, by C. J. Goebel and H. J. Schnitzer, Phys. Rev. 123, 1021 (1961); P. Carruthers, Ann. Phys. (to be published); and K. Itabashi, M. Kato, K. Nakagawa, and G. Takeda, Progr. Theoret. Phys. (Kyoto) 24, 529 (1960). See these papers for references to earlier work.

[14]The formulas we have obtained have also been derived by V. Singh and B. M. Udgaonkar, Phys. Rev. (to be published).

[15]This argument has been given by P. Carruthers, Phys. Rev. Letters 6, 567 (1961).

[16]The model in which the K^--p resonance is explained in terms of K^* production has been considered by S. Minami, Progr. Theoret. Phys. (Kyoto) 25, 863 (1961).

LEPTON PAIRINGS IN THE TWO-NEUTRINO THEORY

G. Feinberg,* F. Gürsey,† and A. Pais‡
CERN, Geneva, Switzerland
(Received July 31, 1961)

In this note we will discuss some possible implications of the assumption that two distinct neutrinos are involved in the weak interactions. In particular, we consider the possibility that the association of the neutrinos with charged leptons in strangeness-changing decays is different from the pairing in strangeness-conserving decays. We will see that this possibility, if fulfilled, would have important consequences for proposed inverse neutrino reactions.

We recall that the existence of two neutrinos was assumed in order to forbid the decay $\mu \to e + \gamma$ by a selection rule,[1] according to which the μ and e are assigned different values of some quantum number. In order to make this consistent with the ordinary μ decay, two distinct neutrinos ν_1 and ν_2 with the same helicity are introduced, and the μ decay is assumed to be of the form

$$\mu^- \to e^- + \bar{\nu}_1 + \nu_2. \tag{1}$$

This follows in a natural way from the common assumption that all strangeness-conserving decays arise from an interaction of the form $J^\dagger J$, provided that $J = \bar{n}p \ldots + e^- \nu_1 + \mu^- \nu_2$. Such a structure implies also that the π decays are

$$\pi^+ \to e^+ + \nu_1, \tag{2}$$

$$\pi^+ \to \mu^+ + \nu_2. \tag{3}$$

These processes will not lead to $\mu \to e + \gamma$ to any order.[2]

It has been usually assumed that the pairings $(\mu\nu_2)$ and $(e\nu_1)$ are, in fact, universal and also occur in strangeness-changing reactions. The purpose of this note is to point out that if two neutrinos exist at all, there is the alternative possibility that in decays with $\Delta S = \pm 1$, the pairings $(e\nu_2)$ and $(\mu\nu_1)$ may occur. In such a theory the two-body leptonic decays of the K^+ would be

$$K^+ \to \mu^+ + \nu_1, \tag{4}$$

$$\to e^+ + \nu_2. \tag{5}$$

We will refer to such decays as "neutrino flip" decays. In the conventional theory the decays would instead be

$$K^+ \to \mu^+ + \nu_2, \tag{6}$$

$$\to e^+ + \nu_1. \tag{7}$$

Clearly, no direct experimental evidence exists at present to decide between the reactions (4), (5) and (6), (7), although the arguments on forbidding $\mu \to e + \gamma$ to all orders implies that they cannot coexist. If the reactions (4), (5) rather than (6), (7) occur, there will be important experimental consequences, some of which we indicate here.

(1) If high-energy neutrinos are obtained from the decay of a beam of positive pions, which has a "contamination" of positive K mesons, the net neutrino beam would be a mixture of ν_1 and ν_2 and therefore could generate both the reactions

$$\nu_1 + n \to e^- + p, \tag{8}$$

and

$$\nu_2 + n \to \mu^- + p. \tag{9}$$

We have been informed[3] that in neutrino experiments in progress, the K contamination of the pion beam may be ~20%. In the presence of neutrino flip decays this might lead to a sizable electron production. If an experiment is performed with neutrinos from a contaminated beam and no electrons are found, it would not only establish the two-neutrino theory, but also rule out the existence of neutrino flip K decays. Conversely, the mere observation of electrons produced by neutrinos would disprove the two-neutrino theory only if a "pure" pion beam was the source of neutrinos. (We neglect the one neutrino in 10^4 coming from $\pi \to e + \nu$ decay.)

(2) A related point is the availability of high-energy ν_1's from K^+ decay if the neutrino flip decay (4) occurs. Such high-energy ν_1's are not obviously available from any other source and would be a good tool in studying the symmetry between muon and electron interactions, by comparing for example the reactions (8) and (9). It will therefore be useful in this connection to be able to distinguish experimentally between inverse neutrino events induced by K^+ neutrinos and by π^+ neutrinos. For this purpose kinematic discriminations in a "contaminated" beam may be sufficient.

(3) The occurrence of neutrino flip K decays necessarily implies the occurrence of neutrino flip in hyperon-lepton interactions with $\Delta S = \Delta Q$. This means that in a neutrino absorption experiment, where the neutrinos are known to be of one type, the charged leptons produced with hyperons will not be the same as those produced with nu-

cleons. In particular the reactions

$$\bar{\nu}_2 + p \to \Lambda^0 + e^+, \tag{10}$$

$$\bar{\nu}_1 + p \to \Lambda^0 + \mu^+, \tag{11}$$

will occur, rather than

$$\bar{\nu}_2 + p \to \Lambda^0 + \mu^+, \text{ etc.} \tag{12}$$

In addition, we would like to make some comments of a more theoretical nature.

(a) If the lepton pairings in strangeness-changing decays are indeed different than those in strangeness-conserving decays, it would suggest that leptons carry a quantum number somehow related to strangeness,[4] and that the weak leptonic interactions are characterized by a selection rule involving both of these numbers. In this connection we mention that the reactions (4), (5) also imply the existence[5] of $\mu^+ \to e^+ + \nu_2 + \bar{\nu}_1$. These points will be taken up elsewhere.

(b) Unless special parity structures of the leptonic, strangeness violating, couplings prevail, it follows that if the K_{l2} modes (4) and (5) do show neutrino flip, all $\Delta S/\Delta Q = +1$ transitions do the same. Thus in the K_{l3}^+ decays and in the ($|\Delta S| = 1$) β and μ decays of Λ, Σ^-, and Ξ^- we would expect also (e, ν_2) and (μ, ν_1) pairings. The same is true in $K^0 \to \pi^- + e^+ + \nu_2$. If $\Delta S/\Delta Q = -1$ transitions occur, it is evidently impossible to determine the nature of the lepton pairing in such reactions from Eqs. (4) and (5). To reconcile the absence[6] of nonleptonic $\Delta S = 2$ transitions with a relatively simple current-current structure, it is attractive to consider the possibility that, if reactions with $\Delta S/\Delta Q = -1$ take place at all, the pairing is (e, ν_1), (μ, ν_2). In this case we would have

$$K^0 \to \pi^- + e^+ + \nu_2 \tag{13}$$

$$\to \pi^+ + e^- + \bar{\nu}_1, \tag{14}$$

$$\bar{K}^0 \to \pi^+ + e^- + \bar{\nu}_2 \tag{15}$$

$$\to \pi^- + e^+ + \nu_1. \tag{16}$$

We now assume CP invariance. Then regardless of the relative pairings in the reactions (14), (16) as compared to (13), (15), we have

$$R_1(\pi^-) = R_1(\pi^+), \tag{17}$$

$$R_2(\pi^-) = R_2(\pi^+), \tag{18}$$

where R_1 (R_2) denote the total rate of decay of K_1 (K_2) into the π with charge as indicated plus the corresponding electron-neutrino pair (and likewise for the μ-neutrino pair). We now consider the following three instances.

(i) No $\Delta S/\Delta Q = -1$ transitions. We have now in addition

$$R_1(\pi^-) = R_2(\pi^-). \tag{19}$$

(ii) $\Delta S/\Delta Q = -1$ transitions occur and the same lepton pairings (e, ν_2), (μ, ν_1) appear in both $\Delta S/\Delta Q = \pm 1$. This means that in Eqs. (14) and (16) $\bar{\nu}_2$ and ν_2 occur, respectively, rather than $\bar{\nu}_1$ and ν_1. The relation (19) is now in general not true due to different coherence effects in K_1 as compared to K_2 decays.

(iii) $\Delta S/\Delta Q = -1$ transitions occur and the lepton pairing is as indicated in Eqs. (13)-(16). Now, for example, the K_1 decay into $\pi^- + e^+ +$ neutrino is the incoherent superposition of the channels (13) and (16). Thus the rate is one half the sum of the partial rates. As a result the relation (19) is true even in the presence of (CP-invariant) $\Delta S/\Delta Q = \pm 1$ transitions.[7] Thus we have here the possibility of an experimental distinction between the cases (ii) and (iii). Observe also that if the $\Delta S/\Delta Q = +1$ transitions satisfy more specifically $|\Delta T| = \frac{1}{2}$, then the following conclusion is immediate: If $\Delta S/\Delta Q = -1$ transitions occur, with pairings as in Eqs. (14) and (16), then the ratio of rates $(K_2^0 \to \pi^\pm + e^\mp + \nu)/(K^+ \to \pi^0 + e^+ + \nu)$ is larger than two.

It should be noted that these last results depend only on the lepton pairing in $\Delta S/\Delta Q = +1$ relative to $\Delta S/\Delta Q = -1$. It is independent of the lepton pairing in $\Delta S/\Delta Q = +1$ relative to strangeness-conserving reactions.

In addition it should be emphasized that if $\Delta S/\Delta Q = -1$ involves (e, ν_1) and (μ, ν_2), as in Eqs. (14) and (16), then for example $\nu_2 + n \to \Sigma^+ + e^-$ remains forbidden, while for pairing (e, ν_2), (μ, ν_1) this reaction is allowed.

(c) It has been surmised that all the weak interactions are generated by a sum of product of currents such as $(\mathcal{J} + j + s)^\dagger \cdot (\mathcal{J} + j + s) + (j_0 + s_0)^\dagger \cdot (j_0 + s_0)$. This extension of the universal Fermi interaction to include strangeness-changing processes has sometimes been questioned, because of the absence of neutral lepton currents and because of the slowness of hyperon decay into leptons compared to the universal rates.[8] Regardless of these problems we would like to emphasize that the existence of the neutrino flip K decays would rule out this particular current-current structure, since different lepton currents occur in $\Delta S = 0$ decays than in $|\Delta S| = 1$ decays. Of course, a more complicated current structure can be envisaged.

(4) If all weak interactions including nonleptonic ones are considered to all orders of perturbation theory, then the absence of $\mu \to e + \gamma$ decay rules

out neutrino flip K decays.[9] This follows because the K meson can convert into a pion through virtual weak nonleptonic interactions, and therefore the chain $\mu \to K + \nu_1 \to \pi + \nu_1 \to e + \gamma$ can occur to third order in weak interactions. From this standpoint there is therefore a cogent objection to our proposal, if the cutoff of weak interactions is very large. However, we believe that this theoretical question is sufficiently open to warrant a direct experimental test of the existence of neutrino flip.

We are grateful to CERN for its kind hospitality and support.

After this note was submitted, Dr. B. d'Espagnat kindly brought to our attention a preprint[10] by Dr. S. Bludman in which the possibility of neutrino flip for a $\Delta S = \Delta Q$ is already considered.

---

*Alfred P. Sloan Foundation Fellow. Permanent address: Columbia University, New York, New York.

†On leave from the University of Istanbul, Istanbul, Turkey.

‡ Permanent address: Institute for Advanced Study, Princeton, New Jersey.

[1]B. Pontecorvo, J. Exptl. Theoret. Phys. (U.S.S.R.) 33, 549 (1957) [translation: Soviet Phys. – JETP 6, 429 (1958)]; K. Nishijima, Phys. Rev. 108, 907 (1957); G. Feinberg, Phys. Rev. 10, 1482 (1958).

[2]See Pontecorvo, reference 1.

[3]G. Bernardini (private communication).

[4]A. Gamba, R. E. Marshak, and S. Okubo, Proc. Natl. Acad. Sci. U.S. 45, 881 (1959). These authors have considered such a possibility in a theory with one neutrino. See also R. G. Sachs, Phys. Rev. 99, 1573 (1955). Another possible connection between strangeness and a neutrino quantum number has recently been discussed by T. Okabayashi, S. Nakamura, and Y. Nisiyama, Progr. Theoret. Phys. (Kyoto) 25, 701 (1961).

[5]This possibility has been discussed by G. Feinberg and S. Weinberg, Phys. Rev. Letters 6, 381 (1961).

[6]L. B. Okun and B. Pontecorvo, J. Exptl. Theoret. Phys. (U.S.S.R.) 32, 1587 (1957) [translation: Soviet Phys. – JETP 3, 989 (1957)]; F. Muller, R. W. Birge, W. B. Fowler, R. H. Good, W. Hirsch, R. P. Matsen, L. Oswald, W. M. Powell, H. S. White, and O. Piccioni, Phys. Rev. Letters 4, 418 (1960).

[7]R. G. Sachs and S. B. Treiman (private communication) first suggested an alternative way of reconciling Eq. (19) with the occurrence of $\Delta S = -\Delta Q$ transitions.

[8]W. E. Humphrey, J. Kirz, A. H. Rosenfeld, J. Leitner, and Y. I. Rhee, Phys. Rev. Letters 6, 478 (1961).

[9]In this connection see the footnote 5 of reference 5.

[10]S. Bludman, University of California Radiation Laboratory Report UCRL 9667 [Phys. Rev. (to be published)].

$\Lambda\pi$ RESONANCE AND s-WAVE K^--p REACTIONS*

Gordon L. Shaw
University of California, La Jolla, California

and

Marc H. Ross,†
Universita di Roma, Rome, Italy

(Received July 3, 1961)

The Y_1^* or $\Lambda\pi$ resonance at 1385 Mev has been observed by several experimental groups.[1] One of the theoretical explanations of the Y_1^* is that it is a quasi-bound state of the s-wave $\bar{K}N$ system. In fact, Dalitz and Tuan,[2] from their rough, constant-scattering-length analysis of the s-wave K^-p data, predicted that such a resonant state might exist. Discovery of the Y_1^* led to a discussion by Ross and Shaw[3] of the possibility of putting the association of the Y_1^* with the $\bar{K}N$ s state to a detailed test by means of an effective-range analysis, and as a result determine the KYN parities.

The purpose of this note is to report on an extensive survey of effective-range solutions of the s-wave K^-p data. The results can be summarized as follows: Assuming that the Y_1^* is associated with K^-p s state, the only acceptable solutions found were for the $\Sigma\pi$ channel in a p state (thus even $K\Sigma N$ parity), whereas the $\Lambda\pi$ channel could be either in an s or p state. In addition, among three different sets of effective ranges, only the one corresponding to a moderately short "range of forces," i.e., 0.4 f, led to satisfactory solutions.

The scattering amplitudes T_{ij} for a system of n coupled two-particle channels in a given state of total angular momentum J, z component J_z, isotopic spin I, parity P, etc., can be expressed as[4]

$$T = k^{l+1/2}(M - ik^{2l+1})^{-1}k^{l+1/2}. \quad (1)$$

The partial cross section from channel i to chan-

nel j is given by

$$\sigma_{ij} = \frac{4\pi}{k_i^2} \frac{2J+1}{2S_i+1} |T_{ij}|^2, \qquad (2)$$

where S_i is the spin of the initial (unpolarized) channel. The $(n \times n)$ matrix M is an even function of all the channel momenta k_i and thus remains real and symmetric when all the channels are not open (below the ith threshold $k_i - i\kappa_i$, $\kappa_i > 0$). The diagonal matrix $k^{l+1/2}$ has entries

$$(k^{l+1/2})_{ij} = \delta_{ij} k_i^{l_i+1/2},$$

where l_i is the angular momentum of the ith channel. According to the effective-range theory developed in A, M has the following energy dependence near any fixed energy E_0 (which we take as the K^-p threshold for the present application):

$$M = M(E_0) + \tfrac{1}{2}\Re[k^2 - k^2(E_0)], \qquad (3)$$

where $\Re$ is a real, approximately energy-independent and diagonal (even for $l_i \neq l_j$) matrix whose elements are roughly interpretable in terms of an interaction range. We have

$$M_{ij} = M_{ij}(E_0) + \tfrac{1}{2}\delta_{ij} R_i^{1-2l_i}[k_i^2 - k_i^2(E_0)], \qquad (4)$$

where $C_0 = 1$, $C_1 = -3$, and R_i is a measure of the range of forces in the ith channel.

The s-wave $I = 0$ $\bar{K}N$ channel is coupled to the $\Sigma\pi$ channel whereas the $I = 1$ system consists of three coupled two-body channels ($\bar{K}N$, $\Sigma\pi$, $\Lambda\pi$). In addition to the energy dependence of the isotopic spin amplitudes there are two charge-dependent modifications which are made: corrections due to the K^-p-$\bar{K}^0n$ mass splitting, and Coulomb corrections due to the charged K^-p channel.

There are eight pieces of data from s-wave K^-p reactions which are used in the present analysis: The capture of K^- mesons from s orbitals in (K^-, p) atoms yields the production ratios[5] $\Sigma^+\pi^-/\Sigma^-\pi^+/\Sigma^0\pi^0/\Lambda\pi^0$. At an incident K^- laboratory momentum of 175 Mev/c there are measurements on the elastic and charge-exchange cross sections as well as the production in the charged hyperon channels $\Sigma^+\pi^-$ and $\Sigma^-\pi^+$.[6] At 400 Mev/c, the p-wave amplitudes become dominant, and there is a very strong restriction[7,8] on the s-wave elastic scattering:

$$\sigma_{el}(400 \text{ Mev}/c) < 22 \text{ mb}.$$

The position (≈ 50 Mev below E_0), width (full width at half maximum < 30 Mev), and $(\Sigma\pi/\Lambda\pi)_{I=1}$ ratio (< 0.2) measurements on the Y_1^* have been fairly well corroborated.[1] We will assume that the Y_1^* has $J = \frac{1}{2}$ and $P(KY_1^*N)$ is even, i.e., the $\Lambda\pi$ resonance is associated with the s-wave $\bar{K}N$ system.

The computational procedure we use is the following: The 11 s-wave $\bar{K}N$ data (8 above-threshold K^-p measurements and 3 resonance parameters) are to be fit using the effective-range formalism (1)-(4) properly modified to take into account the charge-dependent corrections mentioned previously. We use 10 parameters: 9 zero-range $M_{ij}(E_0)$ and one effective-range R, i.e., we assume $R_i = R$ for all i. For each possible combination of $P(K\Sigma N)$ and $P(K\Lambda N)$ we considered more than 10 000 sets of zero-range $M_{ij}(E_0)$. All these sets of $M_{ij}(E_0)$ were chosen so that they fit the at-rest data[5] and yield complex scattering lengths $a_I(E_0)$ for the $\bar{K}N$ channels of the Dalitz-Tuan (a-) type (in order to omit all solutions which seem very unlikely to lead to the Y_1^*). Thus only some of the parameters were chosen arbitrarily [e.g., we let the matrix element

$$(k^{l+1/2} M_{I=1}^{-1} k^{l+1/2})_{\Sigma,\Sigma}$$

evaluated at E_0 take on 7 values between +1.2 and -1.2], whereas others were either determined or more narrowly restricted by these conditions imposed at the beginning of the computer program.

The relationship between the scattering length and the M matrix is, for a given isotopic spin,

$$-1/a(k) = M_{nn} + \mathfrak{M}_{nn}^{-1} \sum_{i \neq n} \mathfrak{M}_{ni} \cdot M_{in} \qquad (5)$$

where $\mathfrak{M}_{ij}$ is the ij minor of $(M - ik^{2l+1})$ and n denotes the $\bar{K}N$ channel. [Note that for the one-channel system, $-1/a(k) = M = k\cot\delta$.] Thus the zero-range approximation, $M = M(E_0)$, is not equivalent to the constant scattering-length approximation, $a(k) = a$; for constant M, $a(k)$ may still have considerable energy dependence. For each set of $M_{ij}(E_0)$, we carried the amplitudes to other energies according to the three different prescriptions: the zero-range approximation $M_{ij} = M_{ij}(E_0)$, $R = 0.4$ f, and $R = 0.7$ f. The calculations required several hours on a C.D.C. 1604 computer.

In the present survey, only 8 solutions satisfied the 11 restrictions. All eight solutions were for the $\Sigma\pi$ channel in a p state, i.e., even $K\Sigma N$ parity [in spite of the fact that twice as many sets of values were investigated for odd $P(K\Sigma N)$ as even]. The number of solutions were evenly divided be-

tween even and odd $P(K\Lambda N)$. In addition, all these solutions had a range of interaction $R = 0.4$ f (yielding strong energy dependence in the $\Sigma\pi$ channel).

Some additional aspects that these "acceptable" solutions have in common are as follows: (i) No isotopic spin zero resonance was found. The energy dependence of $1/a_0(k)$ was very rapid (and nonquadratic) and even those solutions which in the constant-scattering-length approximation would yield a broad $I = 0$ resonance had quite small nonresonant $I = 0$ amplitudes below E_0. (The possibility of having the s-wave $\bar{K}N$ amplitudes accommodating both the Y_1^* and a narrow Y_0^* seems completely ruled out.) (ii) The Σ^-/Σ^+ ratio changes rapidly from 2.18 at rest to ≈ 1 at 175-Mev/c incident K^- laboratory momentum, then remains fairly constant (slightly more $\Sigma^+\pi^-$ than $\Sigma^-\pi^+$). (iii) The $\Lambda/(\Lambda+\Sigma^0)$ ratio increases from at-rest values ≈ 0.2 to ≈ 0.6 at 300 Mev/c. (iv) $(\Sigma/\Lambda)_{I=1}$, which is < 0.2 in the resonance energy region and ≈ 1 at threshold, decreases to a value $\ll 1$ at 300 Mev/c.[9] (v) The charge-exchange scattering remains fairly large, i.e., it does not fall off greatly from its value of ≈ 12 mb at 175 Mev/c.

With the existing above-threshold s-wave K^-p data, we find (nonacceptable) effective-range solutions which fit these data and yield scattering lengths near threshold of the Dalitz-Tuan (a-) type (which would in the constant-scattering-length approximation predict a $\Lambda\pi$ resonance having a position and width corresponding to the observed Y_1^*) and yet show no resonant behavior. Thus definite evidence for the (a-) type K^-p scattering length solution is not in itself conclusive evidence that the Y_1^* must be identified with the s-wave $\bar{K}N$ system. Additional K^-p (and $\bar{K}^0p$) measurements shedding light on the detailed energy dependence of the amplitudes, such as the σ_{el}(400 Mev/c) datum, which cannot be fit in a constant-scattering-length approximation, may change this situation. However, identification of the Y_1^* with the s-wave $\bar{K}N$ system together with the present effective-range survey indicates that the $K\Sigma N$ parity is even. Determination of the angular momentum of the $\Lambda\pi$ channel, for example, from measuring the polarization of the Λ produced in the Y_1^* decay would then give the $K\Lambda N$ parity (there is some indication that the $\Lambda\pi$ is in an s state[1]).

The details of this calculation (including a discussion of the accuracy and applicability of the effective-range formalism for the present problem,[10] e.g., the restriction $|k_i^2 - k_i^2(E_0)|R^2 < 1$ is satisfied over the entire energy range considered) along with a treatment of global symmetry as applied to $\bar{K}N$ reactions will be published elsewhere.

The encouraging results of the present survey (e.g., only a small number of acceptable solutions were found) indicate that a gradient search[11] for the $M_{ij}(E_0)$ and R_i would be warranted in the near future.

We would like to thnak Professor R. H. Dalitz for a very helpful discussion.

---

*Supported in part by the U. S. Atomic Energy Commission.

†National Science Foundation Senior Postdoctoral Fellow on leave from Indiana University, Bloomington, Indiana.

[1]M. Alston, L. Alvarez, P. Eberhard, M. Good, W. Graziano, H. Ticho, and S. Wojcicki, Phys. Rev. Letters 5, 520 (1960); M. Ferro-Luzzi, J. Berge, J. Kirz, J. Murray, A. Rosenfeld, and M. Watson, Bull. Am. Phys. Soc. 5, 509 (1960); H. Martin, L. Leipuner, W. Chinowsky, F. Shively, and R. Adair, Phys. Rev. Letters 6, 283 (1961).

[2]R. Dalitz and S. Tuan, Phys. Rev. Letters 2, 425 (1959); Ann. Phys. 10, 307 (1960).

[3]M. Ross and G. Shaw, Phys. Rev. Letters 5, 578 (1960).

[4]M. Ross and G. Shaw, Ann. Phys. 13, 147 (1961). We shall refer to this paper as A.

[5]We use the values $\Sigma^-/\Sigma^+ = 2.18$, $(\Sigma^- + \Sigma^+)/(\Lambda + \Sigma^0) = 1.8$, and $0.13 < (\Sigma^- + \Sigma^+ + \Lambda - 2\Sigma^0)/3\Sigma^0 < 0.26$. These data give $(\Sigma/\Lambda)_{I=1} \approx 1$ and $\Lambda/(\Lambda + \Sigma^0) \approx 0.2$.

[6]These cross sections (in mb) are taken as $70 < \sigma_{el} < 90$, $11 < \sigma_{ex} < 19$, $33 < [\sigma(\Sigma^+) + \sigma(\Sigma^-)] < 49$, $0.5 < \sigma(\Sigma^+)/\sigma(\Sigma^-) < 2.0$.

[7]P. Nordin, Lawrence Radiation Laboratory Report UCRL-9489, 1960 (unpublished).

[8]We wish to thank R. H. Dalitz for calling this to our attention.

[9]This seems, at first, to be in disagreement with the data recently reported on $\bar{K}^0p$ scattering: E. Hart, D. Luers, I. Mittra, W. Willis, and S. Yamamoto, Bull. Am. Phys. Soc. 6, 350 (1961). However, their results include p-wave $\bar{K}N$ reactions which are known to be considerable above 300 Mev/c.

[10]A general treatment of the accuracy and applicability of the effective-range theory is given in A.

[11]See, for example, G. Breit, M. Hull, K. Lassila, and K. Pyatt, Phys. Rev. 120, 222 (1960).

ANOMALOUS THRESHOLDS AND FINAL-STATE INTERACTIONS IN PRODUCTION PROCESSES*

R. F. Sawyer
University of Wisconsin, Madison, Wisconsin
(Received July 18, 1961)

Evidence for resonant two-body final-state interactions in production processes with three-particle final states has recently been obtained in the form of energy spectrum peaks in numerous experiments involving strange particles.[1] It is less obvious how the effects of nonresonant scattering in strongly interacting three-body systems are to be estimated, and under what circumstances they can be expected to provide the dominant dependence of a production amplitude on some variable. Nevertheless nonresonant S-wave pion-pion effects are now suspected to be the cause of the strange He^3 momentum distribution in the $p+d$ experiment of Abashian, Booth, and Crowe.[2,3] If this explanation is correct, a similar effect should be observed in the final nucleon spectrum in the process $N+\pi \to N+\pi+\pi$. It is the purpose of this note to point out some complicating effects, due to anomalous thresholds, in the latter process. These effects will be common to many production processes (including $p+d \to He^3+2\pi^0$) and may muddle the interpretation considerably. The virtue of the particular process, $N+\pi \to N+\pi+\pi$, is that it allows a quantitative estimate of the difficulties.

We shall devote our attention to the dependence of the production amplitude on a variable, q, which is the momentum of one of the final pions in the center-of-mass system of the two outgoing pions. Only pairs of pions in the $T=0$, $J=0$ state and only small values of q will be considered. Whatever the complete analytic structure of the production amplitude, there should be a cut in the q^2 plane running from zero to infinity, originating in the π-π rescattering. This cut may be taken into account by writing for the production amplitude, A (all variables except q^2 suppressed),[7]

$$A(q^2)=M(q^2)\exp\frac{1}{\pi}\int_0^\infty \frac{\delta(q')}{q'^2-q^2-i\epsilon}dq'.$$

The second factor here is the inverse of the standard denominator function, D,[4] computed from the $T=0$, S-wave π-π phase shift. $M(q^2)$ is analytic in q^2 along the physical π-π cut. One is now tempted to assume (and it is this assumption which we shall criticize) that for small q the function $M(q^2)$ can be approximated by a constant. In a scattering-length approximation with an attractive π-π force, the dependence of the cross section for small q^2 would then be as $(1+q^2a^2)^{-1}$, which for a large scattering length, a, would produce an enhancement for small q^2. This is the basis upon which an attractive, $T=0$, π-π force can be considered an explanation for the $T=0$ anomaly in $p+d$ collisions.[2,3]

As has been pointed out,[5-6] production amplitudes may have a wide variety of complex branch points. Of these there is one particular kind of anomaly which seems to be of importance with respect to the above-mentioned arguments on final-state interactions. This is associated with the reduced graph[8] of Fig. 1(a). We define variables for Fig. 1 as

$$W=-(k_1+p_1)^2,$$
$$\Delta=-(p_1-p_2)^2,$$
$$s=-(k_2+k_3)^2=4(q^2+\mu^2). \qquad (1)$$

A. For sufficiently small values of W, the diagram of Fig. 1(a) has only the normal cut in s. As W is increased an anomalous branch point breaks off from the normal threshold at $s=4\mu^2$ and moves to the left. When W becomes unstable $[W=(M+\mu)^2]$ this branch point moves into the complex plane to the point s_b,[8]

$$s_b=\frac{\mu^2(W+M^2-\mu^2)}{2M^2}-\frac{i}{2M^2}[W^2-2(M^2+\mu^2)W+(M^2-\mu^2)^2]^{1/2}(4M^2-\mu^2)^{1/2}. \qquad (2)$$

B. Let the π-π interaction of Fig. 1(a) be local $(\lambda\varphi^4)$. Then the cut originating at the complex branch point, s_b, is quite deformable. However it must terminate on the normal threshold at $s=4\mu^2$ if ordinary unitarity is to be used along the

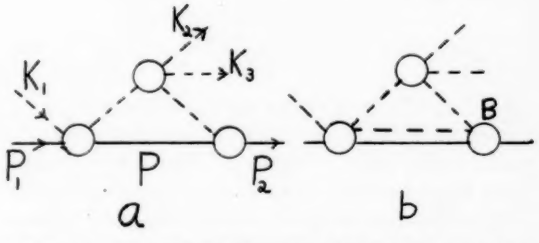

FIG. 1. Two reduced diagrams for $\pi+N \to \pi+\pi+N$. Solid lines are nucleons. Dashed lines are pions.

normal cut, $4\mu^2 < s < \infty$ (this is true at least in perturbation theory). The anomalous cut therefore gives a branch point at $s=4$ which is not removed by factoring out D^{-1}. It remains to estimate the importance of this singularity. For the graph of Fig. 1 the discontinuity across the complex branch cut may be calculated using generalized unitarity,[9] in terms of λ, G (π-N coupling constant), and the π-N scattering amplitude. The π-N scattering will be on the mass shell, but at a complex momentum transfer. We shall return to this calculation.

C. Figure 1(a) seems to be the only contributor to the additional singularity at $s=4\mu^2$ mentioned above, though a further check of some higher order graphs is in progress. Of reduced diagrams which contain the 2π state in the s channel, the next to be considered is that of Fig. 1(b). This graph is not anomalous in s for any value of W. This is by virtue of the internal instability at the vertex, B.[6]

D. If all lines in Fig. 1(a) were boson lines, the discontinuity across the anomalous cut running from $s=s_b$ to $s=4\mu^2$ could be calculated from the expression,[9]

$$\mathrm{disc}A = (\mathrm{KF})\lambda G\int d^4p\ \delta(p^2+M^2)\delta[(p-p_2)^2+\mu^2]\delta[(p-p_1-k_1)^2+\mu^2]T(W,-(p_1-p)^2), \tag{3}$$

where $T(W,t)$ is the π-N scattering amplitude as a function of energy and momentum transfer, and (KF) stands for kinematical factors. One obtains

$$\mathrm{disc}A = (\mathrm{KF})\frac{\lambda G}{4\alpha}\oint\frac{T(W,t)}{(t-t_+)^{1/2}(t-t_-)^{1/2}}dt, \tag{4}$$

where

$$t_\pm = -\frac{\beta^2}{2W}[1-xy\mp(1-x^2)^{1/2}(1-y^2)^{1/2}],$$

$$x=(1/\alpha\beta)(\gamma\delta-2sW), \qquad \beta=(\delta^2-4\mu^2W)^{1/2},$$

$$y=x+(2W/\alpha\beta)(\Delta-\mu^2), \qquad \gamma=W-M^2+s,$$

$$\alpha=(\gamma^2-4sW)^{1/2}, \qquad \delta=W-M^2+\mu^2.$$

The integral in t is around the cut in the denominator. It can be seen that in the high-energy limit, $W\gg M$, Δ, s, the region in the cosine of the π-N scattering angle implied by the integration limits in (4) becomes limited to a small region near $\cos\theta=1$, and that the momentum transfer becomes real (even for the complex values of s under consideration). In fact, for high energies this region in angle remains somewhat within the forward diffraction peak. Therefore we insert in (4) for $T(W,t)$ a diffraction approximation for a black sphere of radius R,

$$T(W,t) = \frac{iQRJ_1[R(-t)^{1/2}]}{(-t)^{1/2}}. \tag{5}$$

E. Considerable complication develops in a proper calculation in which nucleon spin and odd-parity pions enter. For Fig. 1 alone four amplitudes must be introduced and the discontinuity of each calculated along the anomalous cut. This has been done in the high-W limit and in the diffraction approximation described above. Here we quote only the result. The spin dependence is just $\bar{u}(p_2)\gamma_5 u(p_1)$ as in the single-pion pole term. The result will be displayed as the ratio of the contribution of the anomalous cut to that of the pole term, thus eliminating λ, G, and kinematical factors. The isotopic spin dependence of the two contributions is identical in our diffraction approximation. We obtain

$$\frac{A_{\mathrm{anom}}}{A_{\mathrm{pole}}} \approx \frac{i(\Delta-\mu^2)(R\mu)^4}{8\mu^2}\ln\frac{s-4\mu^2}{s-s_b}. \tag{6}$$

For $R\mu\approx 1$ the logarithmic singularity is both large and strongly dependent on s near $s=4\mu^2$. This latter property apparently will cause some difficulty in using scattering-length approximations to treat final-state interactions at low relative momentum.

The domain in which there is such a difficulty is better estimated from a somewhat different comparison. In the one-pion pole contribution to the production process let us insert, instead of $\lambda\varphi^4$, a scattering-length approximation to the pion-pion amplitude,

$$f_{\pi\text{-}\pi} = a/(1-iqa). \tag{7}$$

The contribution of diagram (1a) is calculated as before, taking a coupling constant appropriate to the scattering length in (7). Now we compute the derivatives with respect to q of A_{anom} and A_{pole} in order to give a comparison of the anomalous q dependence with the q dependence of the pole term

implied by (7). One obtains

$$\frac{(d/dq)A_{\text{anom}}}{(d/dq)A_{\text{pole}}} = \frac{(\Delta-\mu^2)(R\mu)^4(1-iqa)^2}{8\mu^2 qa}. \qquad (8)$$

For $\Delta=0$ and $R\mu=1/2^{1/2}$ (as indicated by high-energy π-N total cross sections), we find that we must go to $qa \gg 1/32$ to see the direct q dependence from the π-π scattering amplitude dominate the anomalous q dependence. For example, for $\Delta=10$ there is clearly no domain of $qa<1$ for which the ratio (8) is small. The scattering-length approximation is never valid for very low q. There may or may not be a domain of validity for intermediate q, that is, in a region sufficiently far away from the logarithmic singularity but for small enough qa to justify a scattering-length approximation.

*This work was supported in part by the Research Committee of the University of Wisconsin with funds provided by the Wisconsin Alumni Research Foundation and in part by the National Science Foundation.

[1]M. Alston et al., Phys. Rev. Letters 5, 520 (1960).
[2]A. Abashian, N. E. Booth, and K. M. Crowe, Phys. Rev. Letters 5, 258 (1960).
[3]T. N. Truong, Phys. Rev. Letters 6, 308 (1961).
[4]W. R. Frazer and J. R. Fulco, Phys. Rev. 117, 1609 (1960).
[5]P. V. Landshoff and S. B. Treiman, Nuovo cimento 19, 1249 (1961).
[6]L. F. Cook, Jr., and J. Tarski, Phys. Rev. Letters 5, 585 (1960), and Princeton preprint.
[7]Y. S. Kim, Phys. Rev. Letters 6, 225 (1961).
[8]R. J. Eden, University of Maryland Technical Report No. 211, 1961 (unpublished).
[9]R. E. Cutkosky, J. Math. Phys. 1, 429 (1960), and Phys. Rev. Letters 4, 624 (1960).

ERRATUM

SUPERCONDUCTIVITY IN Nb_3Sn AT HIGH CURRENT DENSITY IN A MAGNETIC FIELD OF 88 kgauss. J. E. Kunzler, E. Buehler, F. S. L. Hsu, and J. H. Wernick [Phys. Rev. Letters 6, 89 (1961)].

Reference 5 is incorrect. Instead of J. C. McLennan et al., Trans. Roy. Soc. Can. 24, 25 (1930), the correct reference should be R. R. Hake, D. H. Leslie, and T. G. Berlincourt, Bull. Am. Phys. Soc. 4, 362 (1959); de Haas and Voogd, Commun. Phys. Lab. Univ. Leiden No. 208b (1930).